Hiroshima University Doctoral Thesis

Regio- and stereoselectivity in the photochemical [2+2] cycloaddition reaction of carbonyl compounds with pyrrole derivatives

(カルボニル化合物とピロール誘導体の光[2+2]付加環化反応における位置及び立体選択性に関する研究)

2018

Department of Chemistry
Graduate School of Science
Hiroshima University

Jianfei Xue

Table of Contents

Main Thesis

Contents

Chapter 1

General Introduction

1-1. Photochemical reaction in organic synthesis

Even though the papers that mentioned "Organic synthesis, Photochemistry" (4970 papers) only occupied ~1% of the papers that mentioned "Organic synthesis" (462402 papers), the significance of application of photochemistry in organic synthesis should not be neglected (searched on SciFinder database in June, 2018). Obviously, the most intriguing merit of the use of photochemistry in organic synthesis is that it could provide people with a method to obtain the target molecule with ease and efficiency that could not achieved by the conventional (thermal) organic reactions easily.[1]

Oxetane, with ~110 kJ/mol of ring strained energy, is significant and widely applied in organic synthesis.[2] In addtion, oxetane derivatives have attracted much attentions since the oxetane structure is found in many biologically active compounds such as merrilactone A, thromboxane A_2, oxetanocin, oxetin, taxane alkaloids and laureacetal-B (Figure 1).[3]

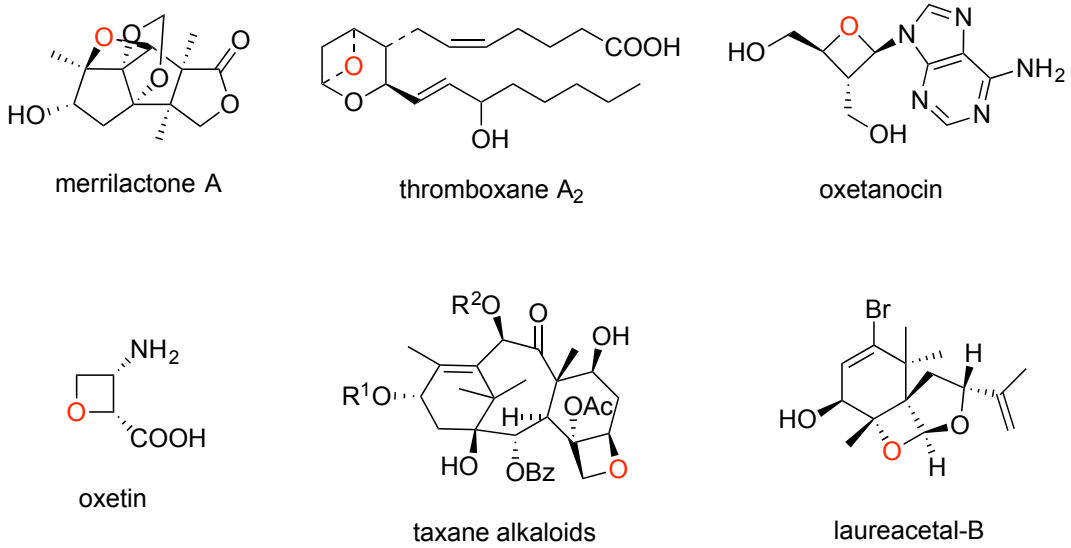

Figure 1. Biologically active compounds containing oxetane rings

Actually, as it is a forbidden process in most cases for the direct [2+2] oxetane formation using thermal reactions, the photochemical reaction (also called Paternò–Büchi reaction) is the most efficient approach for the synthesis of oxetane derivatives because of its good selectivity and

environmentally friendly character without using any other chemical addictive (Scheme 1). It is known that the oxetane could also be afforded from thermal reactions at the expenses of disadvantages that the side reactions, such as fragmentation reaction and elimination reaction, may occur using intramolecular cyclization (Williamson-type reaction)[4] and the ring-expansion reaction using epoxide could be restricted by the less substitution choices[5].

Scheme 1. Oxetane formation reactions

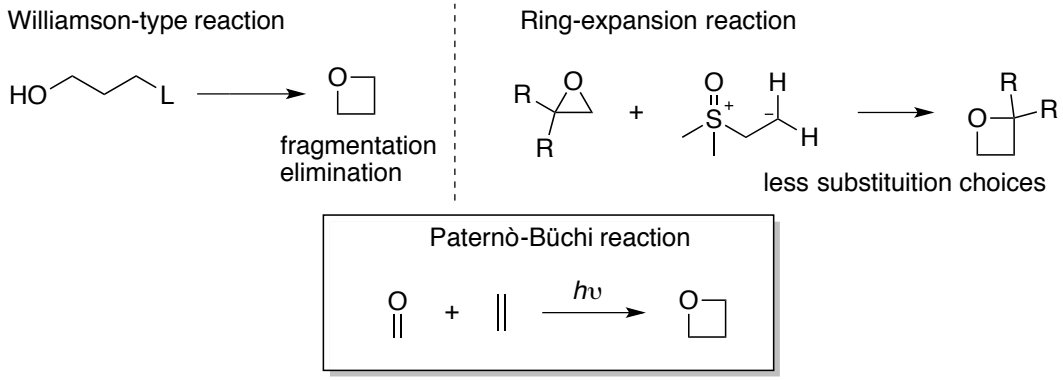

In photochemical reaction, the interaction of organic molecules and light occurs, thus some molecules will absorb one proton to a comparatively unstable state that is called “electronically excited state”. Instead of the direct interaction of the organic molecules in ground state in thermal reaction, organic photochemistry involves the process of excitation. Molecular orbital (MO) theory offers people an easier approach to understand the word “electronically” of “electronically excited state”. For abbreviation, the highest occupied orbital is called HOMO, and the lowest unoccupied orbital is called LUMO. Thus, after absorbing one photon, one electron located in HOMO would “jump” to LUMO that this molecule is in an “electronically excited state”. It is noted that not all of electronically excited state molecules will produce product, sometimes, they would return to the ground state instead. Besides, the ability of the excitation to electronically excited state will be largely depended on the absorption ability of the molecule on the wavelength of the irradiation resources.

The alteration of electron distribution among the molecular orbit makes it

important for providing new methods in organic synthesis. For example, the synthesis of racemic (±)-cedrene could be succeeded by only 4 steps from a chain skeleton molecule as photochemical reaction played as the key step for the cyclic building (Scheme 2).[6] Meanwhile, photochemists are also faced up with the great challenge to control regio- and stereoselectivity using photochemical synthesis.[1a] Despite people are still not fully acquired with the knowledge of photochemical organic reactions, many important findings have disclosed some rules by photochemists' efforts during the recent decade.

Scheme 2. Synthesis of (±)-cedrene

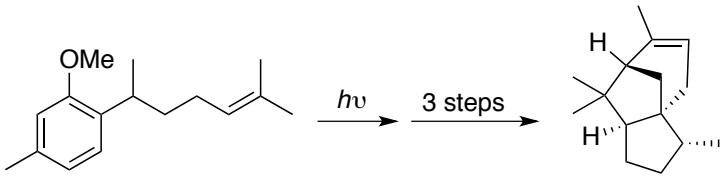

Furthermore, it is also not necessary to be worried about it that the photochemical organic synthesis could not be carried out in large scale.[7] For example, vitamin D3, the total synthesis of which involves the photochemical reaction as a key step, has been manufactured at the amount of several tons every year and the production plant is continuing to build.

1-2. Paternò–Büchi reaction

Carbon-carbon bond formation is an essential topic in the study on organic synthesis. Compared to heat energy, photo-energy is specifically efficient for the excitation of molecules, because the electronic configurations in the molecules will be largely altered under the photochemical irradiation. Paternò and Chieffi reported the first photochemical reaction for oxetane formation in 1909 using 104 days of sunlight irradiation.[8] Till 1954, the same reaction was carried out by Büchi and coworkers that it was the first time to confirm the structure of this photochemical product, oxetane.[9] These photochemical [2+2] cycloaddition reactions directly producing oxetanes were nominated as Paternò–Büchi reaction firstly by Yang in 1964 who explored the regioselectivity of this reaction.[10]

Many chemists have contributed their efforts to elucidate the mechanism of Paternò–Büchi reaction.[11] The intrinsic factor in Paternò–Büchi reaction is the alteration of electron distribution on the carbon oxygen double bond of the carbonyl compound after the carbonyl compound molecule absorbs one photon. The excited carbonyl molecular could be further stabilized by spin overturn (from singlet state to triplet state). This process is called inter system crossing (ISC) (including from triplet state to singlet state also).

Although there are still some ambiguous parts on the explanation of the Paternò–Büchi reaction mechanism, the generally accepted mechanism was shown in Scheme 3. The carbonyl compound will be excited to the singlet excited state under photolysis. As to the cases of aromatic carbonyl compounds, the singlet excited state could be transformed to the triplet excited state through the fast ISC process, because the spin-flip process is spin-allowed. Thus, the molecule in long-lived triplet excited state reacts with alkene to produce the triplet 1,4-diradical intermediate, upon which the singlet 1,4-diradical intermediate will be formed after the ISC process. Nevertheless, when it comes to aliphatic carbonyl derivatives or naphthaldehydes, the singlet 1,4-diradical intermediate could be obtained directly from the interaction of singlet excited state with alkene because of the comparatively long lifetime of singlet excited state. Finally, the singlet 1,4-diradical would give the target product oxetane or decompose to the starting materials. Moreover, it is necessary to notice that the regio- and

stereoselectivity of oxetane is largely depended on the energetic stability and conformation of the triplet 1,4-diradical intermediate.

Scheme 3. Mechanism of Paternò–Büchi reaction

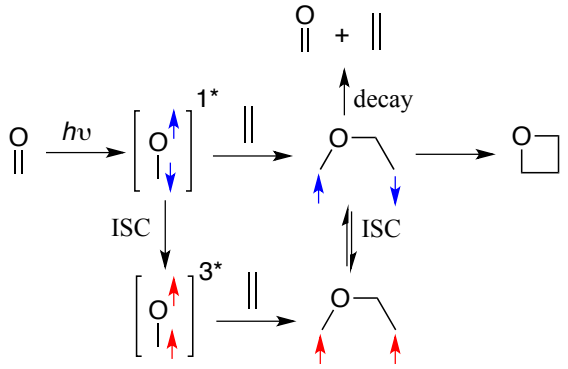

In the Paternò–Büchi reactions of carbonyl compounds with electron-rich alkenes, the photoinduced electron transfer (PET) may occur after excited to the triplet excited state (Scheme 4) when the energy of electron transfer process is spontaneous in the estimation equation based on Rehm–Weller equation: $\Delta G = E(D^+/D) - E(A/A^-) - \Delta E_{exc}$ (ΔG means the Gibbs energy of photoinduced electron transfer; $E(D^+/D)$ and $E(A/A^-)$ correspond to the donor and acceptor ground state potentials, respectively; ΔE_{exc} is the excitation energy between ground state and excited state of the reactant).[12] It could be explained by the interaction of the half-occupied n_p orbital of the oxygen atom in the triplet excited state of carbonyl compound and the HOMO of alkene. The PET induced triplet 1,4-diradical species may also decay to the starting material after ISC process (Scheme 4).

Scheme 4. Mechanism for Paternò–Büchi reaction through PET

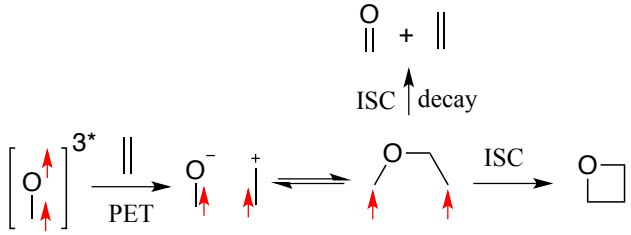

For example, the Paternò–Büchi reaction of naphthaldehyde and siloxyl

dihydrofuran derivative went through a PET process and the oxetane bicyclic product was obtained with excellent regio- and stereoselectivity (Scheme 5).[13]

Scheme 5. Paternò–Büchi reaction of naphthaldehyde and siloxyl dihydrofuran derivative

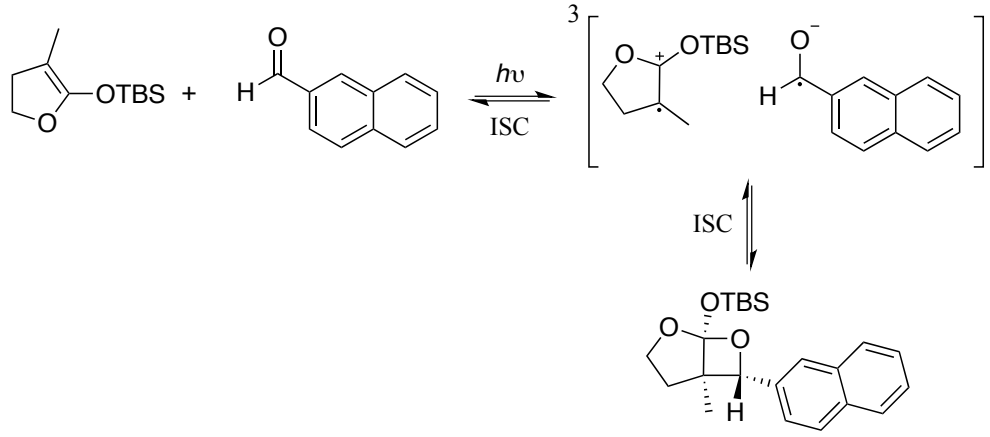

The mechanism is mainly decided by the redox potential of carbonyl compound and alkene. Thus, it is favored to form the radical pair when the energy of electron process is spontaneous.[14] Otherwise, the 1,4-diradical intermediate will be formed directly without PET process.

As is mentioned above, the electron distribution of carbonyl compounds will be tremendously changed under irradiation; therefore, the oxygen atom was altered from the nucleophilic character to the electrophilic character. Upon which, the first C-O bond formation mostly locates on the nucleophilic position of the alkene. Besides, the regio- and stereoselectivity of oxetane product is also largely determined by the conformers of following formed 1,4-diradical intermediates. Abe and his coworkers reported the regioselectivity study of the Paternò–Büchi reactions on the furan derivatives and aromatic compounds.[15] As is shown in Scheme 6, the ratio of photochemical [2+2] adducts, **F-OX1** to **F-OX2**, was 19:81 at 52°C and 42:58 at −76°C. **F-OX2** was more favorable product because the corresponding productive 1,4-diradical conformer is at lower energy and the conformers transformation could be suppressed in low temperature that

explained why the ratio was much more close to 1:1 in -76°C. Besides, higher quantum yield will be obtained at low temperature.

Scheme 6. Paternò–Büchi reaction of 3-methyl furan with benzaldehyde

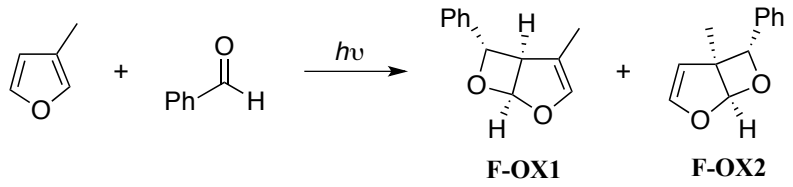

F-OX1 **F-OX2**

Temp.	**F-OX1**: **F-OX2**
52 °C	19 : 81
-76 °C	42 : 58

The stereoselectivity of oxetane formation from 1,4-diradical intermediate is depended on the geometry of 1,4-diradical intermediate influenced by the spin-orbit coupling (SOC) that is rationalized by Griesbeck *et al.* in 1990 (Scheme 7).[16] As shown in Scheme 7, the perpendicular orientation of two radical *p*-orbitals will accelerate the ISC rate to form the corresponding oxetane. This orbital orientation explained why the less thermally stable *endo* isomer was more favorable to be obtained, which is called "Griesbeck model". The conformational dependence of SOC in the 1,4-diradical (Griesbeck model) is also confirmed by computation in 2001 by Kutateladeze.[17]

Scheme 7. The Griesbeck model

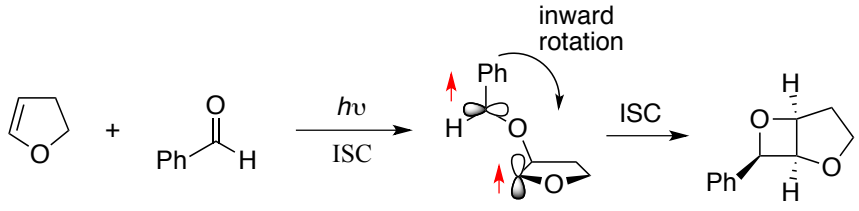

98%

1-3. Photochemical [2+2] cycloaddition reaction

Since Ciamician found the first intramolecular photochemical [2+2] cycloaddtition reaction of carvone (Scheme 8),[18] this synthetic method has been widely applied in organic synthesis.[19] Till now, photochemical [2+2] cycloaddition reaction has become one of the most frequently used and powerful methodologies in ring-formation reactions.

Scheme 8

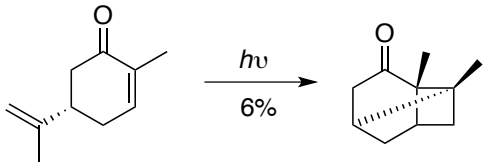

According to the summaries of several books, when it comes to the case of photochemical [2+2] cycloaddition reaction of enone and alkene, the mechanism was believed to go through a triplet excitation process.[20] After one photon absorption, the enone could be excited to singlet excited state by π-π* excitation instead of n-π* excitation in Paternò–Büchi reaction (Scheme 9). After ISC, the enone in triplet excited state could react with alkene to produce the triplet 1,4-diradical, which might give the final cyclobutane product after the ISC. It should be noted that each step is a reversible step that the some excited molecules will be quenched to the ground state.

However, the mechanism will become more straightforward in the photochemical [2+2] cycloaddition reaction of two alkenes. The singlet 1,4-diradical will be formed directly from the interaction of alkene in singlet excited state with another ground state alkene without ISC process (Scheme 10).[19h]

Scheme 9. General mechanism of photochemical [2+2] cycloaddition reaction of enone and alkene

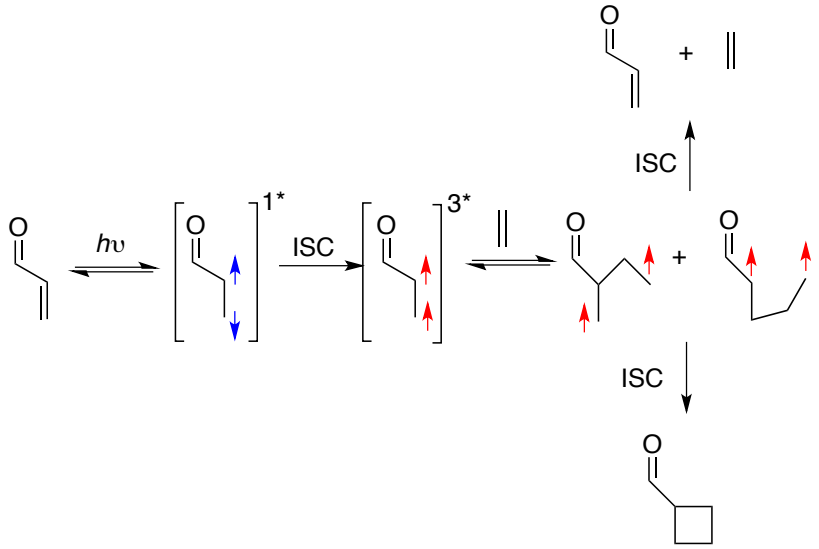

Scheme 10. General mechanism of photochemical [2+2] cycloaddition reaction of two alkenes

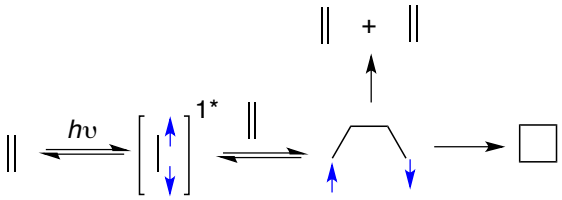

References

1. For reviews, see: (a) Ciana, C. L; Bochet, C. G. *Chimia*, **2007**, *61*, 650. (b) Hoffmann, N.; Gramain, J. C.; Bouas-Laurent, H. *Actual. Chim.* **2008**, *317*, 6. (c) Hoffmann, N. *Chem. Rev.* **2008**, *108*, 1052. (d) Bach, T.; Hehn, J. P. *Angew. Chem. Int. Ed.* **2011**, *50*, 1000.

2. (a) Bertolini, F.; Crotti, S.; Bussolo, V. D.; Macchia, F.; Pineschi, M. *J. Org. Chem.* **2008**, *73*, 8998. (b) Bull, J. A.; Croft, R. A.; Davis, O. A.; Doran, R.; Morgan, K. F. *Chem. Rev.* **2016**, *116*, 12150. (c) Burkhard, J. A.; Wuitschik, G.; Rogers-Evans, M.; Müller, K.; Carreira, E. M. *Angew. Chem. Int. Ed.* **2010**, *49*, 9052.

3. (a) Huang, J; Yokoyama, R.; Yang, C.; Fukuyama, Y. *Tetrahedron Lett.* **2000**, *41*, 6111. (b) Bhagwat, S. S.; Hamann, P. R.; Still, W. C. *J. Am. Chem. Soc.* **1985**, *107*, 6372. (c) Norbeck, D. W.; Kramer, J. B. *J. Am. Chem. Soc.* **1988**, *110*, 7217. (d) Kawahata, Y.; Takatsuto, S.; Ikekawa, N.; Murata, M.; Omura, S. *Chem. Pharm. Bull.* **1986**, *34*, 3102. (e) Miller, P. W. R.; Powell, R. G.; Smith, C. R. Jr. *J. Org. Chem.* 1981, 46, 1469. (f) Suzuki, T.; Kurosawa, E. *Chem. Lett.* **1979**, 301.

4. (a) Derick, C. G.; Bissel, D. W. *J. Am. Chem. Soc.* **1916**, *38*, 2478. (b) Allen, J. S.; Herbert, H. *J. Am. Chem. Soc.* **1951**, *56*, 1398. (c) Searles, S. Jr. *J. Am. Chem. Soc.* **1951**, *73*, 124. (d) Biggs, J. *Tedrahedron Lett.* **1975**, *16*, 4285. (e) Still, W. C. *Tedrahedron Lett.* **1976**, *17*, 2115. (f) Fischer, W.; Grob, C. A. *Helv. Chim. Acta*, **1978**, *61*, 2336. (g) Koell, P.; Schultz, J. *Tedrahedron Lett.* **1978**, *19*, 49. (h) Denmark, S. E. *J. Org. Chem.* **1981**, *46*, 3144. (i) Bats, J. P.; Moulines, J. *Tedrahedron Lett.* **1976**, *17*, 2249.

5. Okuma, K.; Tanaka, Y.; Kaji, S.; Ohta, H. *J. Org. Chem.* **1983**, *48*, 5133.

6. Wender, P. A.; Howbert, J. J. *J. Am. Chem. Soc.* **1981**, *193*, 688.

7. (a) Pape, M. *Pure Appl. Chem.* **1975**, *41*, 535. (b) Roloff, A.; Meier, K.; Riediker, M. **1986**, *58*, 1267. (c) Pfoertner, K. H. *J. Photochem. Photobiol. A.* **1990**, *51*, 81. (d) Braun, A. M. *Speciality Chemicals*, **1997**, *17*, 21.

8. Paternò, E.; Chieffi, G. *Gazz. Chim. Ital.* **1909**, *39*, 341.

9. Büchi, G.; Ihman, C. G.; Lipinsky, E. S. *J. Am. Chem. Soc.* **1954**, *76*, 4327.

10. Yang, N. C.; Nussim, M.; Jorgenson, M. J.; Murov, S. *Tetrahedron Lett.* 1964, **5**, 3657.

11. For reviews, see: (a) Porco, J. A.; Schreiber, S. L. *In Comprehensive Organic Synthesis*; Trost, M. M. *Ed*; Pergamon Press: New York, **1991**, *5*, 168. (b) Abe, M. *J. Chin. Chem. Soc.* **2008**, *55*, 479. (c) Abe, M. Formation of a 4-Membered ring: Oxetanes, in: *Handbook of Synthetic Photochemistry* (Eds: Albini), Wiley-VCH, **2010**, 217. (d) Fréneau, M.; Hoffman, N. *J. Photochem. Photobiol. C.* **2017**, *33*, 83.
12. Rehm, D.; Weller, A. *Isr. J. Chem.* **1970**, *8*, 259.
13. Abe, M.; Ikeda, M.; Shirodai, Y.; Nojima, M. *Tetrahedron Lett.* **1996**, *37*, 5901.
14. (a) Eckert, G.; Goez, M. *J. Am. Chem. Soc.* **1994**, *116*, 11999. (b) Bigot, B.; Devaquet, A.; Turro, N. J. *J. Am. Chem. Soc.* **1981**, *103*, 6.
15. Abe, M.; Kawakami, T.; Ohata, S.; Nozaki, K.; Nojima, M. *J. Am. Chem. Soc.* **2004**, *126*, 2838.
16. Griesbeck, A. G.; Stadtmüller, S. *J. Am. Chem. Soc.* **1990**, *112*, 1281.
17. Kutateladeze, A. G. *J. Am. Chem. Soc.* **2001**, *123*, 9279.
18. Ciamician, G.; Silber, P. *Ber. Dtsch. Chem. Ges*. **1908**, *41*, 1928.
19. For reviews, see: (a) Crimmins, M. T.; Reinhold, T. L. *Org. Reactions*, **1993**, *44*, 297. (b) Schuster, D. I.; Lem, G.; Kaprinidis, N. A. *Chem. Rev.* **1993**, *93*, 3. (c) Winkler, J. D.; Bowen, C. M.; Liotta, F. *Chem. Rev.* **1995**, *95*, 2003. (d) Bach, T. *Synthesis*, **1998**, 683. (e) Namyslo, J. C.; Kaufmann, D. E. *Chem. Rev.* **2003**, *103*, 1485. (f) Lee-Ruff, E.; Mladenova, G. *Chem. Rev.* **2003**, *103*, 1449. (g) Hehn, J. P.; Müller, C.; Bach, T. Formation of a Four-Membered Ring: From a Carbonyl-Conjugated Alkene, in: *Handbook of Synthetic Photochemistry* (Eds: A. Albini; M. Fagnoni) Wiley-VCH, **2010**, P171. (h) Poplata, S.; Tröster, A.; Zou, Y. -Q.; Bach, T. *Chem. Rev.* **2016**, *116*, 9748.
20. For books, see: (a) Gilbert, A.; Baggott, J. *Essentials of Molecular Photochemistry*; Blackwell: Oxford, **1991**. (b) Kopecký, J. *Organic Photochemistry: A Visual Approach*; VCH: Weinheim, **1992**. (c) Klań, P.; Wirz, J. *Photochemistry of Organic Compounds*; Wiley: Chichester, **2009**. (d) Turro, N. J.; Ramamurthy, V.; Scaiano, J. C. *Modern Molecular Photochemistry of Organic Molecules*; University Science Books: Sausalito, **2010**.

Chapter 2

Paternò–Büchi reactions of pyrrole derivatives with aromatic carbonyl compounds

2-1. Introduction

Pyrrole derivative is one of the basic aromatic compounds. Many bioactive compounds contain pyrrole rings such as Tolmetin, Atorvastatin, Sunitinib and Ketorolak with some specific medical use (Figure 1).

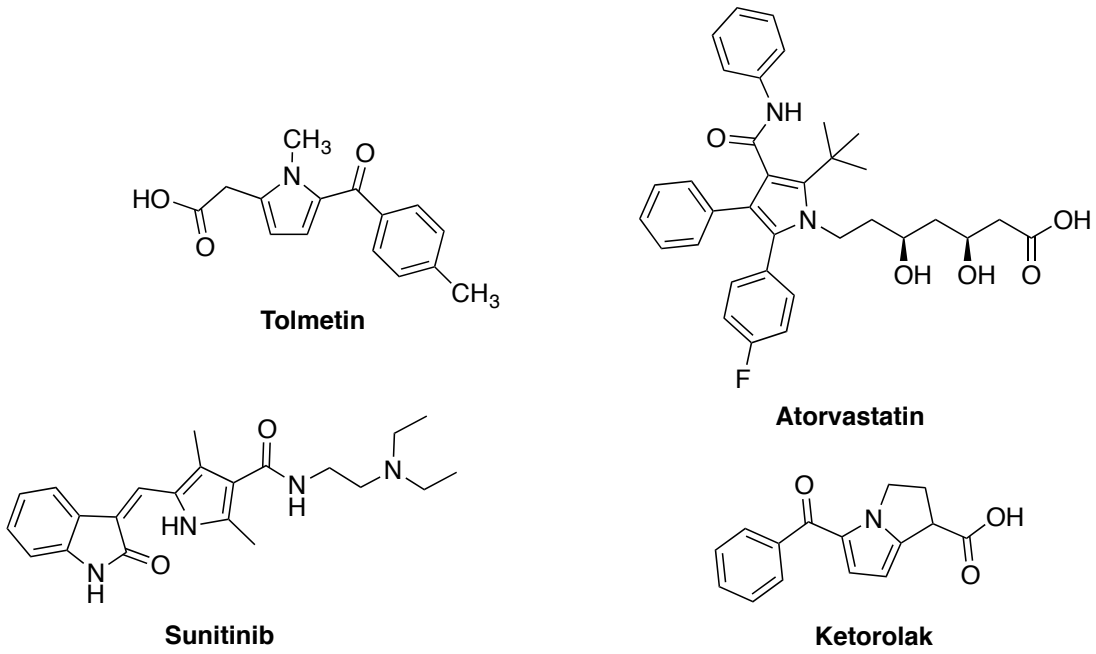

Figure 1. Examples of bioactive compounds contain pyrrole ring

Due to the nucleophilic character of pyrrole derivatives, Lewis acid promoted reactions using pyrrole derivatives were studied well in the past.[1] For example, the carbon-carbon bond formation would occur at more nucleophilic, Cα of pyrrole, when reacted with carbonyl chloride (Scheme 1).[2] The same rule could also be applied in the reaction of 2-siloxyl substituted pyrrole with benzophenone, the newly formed carbon-carbon bond was located at C5 of the pyrrole (Scheme 2).[3]

Scheme 1

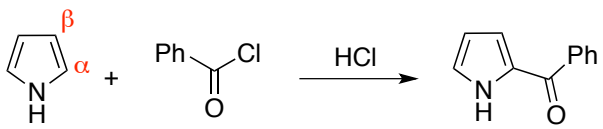

Scheme 2

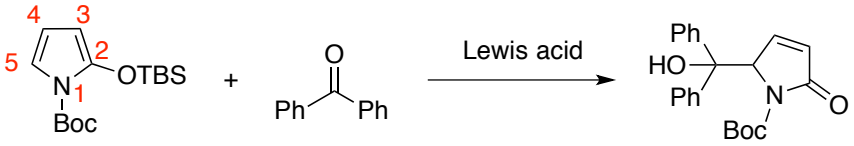

As is discussed in the Chapter 1, the substrates scope and mechanism study has been investigated in detail in the Paternò–Büchi reactions using furan derivatives.[4] Surprisingly, only a few reports have been published on Paternò–Büchi reactions of the pyrrole derivatives. The bicyclic oxetane has not been isolated because of the instability, though the following decomposed alcohol may imply that the pyrroly-oxetane probably formed as the intermediate (Scheme 3).[5]

Scheme 3

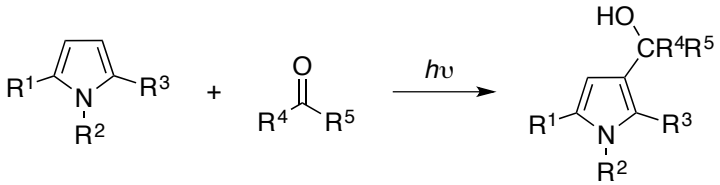

R^1, R^2, R^3, R^4 and R^5 are aliphatic carbon groups

In this chapter, the bicyclic oxetanes **4ba** and **4ca** (X = NBoc and R^1 = OSi^{t}BuMe$_2$(OTBS) or OSi^{t}BuPh$_2$ (OTBDPS)) were isolated in high yields from the regioselective Paternò–Büchi reaction of 2-siloxy-1*H*-pyrrol derivatives **1b** and **1c** with benzophenone **2a** (Scheme 4). The oxetanes **4** are potential precursors for synthetically important pyrrol-2-one derivatives, i.e., γ-lactams **5b** (X = NBoc). The introduction of substituents at the C3 position of pyrrol-2-one is possible using the photochemical PB reaction of 2-siloxypyrrole derivatives with carbonyl compounds. Conversely, the Lewis-acid-induced coupling reaction is known to selectively afford the C5-substituted γ-lactams **6** (X = NR).[3, 6]

Scheme 4. Comparison of the photochemical Paternó-Büchi (PB) reaction and Lewis-acid-promoted reaction of furan or pyrrole derivatives with carbonyl compounds

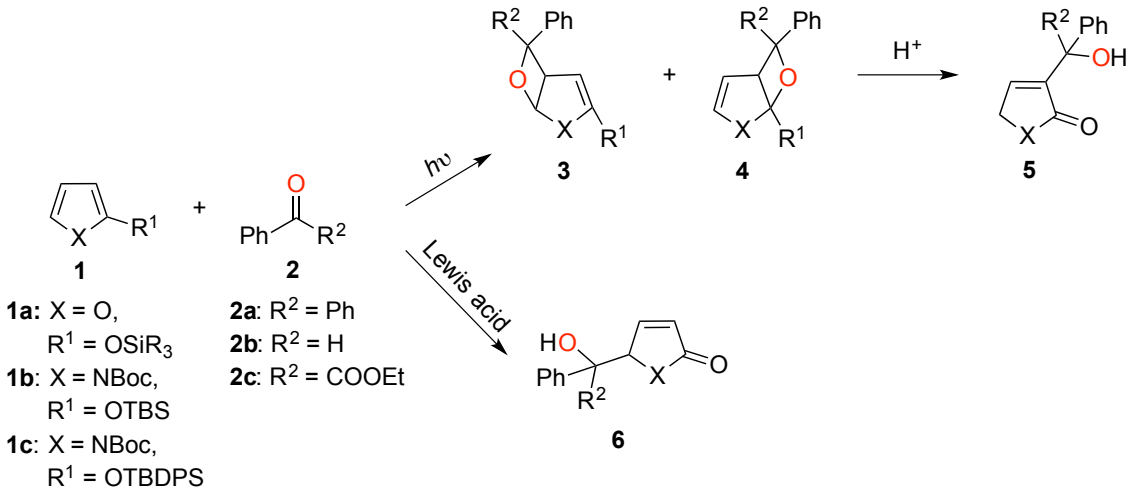

1a: X = O, $R^1 = OSiR_3$
1b: X = NBoc, R^1 = OTBS
1c: X = NBoc, R^1 = OTBDPS

2a: R^2 = Ph
2b: R^2 = H
2c: R^2 = COOEt

2-2. Results and discussion

The 2-siloxypyrrole derivatives **1b** and **1c** were prepared according to previously reported methods.[3] First, the photochemical reaction of **1b** (0.49 M) with benzophenone **2a** (0.33 M) was carried out in a sealed nuclear magnetic resonance (NMR) tube in C_6D_6 under nitrogen. After 1.5 h irradiation with a 365-nm light-emitting diode (LED) at 25 °C, new signals at ca. δ 7.4, 6.2, 4.4, and 4.0 ppm were clearly observed, with a concomitant decrease of the benzophenone signals at δ ca. 7.8 ppm, as shown by comparing Figure 2c with 1e. After the solvent was removed under reduced pressure, the major product responsible for the new signals was isolated using gel permeation chromatography (GPC).

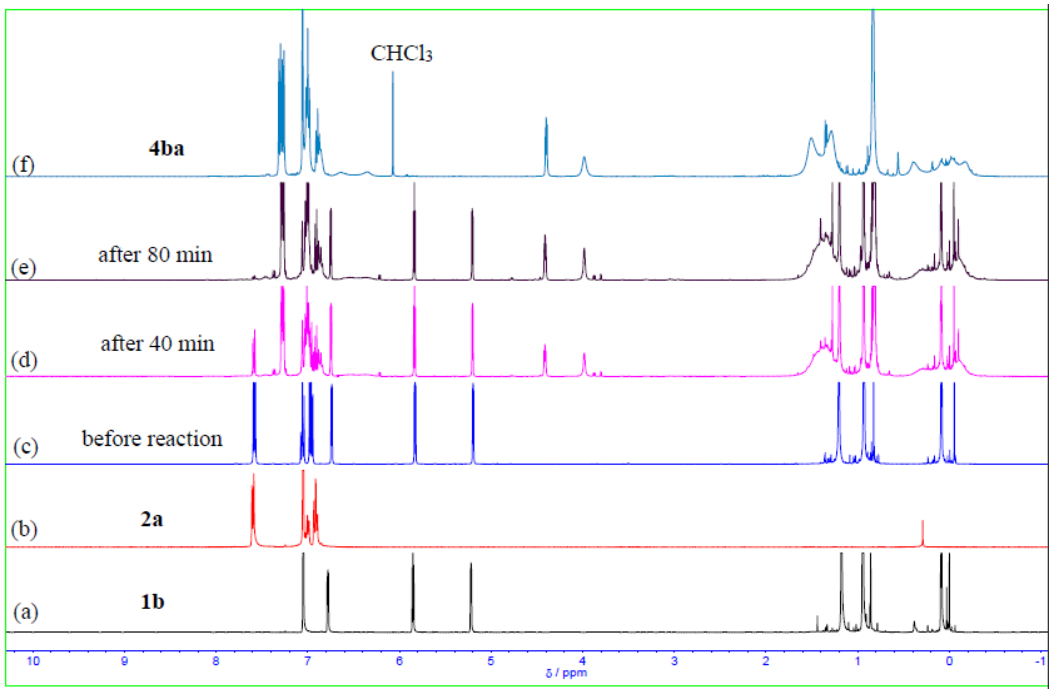

Figure 2. ^{1}H NMR (400 MHz, C_6D_6) spectroscopic analysis of the photochemical reaction of **1b** with **2a** under irradiation at 365 nm (a) **1b**, (b) **2a**, (c) before photolysis at 25 °C, (d) after 40 min irradiation at 365 nm, (e) after 80 min irradiation at 365 nm, and (f) isolated **4ba**

The 1D- and 2D-NMR (^{1}H, ^{13}C, H-H COSY, H-C HSQC, and H-C HMBC) data and mass spectroscopic analysis confirmed that the major

product was the bicyclic oxetane 1-siloxy-6,6-diphenyl-7-oxa-2-azabicyclo -[3.2.0]hept-3-ene **4ba**. In the 2D-NMR analyses, the two vinyl protons and one aliphatic proton are assigned as H_a (δ 6.31 ppm), H_b (δ 4.81 ppm), and H_c (δ 4.15 ppm), respectively. As shown in Figures 3 and 4, H_b was correlated with both H_a and H_c in the H-H COSY spectrum, and the protons H_a, H_b, and H_c were correlated with the carbons at δ ca. 133.5, 103.4, and ca. 60.8 ppm, respectively, in the H-C HSQC spectrum. The regioisomer **3ba** contains one vinyl proton and two aliphatic protons; thus, the observed NMR spectra do not correspond to compound **3ba**. Furthermore, in the H-C HMBC spectrum (Figure 5), the correlation of H_c with the quaternary carbons in phenyl rings C_d (146.1 ppm) was observed; thus the formation of **7ba** may also be discounted.

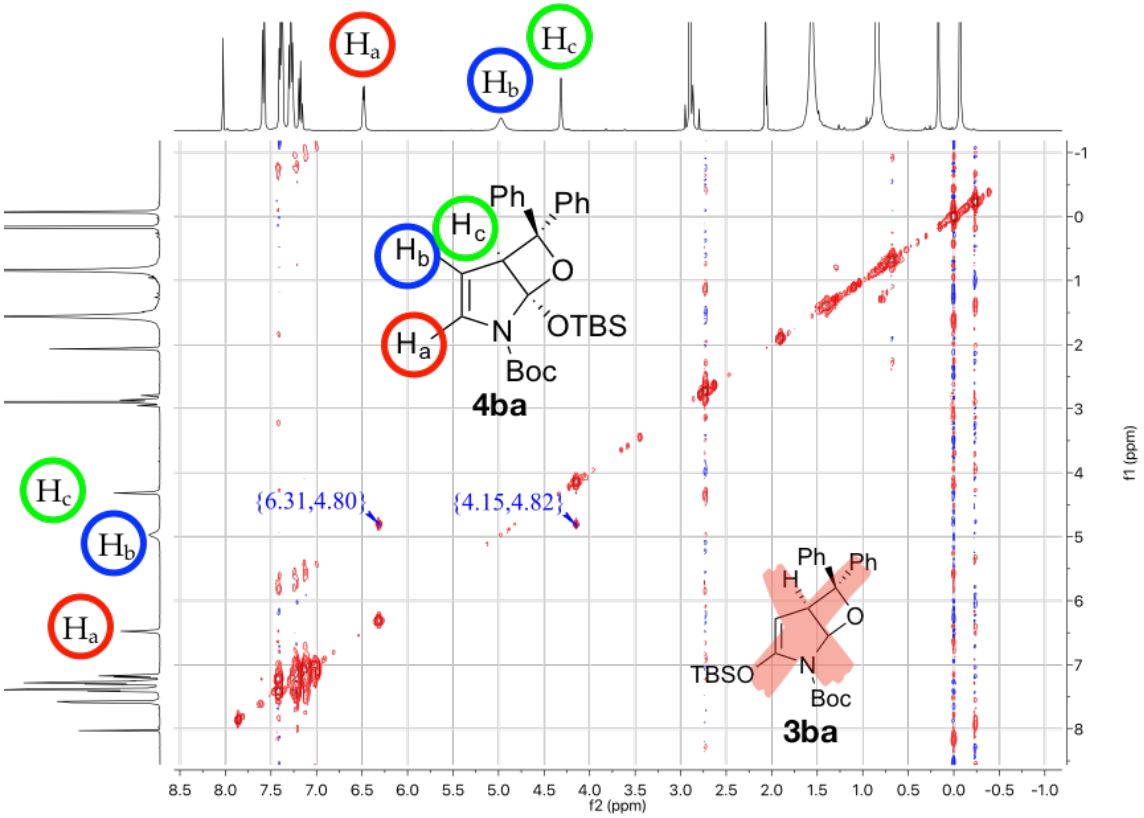

Figure 3. H-H COSY spectrum of **4ba** (Acetone-d_6)

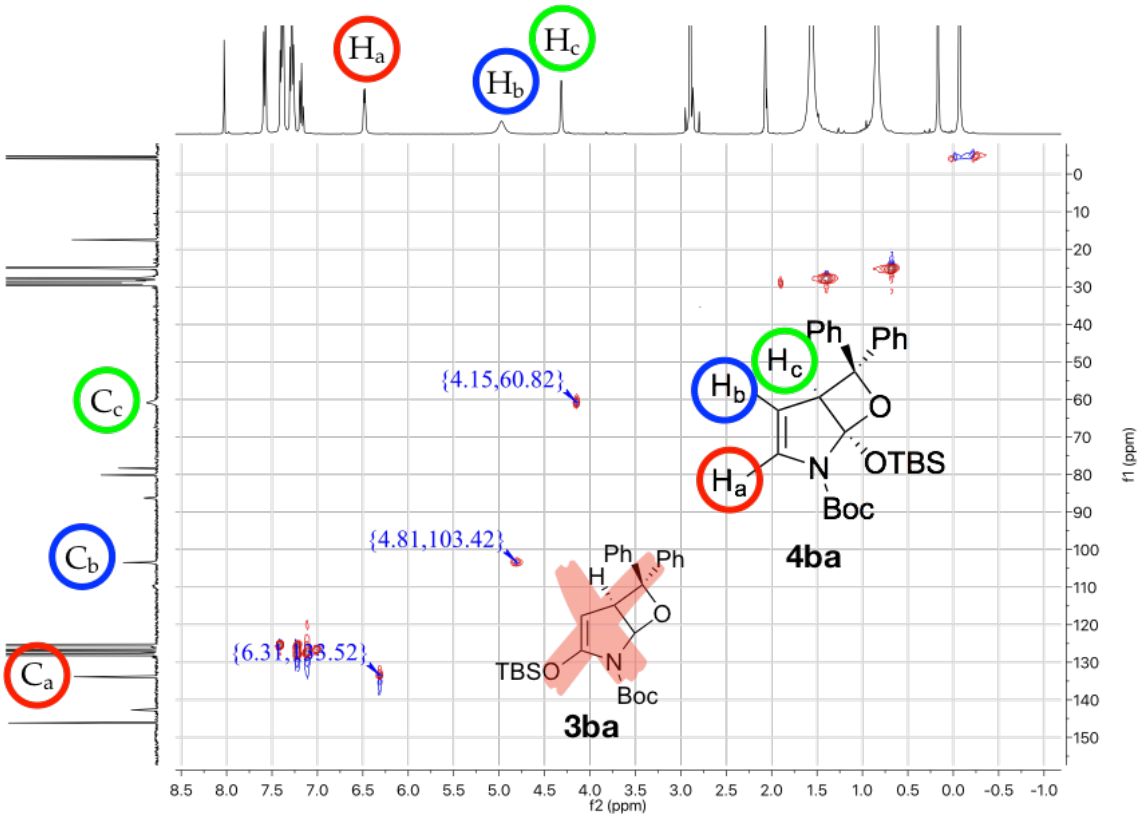

Figure 4. H-C HSQC spectrum of **4ba** (Acetone-d_6)

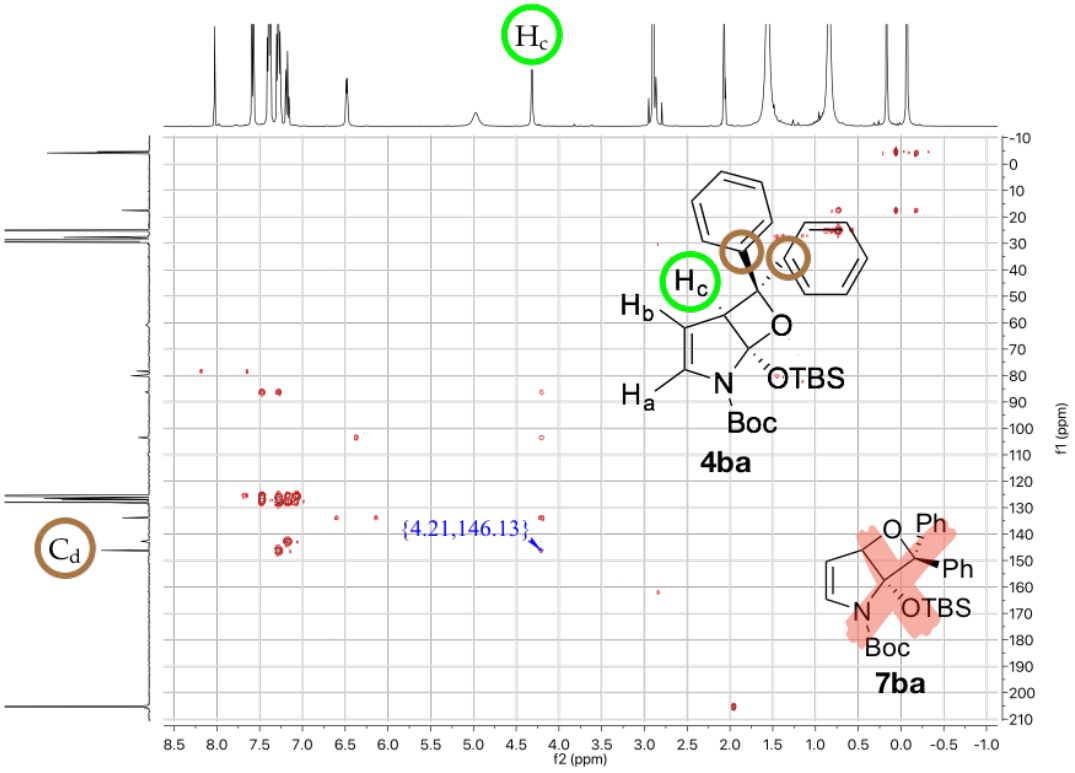

Figure 5. H-C HMBC spectrum of **4ba** (Acetone-d_6)

The reaction conditions were then optimized to obtain the synthetically important bicyclic oxetane **4ba** in high yield (Table 1). First, the optimum ratio of the two starting materials was explored (entries 1–4). The yield was low when the ratio was 1:1 (entry 4), probably because the bicyclic oxetane formed in the PB reaction was more reactive towards benzophenone than the starting pyrrole.[5a] The yield was largely unchanged when the reaction was performed at both high and low temperatures (entries 5–7). Thus, using **1a** and **2a** at a molar ratio of 1.5:1 under 365-nm irradiation at room temperature was decided to be the optimized condition for the PB reaction.

Table 1. Optimization of the reaction conditions for the PB reaction of **1b** with **2a**[a]

Entry	Temp (°C)	Reactant ratio (pyrrole **1b**:BP **2a**)	Yield[b] of **4ba**
1	25	3:1	92%
2	25	2:1	89%
3	25	1.5:1	86%
4	25	1:1	53%
5	−20[c]	1.5:1	79%
6	−78[c]	1.5:1	83%
7	60	1.5:1	82%

[a] Benzene was used as the reaction solvent using an LED lamp at 365 nm for 1.5 hours; [b] Isolation yield after GPC; [c] Toluene was used as the solvent.

The regioisomer **3ba** was not isolated from the reaction mixture, although the signals at δ ca. 3.8, 3.9, and 6.2 ppm seem to be attributed to **3ba** (Table 2, Figure 6). Thus, highly selective formation of **4ba** was observed in the PB reaction of **1b**, similarly to the high regioselectivity of the PB reaction of furan derivative **1a**.[7]

Table 2. Product ratio of **3ba** and **4ba**

Entry	Temp/^{o}C	Reactant ratio[a] (**3ba** : **4ba**)
1	-78	1 : 10
2	-20	1 : 19
3	25	1 : 22
4	60	1 : 69

[a]The ratio was calculated by the NMR integration.

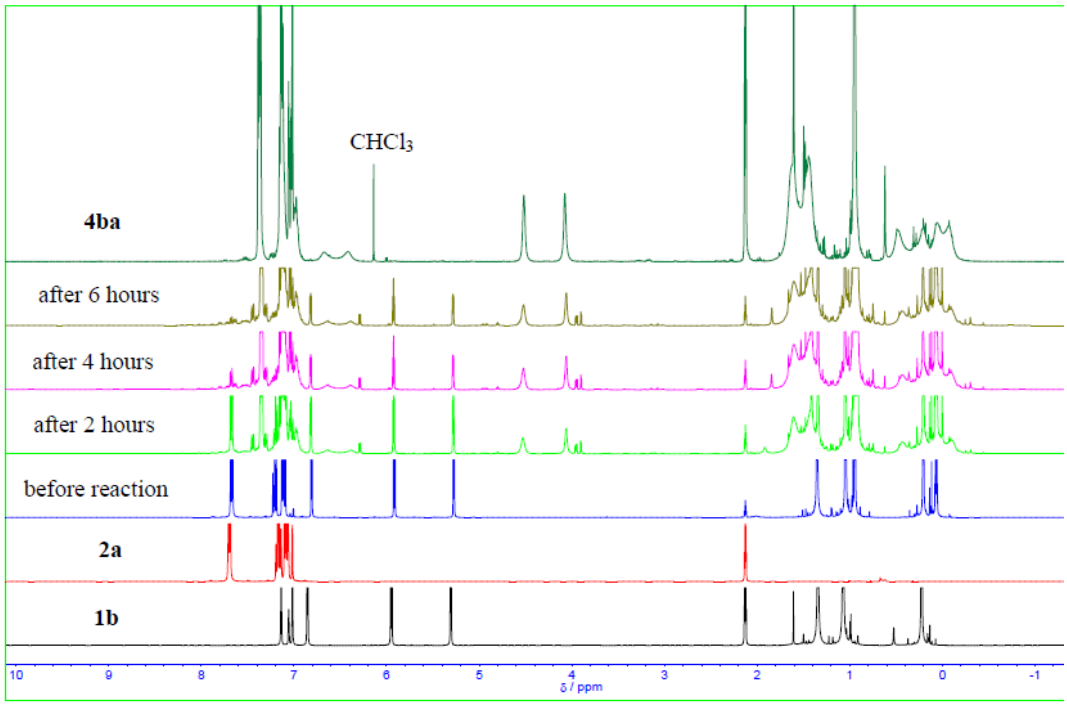

Figure 6. ^{1}H NMR (400 MHz, Toluene-d_8) spectroscopic analysis of the photochemical reaction of **1b** with **2a** under irradiation at 365 nm in -78 ^{o}C

Even when the more bulky siloxyl group was introduced to the pyrrole ring, the expected isomer **4ca** (X = NBoc, R^1 = OTBDPS, and R^2 = Ph) was obtained in good yield (84%) (Figure 7). The photochemical reaction of **1b** with **2b** or **2c** afforded a complex mixture of products; thus, the stereoselectivity of this PB reaction was not determined (Figures 8 and 9).

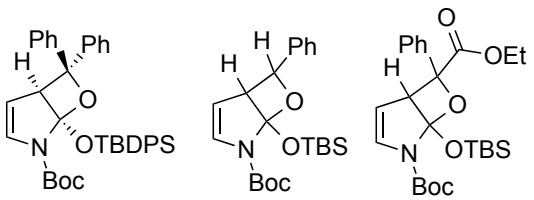

Figure 7. Scope and limitations of the PB reaction

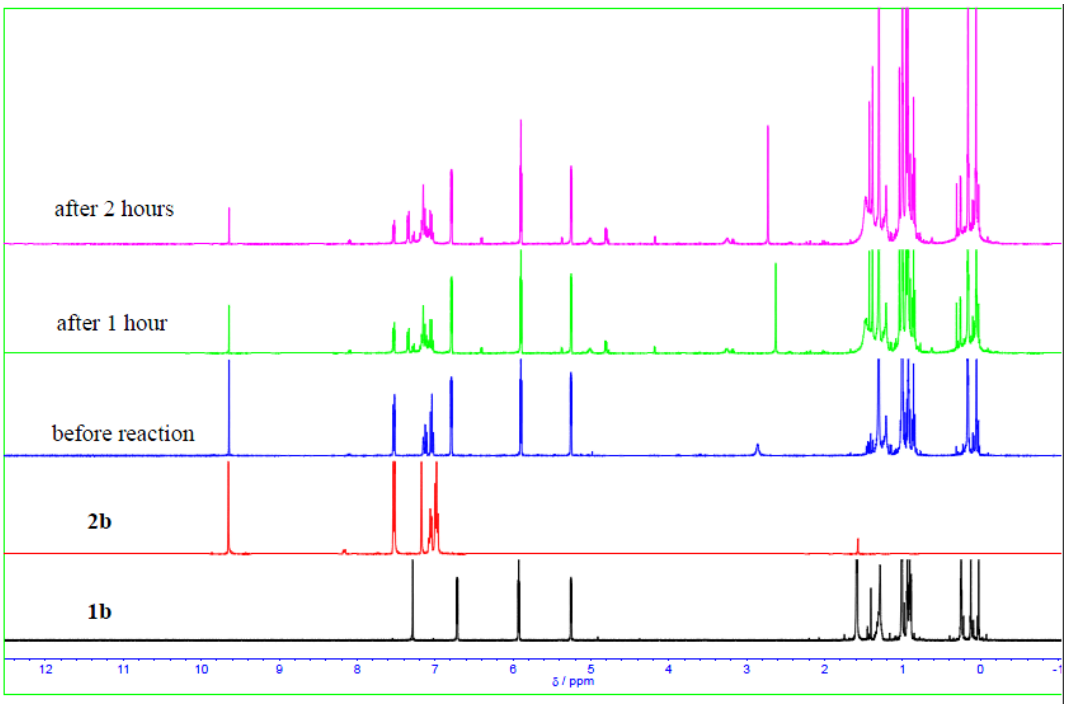

Figure 8. ^{1}H NMR (400 MHz, C_6D_6) spectroscopic analysis of the photochemical reaction of **1b** with **2b** under irradiation at 365 nm in 25 ^{o}C

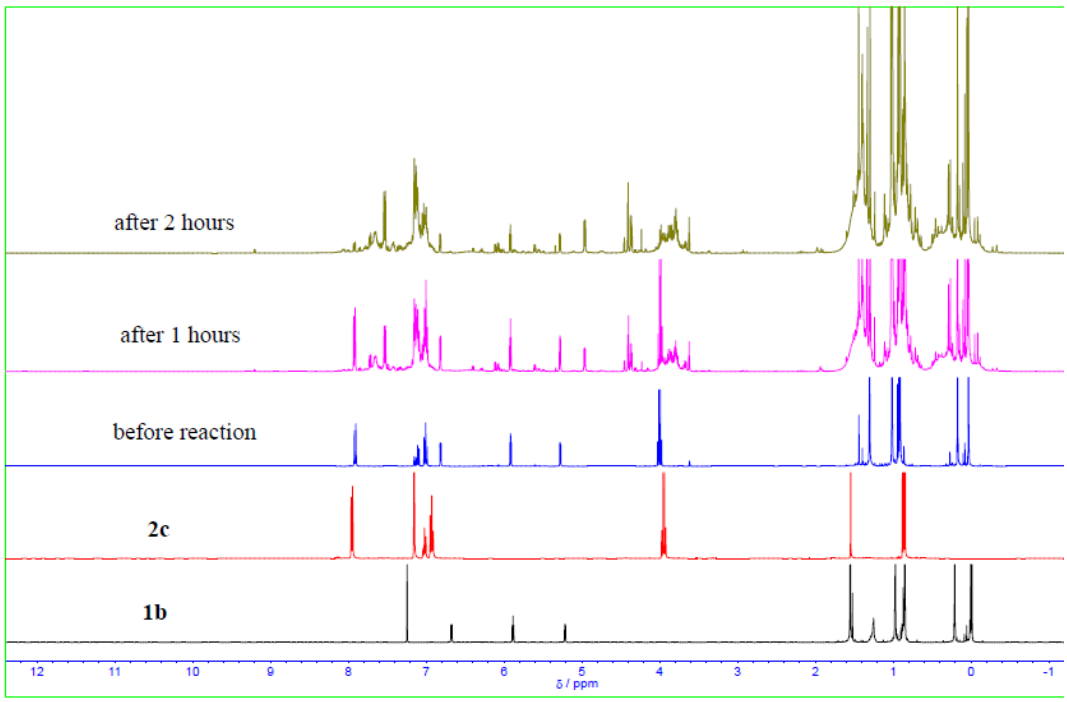

Figure 9. ^{1}H NMR (400 MHz, C_6D_6) spectroscopic analysis of the photochemical reaction of **1b** with **2c** under irradiation at 365 nm in 25 °C

According to UV-absorption spectrum of **1b** and **2a**, **1b** had much less absorption than **2a** that can be neglected (Figure 10). To obtain information about the reaction mechanism for the selective formation of **4ba**, the quenching rate constant k_q of triplet-state benzophenone (^{3}**2a**) monitored at λ_{max} 535 nm by **1b** was first determined by Stern–Volmer analysis using laser flash photolysis (LFP) experiments, where $k_{obs}/k_d = 1 + (k_q/k_d)$[**1b**] (Figures 11 and 12). As shown in Figure 11, the lifetime of the transient ^{3}**2a*** was significantly reduced in the presence of **1b**. From the Stern–Volmer plot (Figure 12), the value of k_q was determined to be 2.95×10^9 M^{-1} s^{-1} by plotting k_{obs} as a function of [**1b**]. The quenching rate constant of ^{3}**2a** in the presence of **1b** (= 0.49 M) is 1.45×10^9 s^{-1}. The decay rate constant k_d of ^{3}**2a** itself is known to be ca. 1.6×10^5 s^{-1}. The quantum yield (Φ) of the quenching process of ^{3}**2a** by **1b** was calculated to be ca. 1.0. However, Φ for the formation of **4ba** was determined to be 0.02, which was much smaller than that for ^{3}**2a*** (ca. 1.0). The quantum yield was measured by the

photoreduction of potassium ferrioxalate (Hatchart-Parker actinometer).[8]

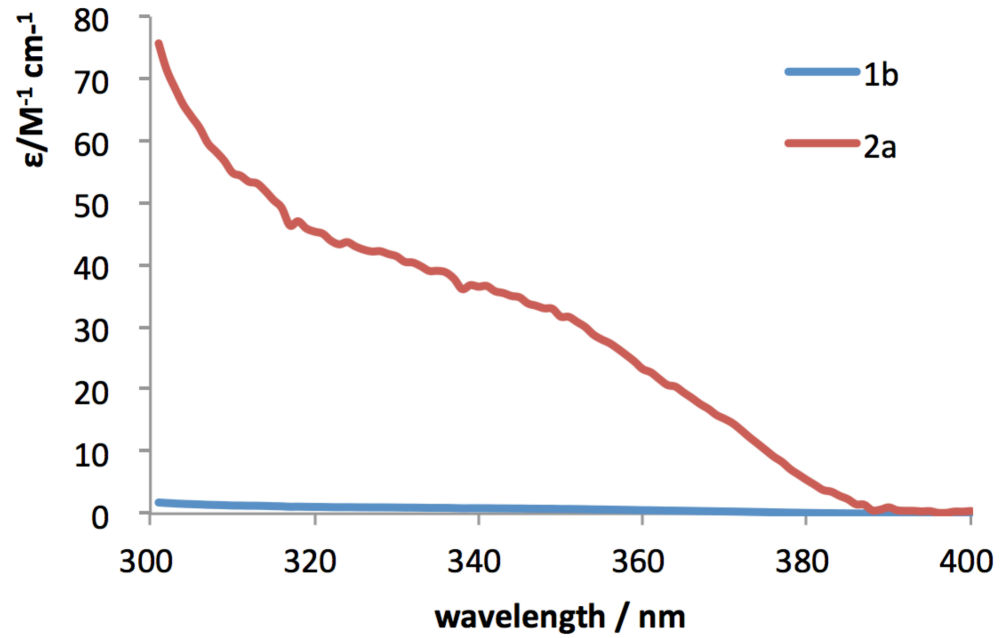

Figure 10. UV-absorption spectrum of **1b** (8.4 mM) and **2a** (0.34 mM) in benzene

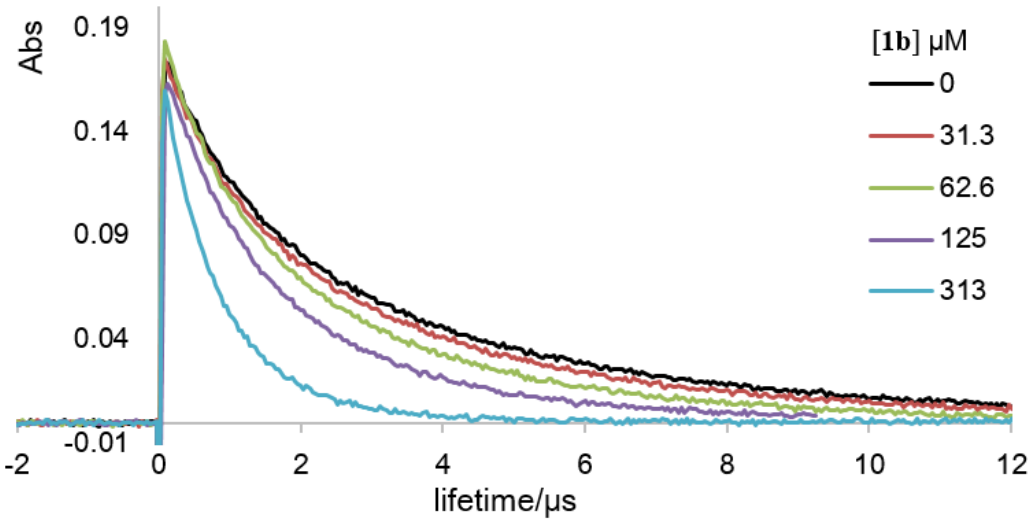

Figure 11. Decay curves of ^{3}**2a*** at 535 nm, which was generated by 355-nm laser flash photolysis in degassed benzene solution in the presence of [**1b**] at room temperature

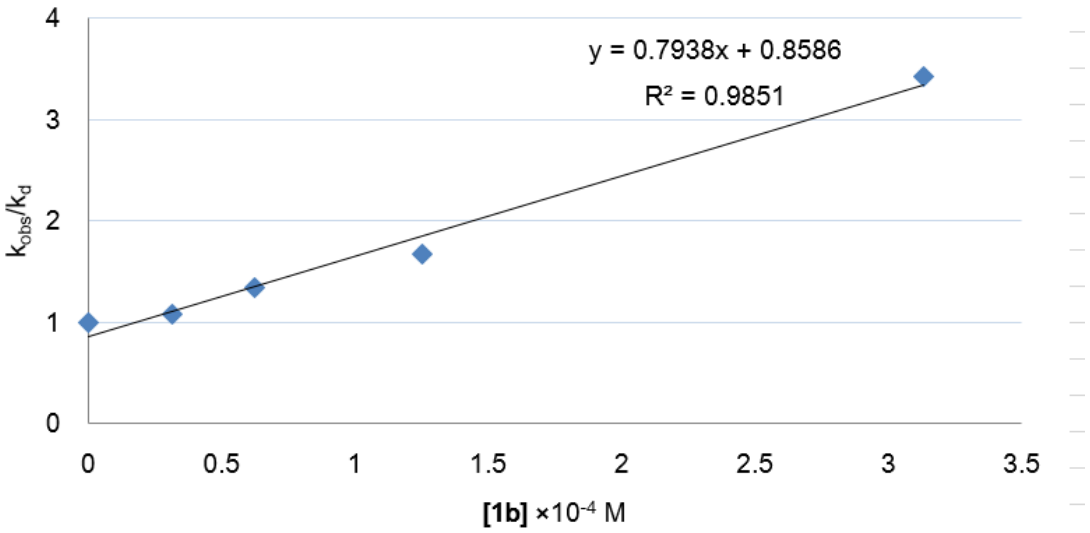

Figure 12. The Stern–Volmer plot ($k_{obs}/k_d = 1 + k_q/k_d$[**1b**]) for the quenching reaction of ^{3}**2a*** by **1b** in degassed benzene at room temperature

Based on the quenching rate constant for ^{3}**2a*** and the quantum yield of the production of **4ba**, a plausible mechanism for the selective formation of **4ba** is proposed, as shown in Scheme 5. Upon excitation of **2a**, the long-lived triplet excited state of benzophenone ^{3}**2a*** is generated after the fast intersystem crossing (ISC, k_{ISC} = ca. 10^{12} s^{-1}) from the singlet excited state of **2a**. The electrophilic ^{3}**2a*** adds to the nucleophilic C2 and C5 carbon of the pyrrole to give the triplet 1,4-diradical intermediates T-**DR3** and T-**DR4**, which are the precursors of oxetanes **3ba** and **4ba**, respectively. There are three possible conformers in each of the triplet diradicals, i.e., inside gauche (ig), outside gauche (og), and outside anti (oa) conformers. The ig and og conformers produce the oxetane products **3ba** and **4ba** and the starting materials after ISC, while the oa conformer produces only the staring materials **1b** and **2a**. According to our previous findings on the PB reaction of furan derivatives **1a**,[9] the population of the productive conformers ig and og among all the conformers determines the product selectivity, i.e., **3ba**:**4ba**, if there is no difference in the relative rate constants in the ISC, bond-formation, and bond-breaking processes (Equation 1).

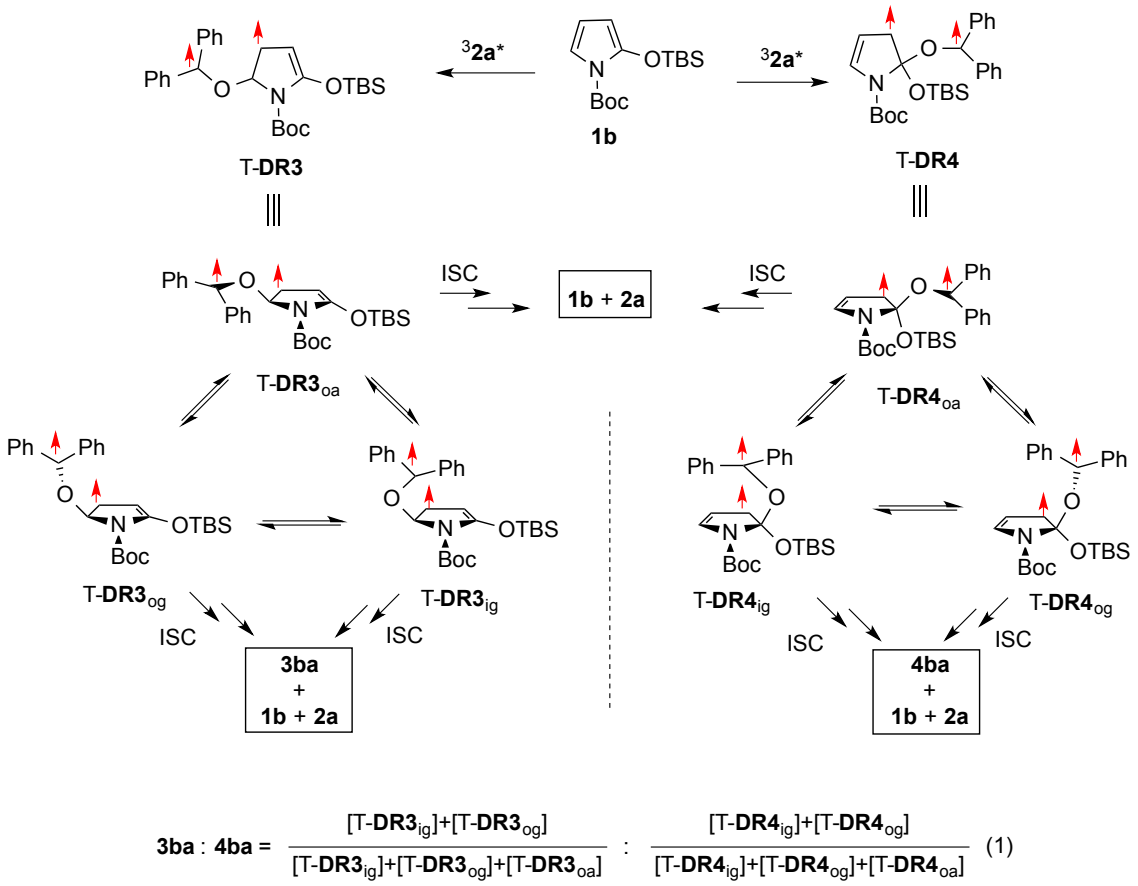

$$\mathbf{3ba} : \mathbf{4ba} = \frac{[\text{T-DR3}_{ig}]+[\text{T-DR3}_{og}]}{[\text{T-DR3}_{ig}]+[\text{T-DR3}_{og}]+[\text{T-DR3}_{oa}]} : \frac{[\text{T-DR4}_{ig}]+[\text{T-DR4}_{og}]}{[\text{T-DR4}_{ig}]+[\text{T-DR4}_{og}]+[\text{T-DR4}_{oa}]} \quad (1)$$

Scheme 5. Proposed mechanism for the selective formation of **4ba**

To gain more insight into the mechanism, the potential energy surfaces (PESs) around the dihedral angle θ° were calculated for the model triplet diradicals T-**DR3′** (X = NCO_2Me, X = OTMS) and T-**DR4′** (X = NCO_2Me, X = OTMS) at the UB3LYP/6-31G(d)[10] level of theory in the GAUSSIAN 09[11] suite of programs (Figure 13). The two energy-minimum structures, i.e., oa (θ = ca. 150°) and og (θ = ca. 320°) conformers, were found on the PESs. The oa conformers T-$\mathbf{DR3}_{oa}$′ and T-$\mathbf{DR4}_{oa}$′ would reform the starting compounds after ISC. Conversely, the og conformers T-$\mathbf{DR3}_{og}$′ and T-$\mathbf{DR4}_{og}$′ can be transformed into the oxetane products.

It should be noted that the productive conformer T-$\mathbf{DR4}_{og}$′ was calculated to be more stable than the unproductive conformer T-$\mathbf{DR4}_{oa}$′ by ca. 2.4 kcal mol^{-1} (Figure 13). However, the productive conformer T-$\mathbf{DR3}_{og}$′ was calculated to be less stable than the unproductive conformer T-$\mathbf{DR3}_{oa}$′

by ca. 2.0 kcal mol^{-1}. The energy barriers between the two conformers are less than 2.5 kcal mol^{-1}, indicating that the two conformers fully equilibrate even at low temperatures. Thus, the population of the productive conformer T-**DR4**$_{og}$′ is higher than that of the unproductive conformer T-**DR4**$_{oa}$′ in the T-**DR4′** regioisomer, while the population of the unproductive conformer T-**DR3**$_{oa}$′ is higher than that of the productive conformer T-**DR3**$_{og}$′ in the T-**DR3′** regioisomer. The computational results are consistent with the selective formation of **4ba** derived from the triplet diradical T-**DR4**. However, the lower quantum yield for the formation of **4ba** (0.02) than that of the ^{3}**2a*** quenching process (1.0) is not currently fully understood, because the selective formation of the productive conformer T-**DR4**$_{og}$ should give a high quantum yield of **4ba**.

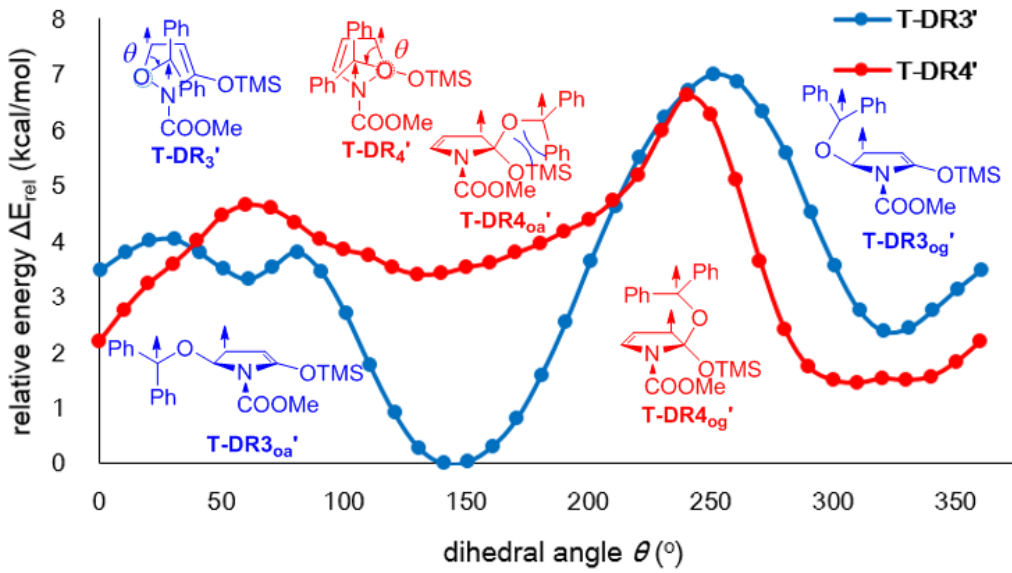

Figure 13. PES analyses around the dihedral angle (θ°) of diradicals T-**DR3′** and T-**DR4′**. The energies, ΔE_{rel} in kcal mol^{-1}, are relative to the most stable conformer T-**DR3**$_{oa}$′.

To obtain information about the energy barriers for the reaction of ^{3}**2a*** with **1b**, the PES for the bond formation process of ^{3}**2a*** with the pyrrole derivative was computed (Figure 14). The barrier-less processes for the formation of diradicals T-**DR3′** and T-**DR4′** was calculated, indicating that

there is no regioselectivity in the step during which the triplet state benzophenone ^{3}**2a*** adds to the pyrrole **1b** (Scheme 5). Thus, the triplet diradicals T-**DR3** and T-**DR4** should be equally formed in the reaction of ^{3}**2a*** with **1b**. Most of the resulting T-**DR3** returns to the starting compounds **2a** and **1b** after ISC, because the unproductive conformer T-**DR3**$_{oa}$ is the most stable. That is why the quantum yield for the formation of **4ba** is much lower than unity.

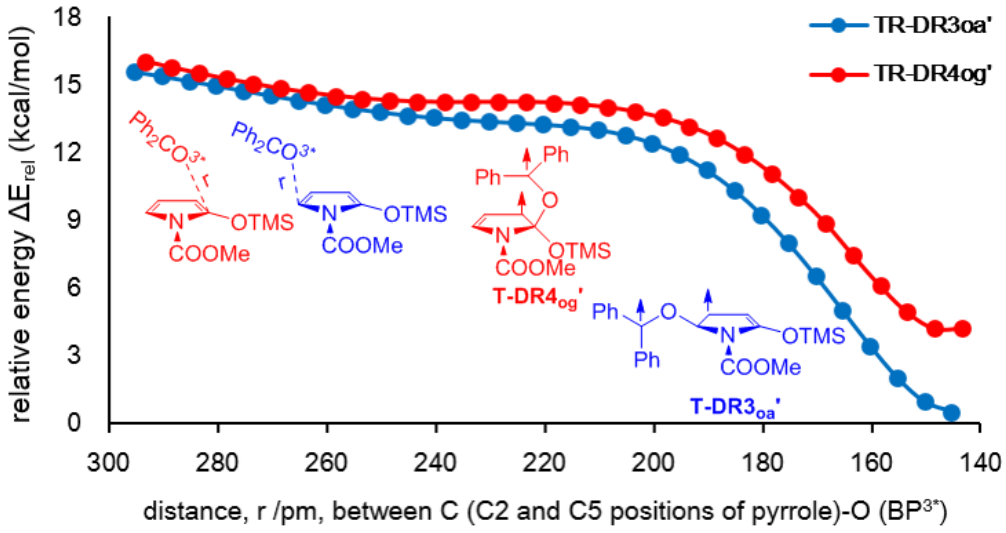

Figure 14. PES analyses of the distance r (pm) of the pyrrolic C2 and C5 to the O of **2a**. The energies, ΔE_{rel} in kcal mol^{-1}, are relative to the most stable diradical T-**DR3′**$_{oa}$.

In this chapter, the Paternò–Büchi reaction of 2-siloxy-substituted pyrrole derivatives **1** to obtain synthetically useful bicyclic oxetanes was investigated. The highly regioselective formation of **4ba** in high isolation yield was achieved for the first time via the reaction of benzophenone with **1b**. The quantum yield for the formation of **4ba** was determined to be 0.02. Product analysis and quenching experiments indicated the formation of the intermediary triplet diradicals T-**DR3** and T-**DR4**, and quantum chemical calculations on the model diradicals T-**DR3′** and T-**DR4′** provided a reasonable mechanism for the regioselective formation of **4ba** in the Paternò–Büchi reaction of **1b** with **2a**.

2-3. Experimental section

All the reagents and solvents were obtained at reagent grade and used without further purification. Thin layer chromatography (TLC) analysis was performed on silica gel plates and imagined under ultraviolet light. ^{1}H NMR and ^{13}C NMR data were recorded with a 400 MHz NMR spectrometer (Bruker Magnet System 400'54 system). Toluene-d_8, acetone-d_6, C_6D_6 and $CDCl_3$ (0.03% TMS) were used as deuterated solvents. Chemical shifts were described in parts per million (ppm) relative to trimethylsilane (δ = 0.00 ppm), and the coupling constants (J) were stated in Hertz (Hz). High-resolution mass spectroscopic (HRMS) analyses were conducted using an Orbitrap XL instrument using the positive ion mode. UV spectra were obtained by SHIMADZU UV-3600 Plus. The photochemical reactions were carried out using the LED lamp *Awill* manufactured by ARK TECH incorporation. An Nd:YAG laser producing 4–6 ns pulses of up to 7 mJ at 355 nm served as the excitation source for the LFP system. The monitoring system comprised a 150-W Xe lamp as the light source, a UNISOKU-MD200 monochromator, and a photomultiplier. The geometries of the stationary species and transition states were all computationally located and the vibrational analyses were performed with the Gaussian 09 suite program.

The synthesis route to **1b** was carried out according to the literature (Scheme 6).[3]

Scheme 6. The synthesis route to **1b**

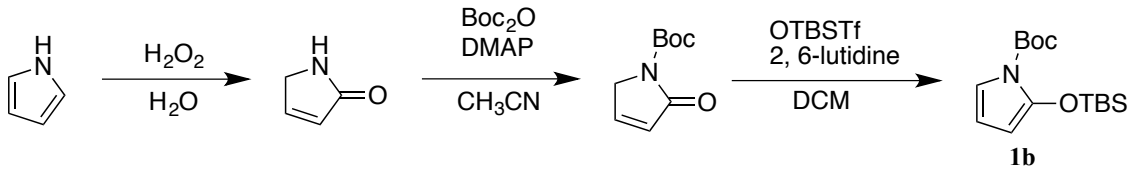

1b

1,5-Dihydro-2*H*-pyrrol-2-one

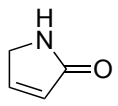

To a round-bottomed flask fitted with a magnetic stir bar were sequentially added pyrrole (10.4 mL, 150 mmol), $BaCO_3$ (3 g, 15 mmol), H_2O (450 mL), and 35% H_2O_2 (22 mL) at room temperature. The resulting reaction mixture was refluxed by heating with a thermal mantle for 4 h, after which time PbO_2 was carefully added until complete disappearance of effervescence. The mixture was filtered through filter paper and the (still hot) water solvent removed under reduced pressure using rotary evaporation to give a dark-red residue. The residue was picked up with 1,4-dioxane (50 mL × 2) and vigorously stirred for 10 min. The mixture was filtered through filter paper and the residue was subjected to the same operation two times again. The orange filtrates were combined and concentrated under reduced pressure to furnish an oily brown residue (crude 1*H*-pyrrol-2(5*H*)-one) (8.0 g, 96 mmol, yield 64%), which was used as such in the subsequent transformation.

^{1}H NMR (400 MHz, $CDCl_3$) δ 7.43 (s, 1H), 7.23-7.10 (m, 1H), 6.20-6.18 (m, 1H), 4.15-3.95 (m, 2H).

***tert*-Butyl 2-oxo-2,5-dihydro-1*H*-pyrrole-1-carboxylate**

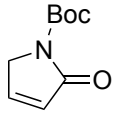

To a stirring solution of 1,5-dihydro-2*H*-pyrrol-2-one (4.2 g, 49 mmol) in CH_3CN (43 mL) were sequentially added Boc_2O (10.5 g, 49 mmol) and DMAP (0.30 g, 2.45 mmol) at room temperature. The resulting dark-brown mixture was stirred for 45 min at room temperature, whereupon the solvent was removed under reduced pressure. The crude black residue was treated with silica gel and EtOAc and the mixture was filtered through filter paper. The filtrate was then concentrated under vacuum to give a residue that was purified by silica gel flash chromatography eluting with 1:1 hexanes/EtOAc mixture. Pure product was obtained as yellow solid (2.6 g, 14 mmol, yield 31%).

^{1}H NMR (400 MHz, $CDCl_3$) δ 7.22-7.19 (m, 1H), 6.20-6.17 (m, 1H), 4.37 (t, J = 2.0 Hz, 2H), 1.58 (s, 9H).

***tert*-Butyl 2-((*tert*-butyldimethylsilyl)oxy)-1*H*-pyrrole-1-carboxylate (1b)**

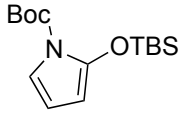

To a solution of *tert*-butyl 2-oxo-2,5-dihydro-1*H*-pyrrole-1-carboxylate (0.65 g, 3.55 mmol) in dry CH_2Cl_2 (5.3 mL) were added TBSOTf (1.7 mL, 7.1 mmol) and 2,6-lutidine (1.2 mL, 10.6 mmol) under N_2 at room temperature. The resulting solution was stirred for 45 min at room temperature, whereupon $NaHCO_3$ saturated aqueous solution was added. The biphasic mixture was stirred vigorously and hexane was added. The phases were then separated and the aqueous layer was washed with petroleum ether. The combined organic extracts were dried over $MgSO_4$, filtered, and the filtrate was concentrated in vacuo. After flash chromatographic purification (hexane /EtOAC, 95:5), pure compound **1b** was obtained as yellow oil (0.45 g, 1.5 mmol, yield 42%). **1b** should be reserved under N_2 atmosphere, −40 °C. **1b** was purified by gel permeation chromatography before use.

^{1}H NMR (400 MHz, $CDCl_3$) δ 6.72 (dd, J = 3.9, 2.0 Hz, 1H), 5.93 (t, J = 3.7 Hz, 1H), 5.26 (dd, J = 3.5, 2.0 Hz, 1H), 1.59 (s, 9H), 1.01 (s, 9H), 0.25 (s, 6H).

The synthesis route to **1c** was carried out according to the literature (Scheme 7).[3]

Scheme 7. The synthesis route to **1c**

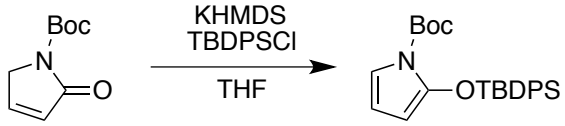

1c

***tert*-butyl 2-((*tert*-butyldiphenylsilyl)oxy)-1*H*-pyrrole-1-carboxylate (1c)**

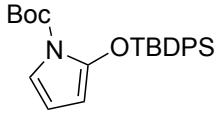

To a flame-dried 50-mL round-bottomed flask fitted with a magnetic stir bar, KHDMS (8.7 mL, 4.4 mmol) and 7.5 mL of anhydrous THF were added.

The solution was cooled to –78 °C and then *tert*-butyl 2-oxo-2,5-dihydro-1*H*-pyrrole-1-carbo-xylate (0.49 g, 2.7 mmol) in 5 mL THF was added slowly dropwise over 10 min via syringe. The resulting orange solution was stirred for 20 min at –78 °C prior to addition of TBDPSCl (0.85 mL, 3.8 mmol) via syringe. The resulting mixture was stirred at –78 °C for 5 min and then the reaction flask was removed from the cooling bath and was allowed to warm to r. t. The reaction mixture was stirred for 1 h at 23 °C, then was concentrated by rotary evaporation. The dark brown oily residue was dissolved in hexane (20 mL) and filtered through a pad of Celite and the filtrate was concentrated in vacuo. After flash chromatographic purification (hexane /EtOAC, 95:5), pure compound **1c** was obtained as orange oil (0.16 g, 0.38 mmol, yield 14%). **1c** should be reserved under N_2 atmosphere, −40 °C. **1c** was purified by gel permeation chromatography before use.

^{1}H NMR (400 MHz, $CDCl_3$) δ 7.78 – 7.75 (m, 4H), 7.53 – 7.31 (m, 6H), 6.67 (dd, J = 3.8, 2.0 Hz, 1H), 5.71 (t, J = 3.7 Hz, 1H), 4.76 (dd, J = 3.5, 2.0 Hz, 1H), 1.61 (s, 9H), 1.15 (s, 9H).

General procedure for the photoreaction of **1** and **2**: A degassed solution of **1** and **2** in Pyrex NMR tube was irradiated by LED (365 nm) for 1.5 hours, whereupon the solvent was removed under reduced pressure using rotary evaporation. After the gel permeation chromatography separation, **4** was obtained under vacuo. Since the product was sensitive to acid, we used deuterium benzene or acetone for the NMR spectrum measurement.

***tert*-Butyl-1-((*tert*-butyldimethylsilyl)oxy)-6,6-diphenyl-7-oxa-2-azabicyclo[3.2.0] hept-3-ene-2-carboxylate (4ba)**

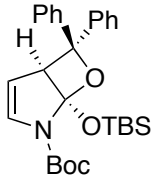

^{1}H NMR (400 MHz, Acetone-d_6) δ 7.58 (d, J = 7.4 Hz, 2H), 7.43 – 7.13 (m, 8H), 6.48 (d, J = 4.5 Hz, 1H), 4.97 (broad s, 1H), 4.31 (d, J = 2.4 Hz, 1H), 2.97 (s, 9H), 0.84 (s, 9H), 0.16 (s, 3H), -0.08 (s, 3H). ^{13}C NMR (101 MHz, Acetone-d_6) δ 146.2, 142.7, 133.9, 128.0, 127.6, 127.0, 126.6, 125.6, 125.4, 103.4, 80.2, 78.3, 27.7, 25.0, 17.5, -4.2, -4.8. HRMS m/z: $[M + Na]^+$ anal.

calcd for $C_{28}H_{37}NO_4SiNa$ 502.23841, found 502.23874.

***tert*-Butyl-1-((*tert*-butyldiphenylsilyl)oxy)-6,6-diphenyl-7-oxa-2-azabicyclo[3.2.0] hept-3-ene-2-carboxylate (4ca)**

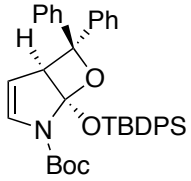

^{1}H NMR (400 MHz, Acetone-d_6): δ 7.54 – 7.01 (m, 20H), 6.02 (d, J = 47.2 Hz, 1H), 4.41 (broad s, 1H), 3.81 (broad s, 1H), 1.43 (m, 9H), 0.89 (s, 9H). ^{13}C NMR (101 MHz, Acetone-d_6): δ 146.0, 142.9, 135.9, 135.8, 130.0, 129.6, 128.1, 127.6, 127.3, 126.8, 126.5, 125.4, 125.0, 102.9, 78.3, 59.2, 27.8, 26.1, 19.0. HRMS m/z: $[M + Na]^+$ anal. calcd for $C_{38}H_{41}NO_4SiNa$ 626.26971, found 626.27014.

The quantum yield measurement used Hatchart-Parker actinometer as the photons counter.[8] The mechanism was shown in Scheme 8.[11]

Scheme 8

$$Fe(C_2O_4)_3^{3-} \xrightarrow{h\upsilon} Fe^{2+} + C_2O_4^{\bullet-} + 2C_2O_4^{3-}$$

$$Fe(C_2O_4)_3^{3-} \xrightarrow{\Delta} Fe^{2+} + 2CO_2^{\bullet-} + 2C_2O_4^{3-}$$

Firstly, the potassium ferric oxalate solution was prepared that 0.156 g of potassium ferric oxalate was added to the 100 mL of 0.05 M sulfuric acid solution. After then, buffered phenathroline (0.1%) solution was prepared that 22.5 g sodium acetate trihydrate, and 0.1 g of phenanthroline was mixed with 100 mL of 0.5 M sulfuric acid solution.

The 3 mL of prepared potassium ferric oxalate solution in cell was irradiated by LED lamp by 0.5s, 0.7s. 0.9s, 1.1s separately. Meanwhile, the experiment equipment were set up as in Figure 15.

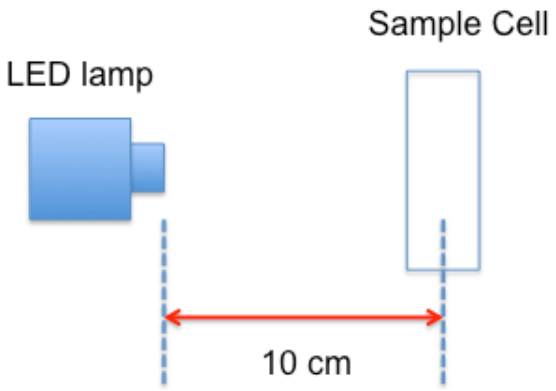

Figure 15. Equipment set-up for the quantum yield measurement

After irradiation, 0.5 mL of prepared buffered phenathroline (0.1%) solution was added to the cell and UV spectrum was measured immediately (Figure 16). 3 mL of 0.15 M **1b** and 0.34 M **2a** in benzene (20 min N_2 bubbled) was irradiated as the exact same condition of potassium ferric oxalate solution by 624 s (chemical yield 3%). The product and yield was calculated by the inner standard (Ph_3CH), according to the plot, (Figure 17) and the quantum yield was calculated to be 0.02 (Scheme 9). [11]

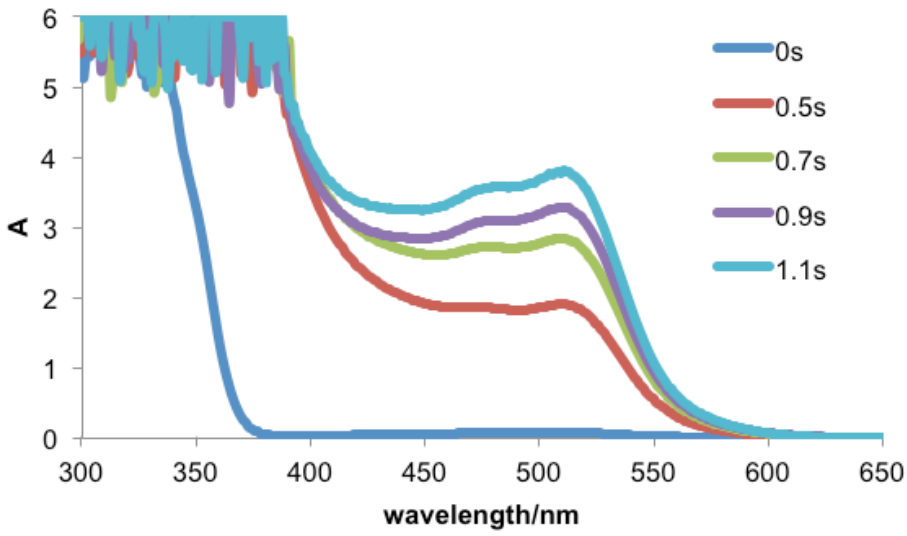

Figure 16. UV spectrum of potassium ferric oxalate solution mixed with phenathroline after irradiation

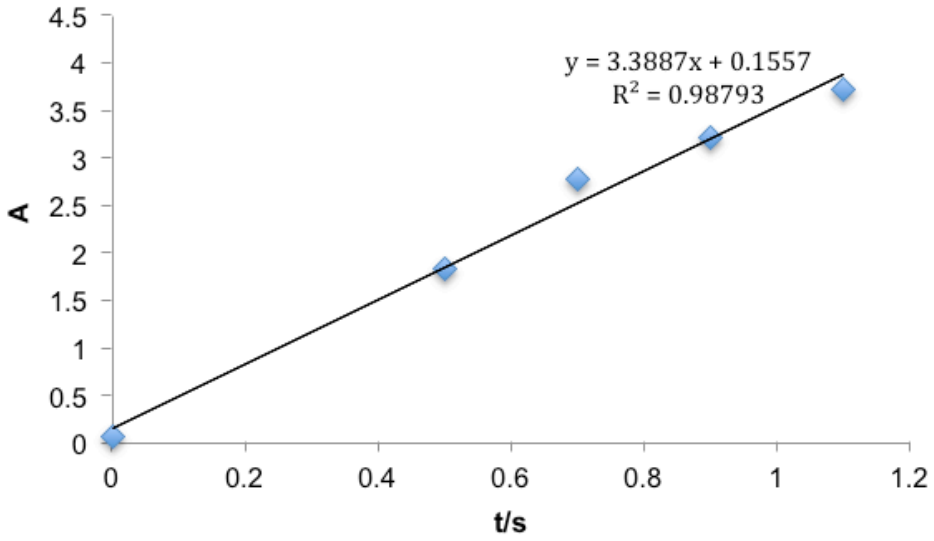

Figure 17. The relative plot of absorption and irradiation of potassium ferric oxalate solution mixed with phenathroline using LED-365 nm lamp

Scheme 9

$$moles\ Fe^{2+} = \frac{V_1 \times V_3 \times \Delta A(510\ nm)}{10^3 \times V_2 \times l \times \varepsilon(510\ nm)}$$

$$Nh\frac{\nu}{t} = \frac{moles\ Fe^{2+}}{\Phi_{363.8\ nm} \times t \times F} = \frac{V_1 \times V_3 \times \Delta A(510\ nm)}{10^3 \times V_2 \times l \times \varepsilon(510\ nm) \times \Phi_{363.8\ nm} \times t \times F}$$

$$= \frac{3 \times 3.5 \times 3.38}{1000 \times 3 \times 1 \times 11100 \times 1.28 \times 1} = 8.3 \times 10^{-4} mmol/s$$

$$\Phi_{PB} = \frac{moles\ of\ oxetane}{Nh\frac{\nu}{t} \times T_{iradiation}} = \frac{0.01}{8.3 \times 10^{-4} \times 624} = 0.02$$

V_1: the radiated volume; (3 mL)

V_2: the aliquot of the irradiated solution taken for the determination of the ferrous ions; (3 mL)

V_3: the final volume after complexation with phenanthroline; (3.5 mL)

$\varepsilon = 11100$ L mol^{-1} cm^{-1}

$\Phi_{\lambda = 363.8\ nm} = 1.28$

F: the mean fraction of light absorbed by the ferrioxalate solution.

2-4. Supplementary material

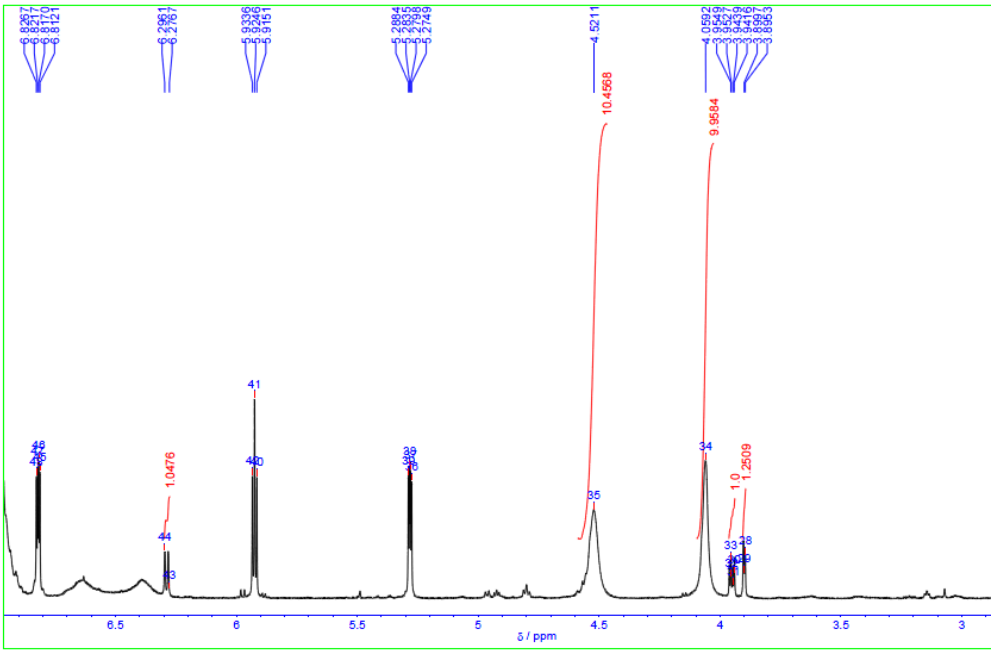

Figure 18. Mixture of **1b** and **2a** in benzene after reaction at -78°C monitored by ^{1}H NMR (400 MHz, Toluene-d_8)

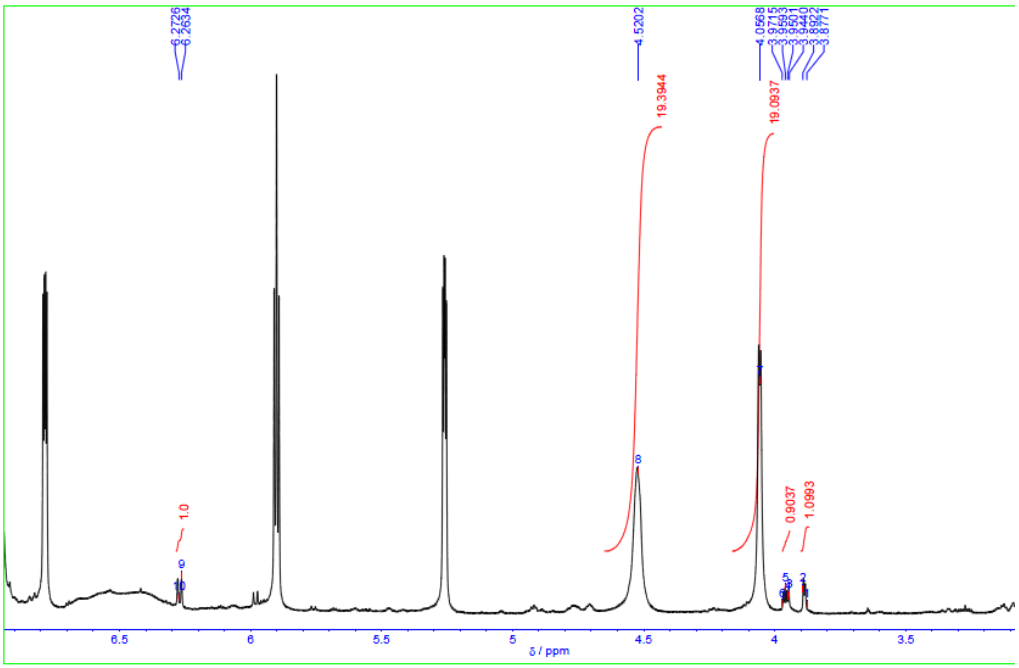

Figure 19. Mixture of **1b** and **2a** in benzene after reaction at -20°C monitored by ^{1}H NMR (400 MHz, Toluene-d_8)

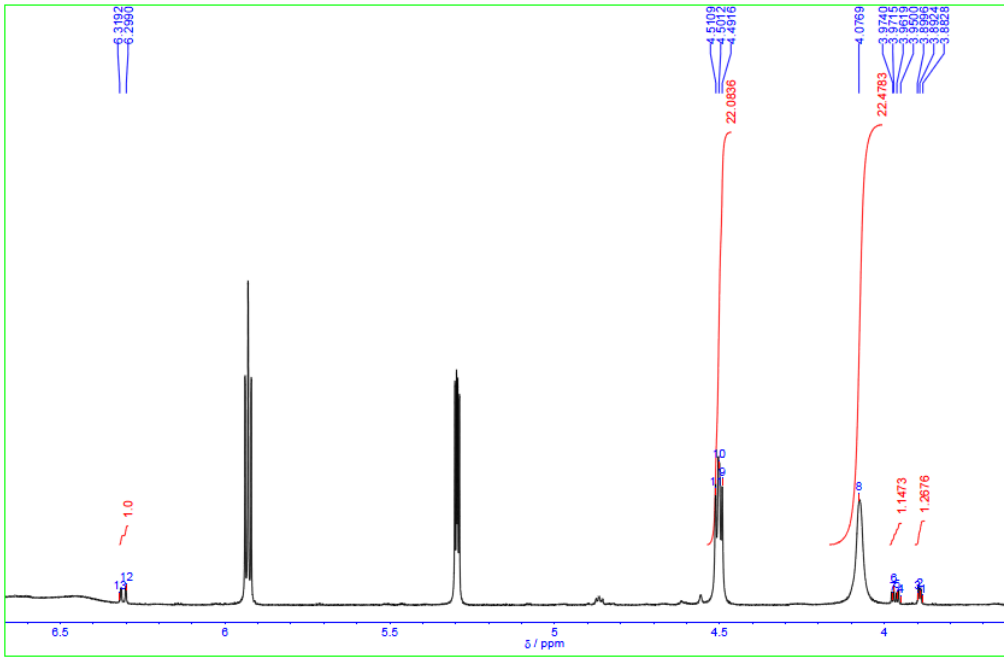

Figure 20. Mixture of **1b** and **2a** in benzene after reaction at 25°C monitored by ^{1}H NMR (400 MHz, C_6D_6)

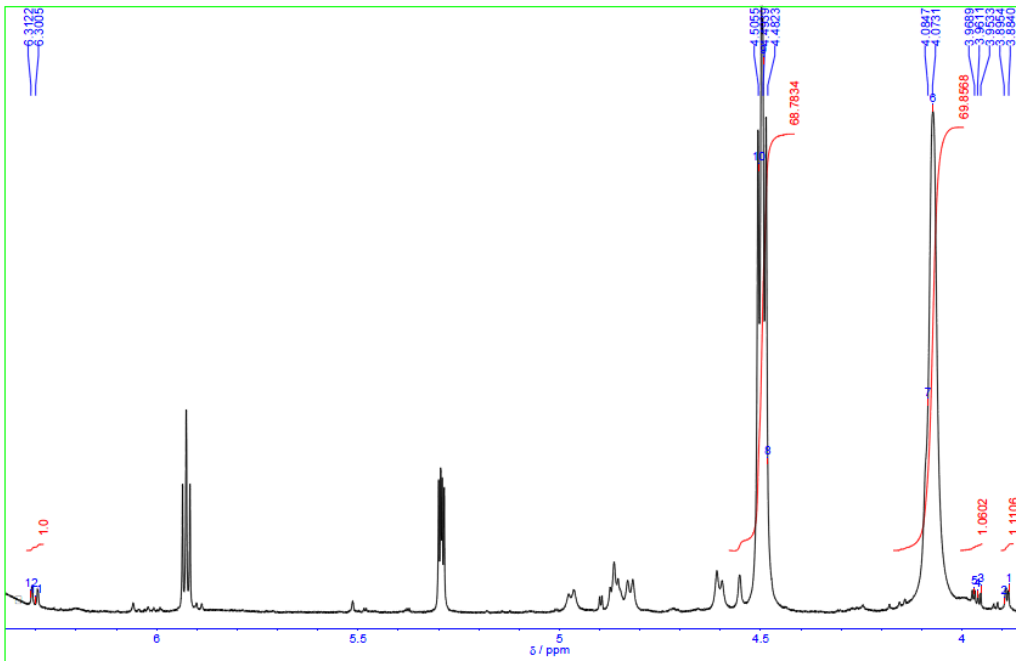

Figure 21. Mixture of **1b** and **2a** in benzene after reaction at 60°C monitored by ^{1}H NMR (400 MHz, C_6D_6)

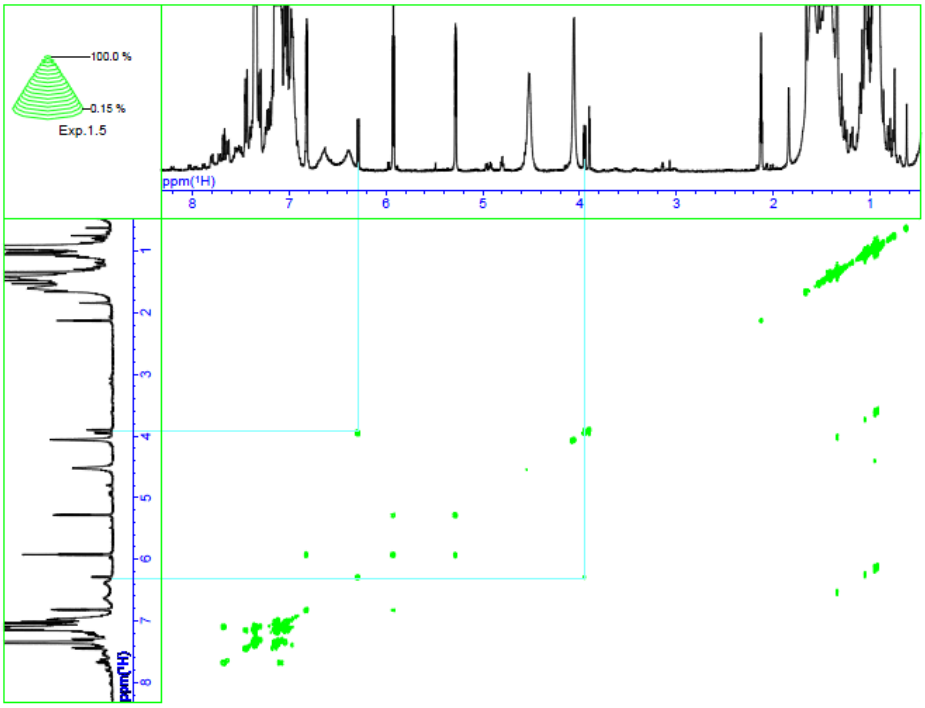

Figure 22. Mixture of **1b** and **2a** in benzene after reaction at -78°C monitored by H-H COSY NMR (Toluene-d_8)

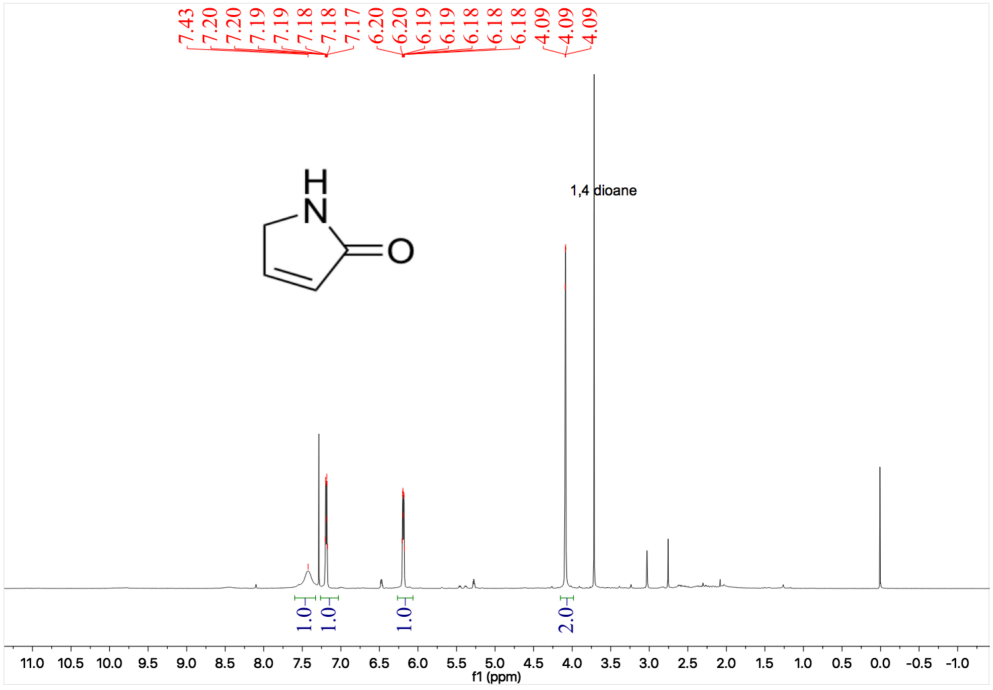

Figure 23. ^{1}H NMR (400 MHz, $CDCl_3$) of 1,5-Dihydro-2*H*-pyrrol-2-one

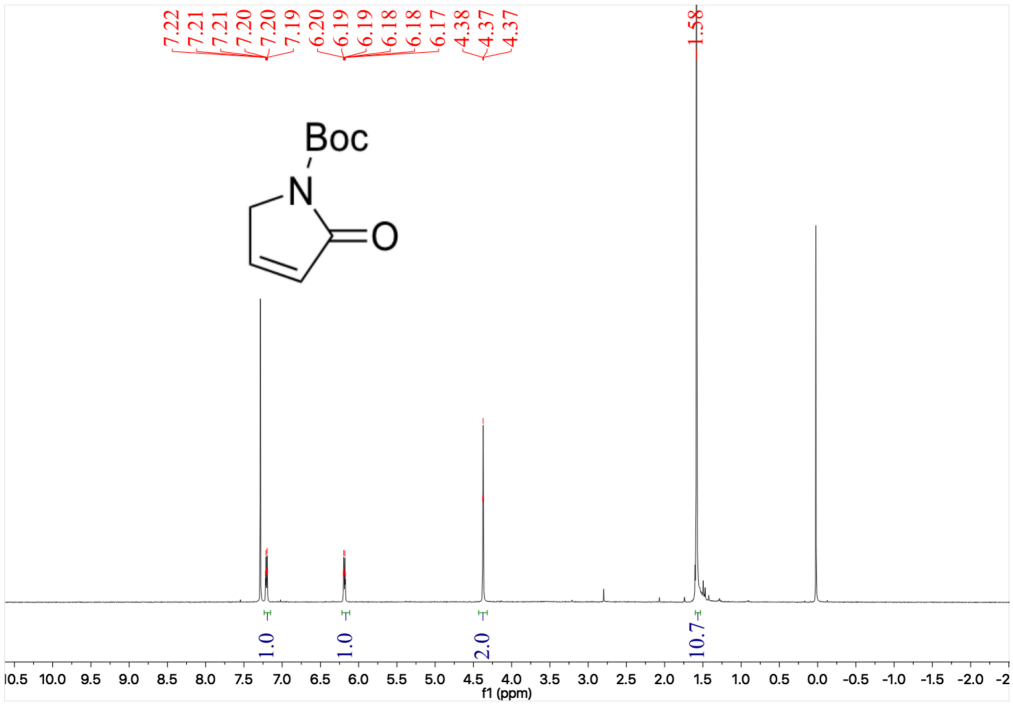

Figure 24. ^{1}H NMR (400 MHz, $CDCl_3$) of *tert*-butyl 2-oxo-2,5-dihydro-1*H*-pyrrole-1-carboxylate

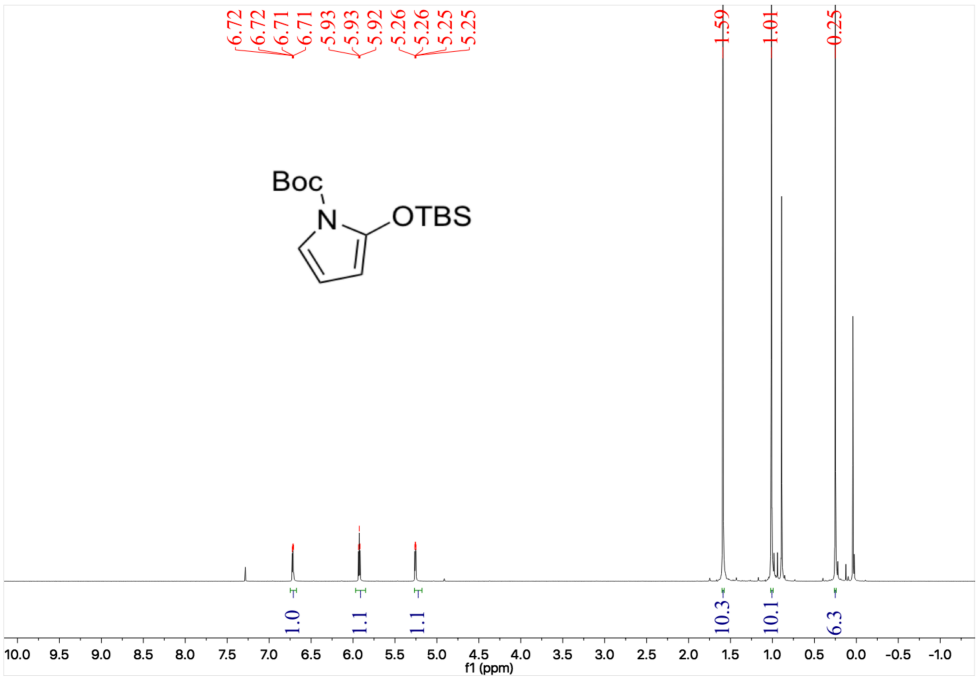

Figure 25. ^{1}H NMR (400 MHz, $CDCl_3$) of **1b** (before GPC)

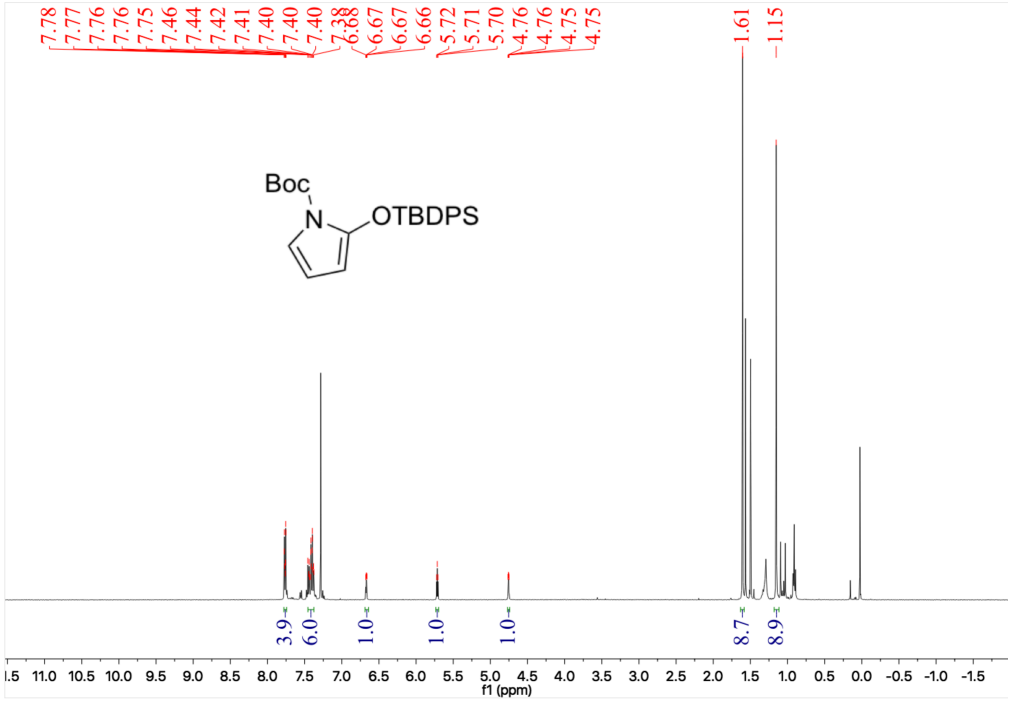

Figure 26. ^{1}H NMR (400 MHz, $CDCl_3$) of **1c** (before GPC)

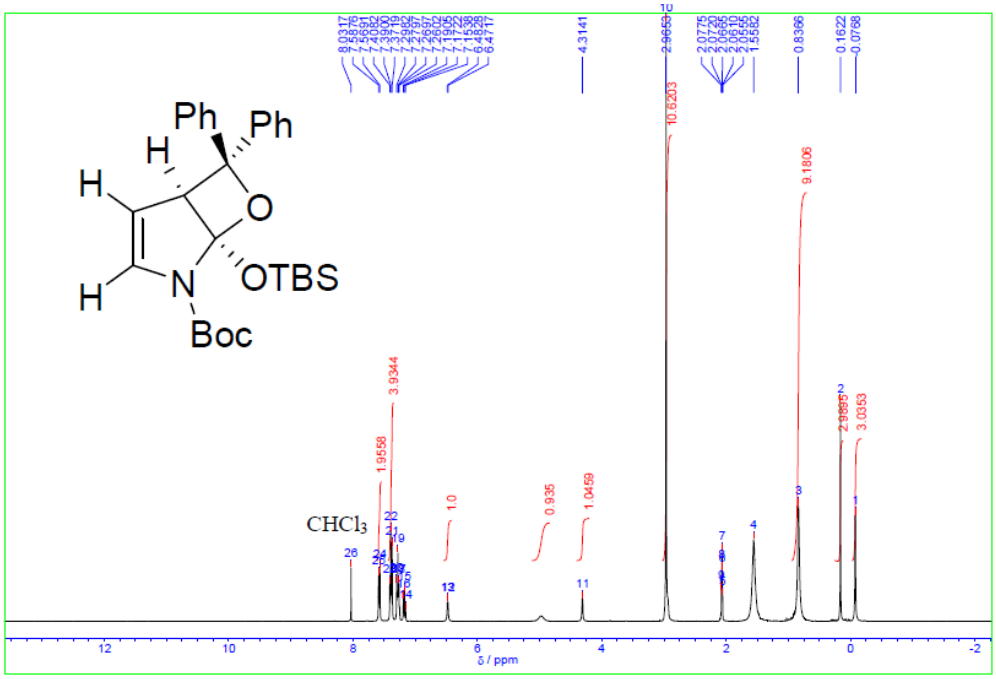

Figure 27. ^{1}H NMR (400 MHz, Acetone-d_6) of **4ba**

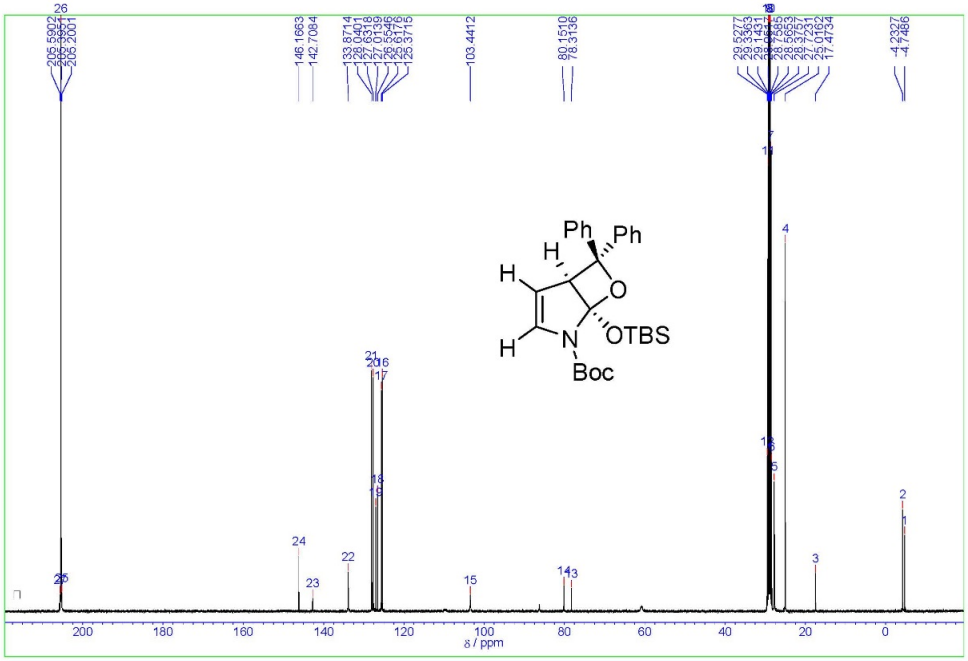

Figure 28. ^{13}C NMR (101 MHz, Acetone-d_6) of **4ba**

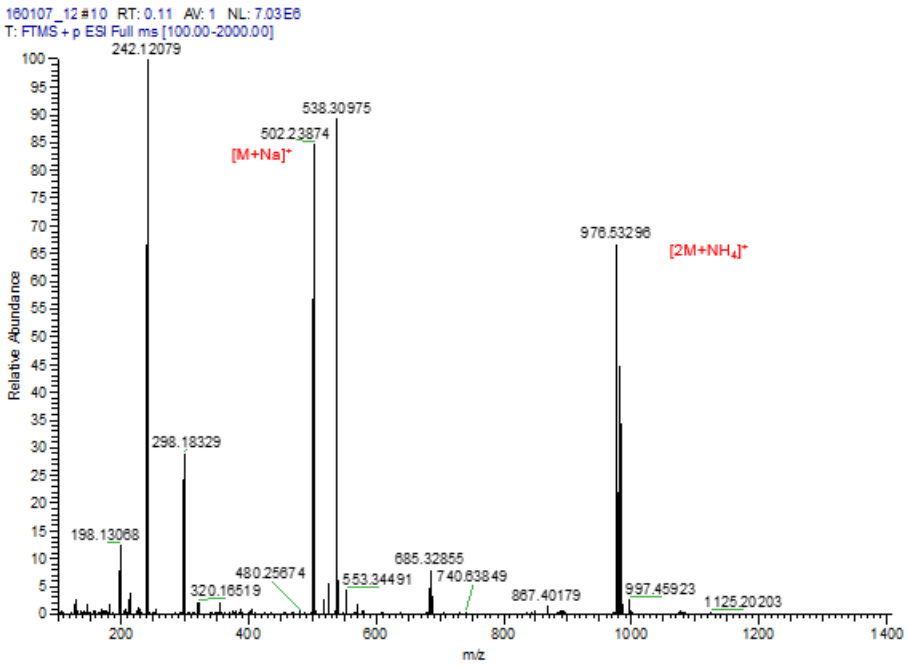

Figure 29. ESI-HRMS analysis of **4ba**

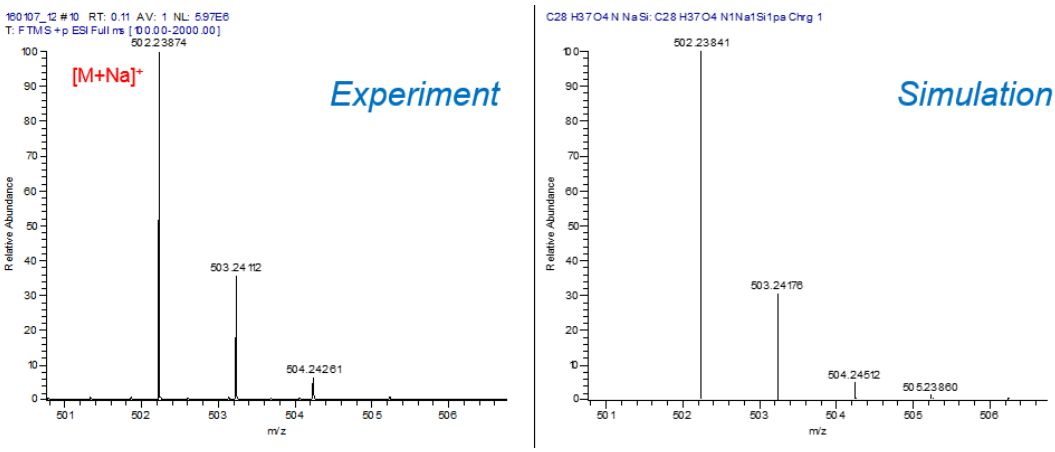

Figure 30. ESI-HRMS analysis of **4ba** (expansion and simulation)

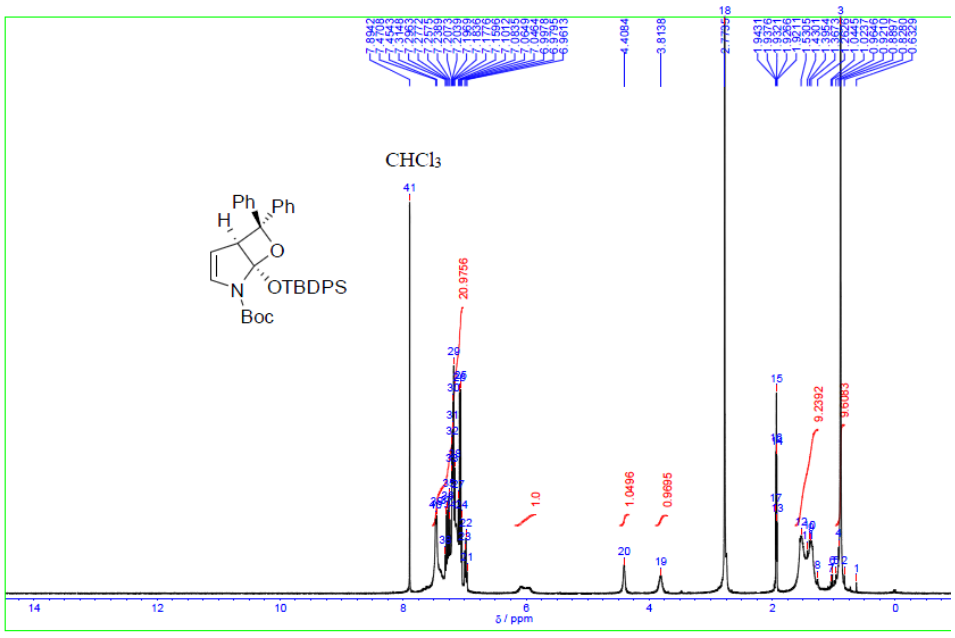

Figure 31. ^{1}H NMR (400 MHz, Acetone-d_6) of **4ca**

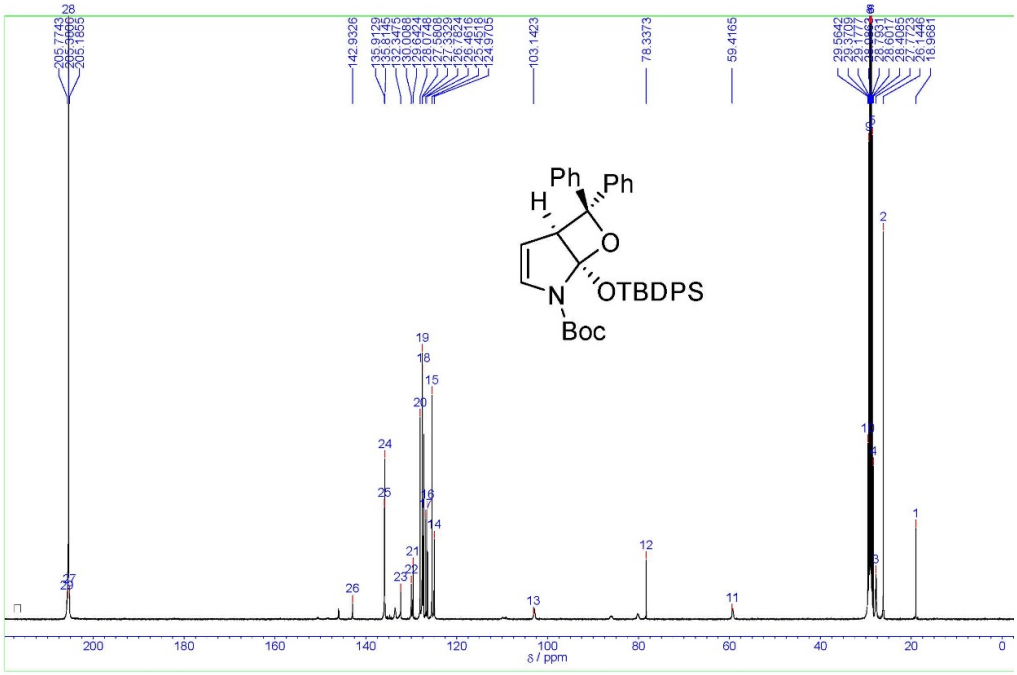

Figure 32. ^{13}C NMR (101 MHz, Acetone-d_6) of **4ca**

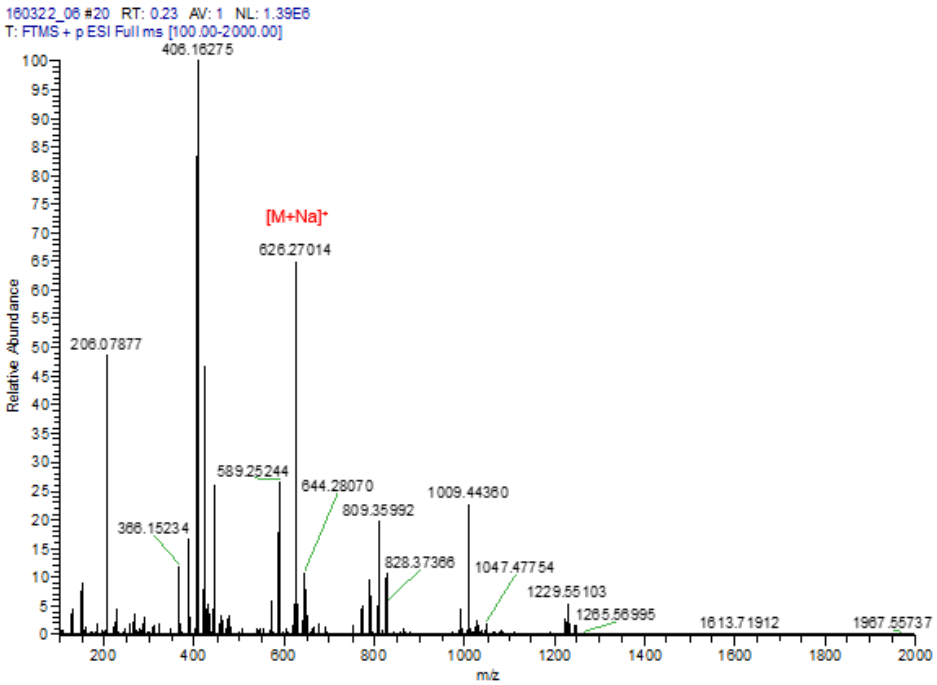

Figure 33. ESI-HRMS analysis of **4ca**

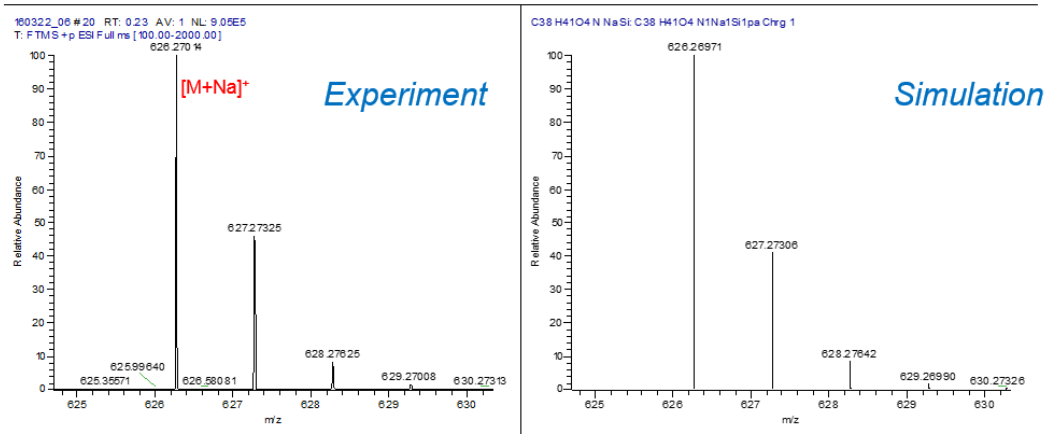

Figure 34. ESI-HRMS analysis of **4ca** (expansion and simulation)

Table 3. T-**DR3'** dihedral angle scan

UB3LYP/6-31G(d) level of theory in the GAUSSIAN 09 Scan of Total Energy **X**-Axis: Scan Coordinate Dihedral Angle, θ (°) **Y**-Axis: Total Energy (+ 940347) (kCal/mol)	
X	**Y**
0.043099	2.19105
10.0431	2.755438
20.0431	3.227256
30.0431	3.58525
40.0431	3.995083
50.0431	4.45021
60.0431	4.652625
70.0431	4.585432
80.0431	4.339674
90.0431	4.023478
100.0431	3.843238
110.0431	3.743188
120.0431	3.518025
130.0431	3.400054
140.0431	3.414085
150.0431	3.525894
160.0431	3.607653
170.0431	3.782263
180.0431	3.948848
190.0431	4.174413
200.0431	4.38589
210.0431	4.720547
220.0431	5.193677
230.0431	5.985631
240.0431	6.613323

250.0431	6.263957
260.0431	5.096231
270.0431	3.645021
280.0431	2.415629
290.0431	1.726072
300.0431	1.490153
310.0431	1.442575
320.0431	1.5191
330.0431	1.490517
340.0431	1.559662
350.0431	1.81659

Table 4. T-**DR4'** dihedral angle scan

UB3LYP/6-31G(d) level of theory in the GAUSSIAN 09 Scan of Total Energy **X**-Axis: Scan Coordinate Dihedral Angle, θ (°) **Y**-Axis: Total Energy (+ 940347) (kCal/mol)	
X	**Y**
0.877605	3.484378276
10.87761	3.789090614
20.87761	4.000103233
30.87761	4.031968166
40.87761	3.799695524
50.87761	3.501986192
60.87761	3.313331736
70.87761	3.527626231
80.87761	3.803579808
90.87761	3.453234979
100.8776	2.699558419
110.8776	1.758545173
120.8776	0.902333561
130.8776	0.280892078
140.8776	0.000000000
150.8776	0.036954035
160.8776	0.308816250
170.8776	0.802534450
180.8776	1.588684627
190.8776	2.533550781
200.8776	3.623967764
210.8776	4.634069806
220.8776	5.511880296
230.8776	6.212281299
240.8776	6.710366965

250.8776	6.994660144
260.8776	6.867231789
270.8776	6.331514379
280.8776	5.571725877
290.8776	4.512960473
300.8776	3.542642533
310.8776	2.752884177
320.8776	2.376416127
330.8776	2.430538822
340.8776	2.749828205
350.8776	3.134221700

Table 5. T-**DR3$_{oa}$'** bond formation scan

UB3LYP/6-31G(d) level of theory in the GAUSSIAN 09 Scan of Total Energy **X**-Axis: Scan Coordinate Distance, r (pm) **Y**-Axis: Total Energy (+ 940348) (kCal/mol)	
X	**Y**
145.317	0.498916
150.317	0.939547
155.317	2.004882
160.317	3.417513
165.317	4.97341
170.317	6.525141
175.317	7.972065
180.317	9.250189
185.317	10.33105
190.317	11.21113
195.317	11.8979
200.317	12.40824
205.317	12.76597
210.317	13.00131
215.317	13.14853
220.317	13.24078
225.317	13.30657
230.317	13.36807
235.317	13.44033
240.317	13.53145
245.317	13.64493
250.317	13.78093
255.317	13.93856
260.317	14.11616
265.317	14.31022

270.317	14.51659
275.317	14.73103
280.317	14.94883
285.317	15.1649
290.317	15.37307
295.317	15.56945

Table 6. T-**DR4$_{og}$'** bond formation scan

UB3LYP/6-31G(d) level of theory in the GAUSSIAN 09 Scan of Total Energy **X**-Axis: Scan Coordinate Distance, r (pm) **Y**-Axis: Total Energy (+ 940348) (kCal/mol)	
X	**Y**
143.4343	4.186973
148.4343	4.184677
153.4343	4.917915
158.4343	6.088904
163.4343	7.456003
168.4343	8.865006
173.4343	10.04503
178.4343	11.07526
183.4343	11.93812
188.4343	12.63362
193.4343	13.16013
198.4343	13.53055
203.4343	13.80164
208.4343	13.99352
213.4343	14.12296
218.4343	14.20042
223.4343	14.23304
228.4343	14.23275
233.4343	14.22052
238.4343	14.2229
243.4343	14.24444
248.4343	14.2982
253.4343	14.38472
258.4343	14.50246
263.4343	14.64884

268.4343	14.82085
273.4343	15.03068
278.4343	15.25013
283.4343	15.49555
288.4343	15.75657
293.4343	16.02616

References

1. Krimen, L. I. *Chem. Rev.* **1963**, *63*, 511.
2. Jacob, K.; Treibs, A.; Roomi, M. W. *Liebigs Ann.* **1969**, *724*, 137.
3. Curti, C.; Ranieri, B.; Battistini, L.; Rassu, G.; Zanardi, F. *Adv. Synth. Catal.* **2010**, *352*, 2011.
4. For reviews, see: (a) Porco, J. A.; Schreiber, S. L. *In Comprehensive Organic Synthesis*; Trost, M. M. *Ed*; Pergamon Press: New York, **1991**, *5*, 168. (b) Abe, M. *J. Chin. Chem. Soc.* **2008**, *55*, 479. (c) Abe, M. Formation of a 4-Membered ring: Oxetanes, in: *Handbook of Synthetic Photochemistry* (Eds: A. Albini), Wiley-VCH, **2010**, 217–239.
5. (a) Rivas, C. R.; Bolívar, A. *J. Heterocyclic Chem.* **1976**, *13*, 1037. (b) Guilford, J.; Helmuch, M. G.; Julie, L. *J. Org. Chem.* **1979**, *44*, 2949.
6. J. M. Brittain, R. A. Jones, J. S. Arques, T. A. Saliente, *Synth. Commun.* **1982**, *12*, 231.
7. Abe, M.; Torii, E.; Nojima, M. *J. Org. Chem.* **2000**, *65*, 3426.
8. (a) Hatchard, C. G.; Parker, C. A. *Proc. R. Soc. London,* **1956**, *A235*, 518. (b) Parker, C. A. *Proc. R. Soc. London,* **1953**, *A220*, 104.
9. Abe, M.; Kawakami, T.; Ohata, S.; Nozaki, K.; Nojima, M. *J. Am. Chem. Soc.* **2004**, *126*, 2838.
10. Gaussian 09, Revision A.02, 21), Frisch, M. J.; Trucks, G. W.; Schlegel, H. B.; Scuseria, G. E.; Robb, M. A.; Cheeseman, J. R.; Scalmani, G.; Barone, V.; Mennucci, B.; Petersson, G. A.; Nakatsuji, H.; Caricato, M.; Li, X.; Hratchian, H. P.; Izmaylov, A. F.; Bloino, J.; Zheng, G.; Sonnenberg, J. L.; Hada, M.; Ehara, M.; Toyota, K.; Fukuda, R.; Hasegawa, J.; Ishida, M.; Nakajima, T.; Honda, Y.; Kitao, O.; Nakai, H.; Vreven, T.; Montgomery, Jr., J. A.; Peralta, J. E.; Ogliaro, F.; Bearpark, M.; Heyd, J. J.; Brothers, E.; Kudin, K. N.; Staroverov, V. N.; Kobayashi, R.; Normand, J.; Raghavachari, K.; Rendell, A.; Burant, J. C.; Iyengar, S. S.; Tomasi, J.; Cossi, M.; Rega, N.; Millam, J. M.; Klene, M.; Knox, J. E.; Cross, J. B.; Bakken, V.; Adamo, C.; Jaramillo, J.; Gomperts, R.; Stratmann, R. E.; Yazyev, O.; Austin, A. J.; Cammi, R.; Pomelli, C.; Ochterski, J. W.; Martin, R. L.; Morokuma, K.; Zakrzewski, V. G.; Voth, G. A.; Salvador, P.; Dannenberg, J. J.; Dapprich, S.; Daniels, A. D.; Farkas, Ö.; Foresman, J. B.; Ortiz, J. V.; Cioslowski, J.; Fox, D. J. Gaussian 09, Revision A.02; Gaussian, Inc.: Wallingford, CT,

2009.
11. Montalti, M.; Credi, A.; Prodi, L.; Gandolfi, M. T. *Handbook of Photochemistry*, 3rd Eds, **2006**, P601.

Chapter 3

Photochemical [2+2] cycloaddition reactions of pyrrole derivatives with enone derivatives

3-1. Introduction

2-Cyclopenten-1-one, as one of the *α, β*-unsaturated ketones (enones), is often used for the intermolecular photochemical [2+2] cycloaddtion reactions through a process of triplet state diradical intermediate.[1] The stability of triplet 1,4-diradical intermediate will greatly determine the stereoselectivity of cyclobutane product. As is shown in Scheme 1, diastereomeric mixture of **9a** and **9b** was produced when six-membered cyclic alkene was applied in this photochemical [2+2] cycloaddtion reaction.[2] Nevertheless, higher stereoselectivity was observed at the expense of relatively lower yield in the case of more strained cyclic alkene, cyclopentene, because of the steric effect.

Scheme 1. Photochemical [2+2] cycloaddtion reactions of 3-methyl cyclopentenone with cyclopentene and cyclohexene

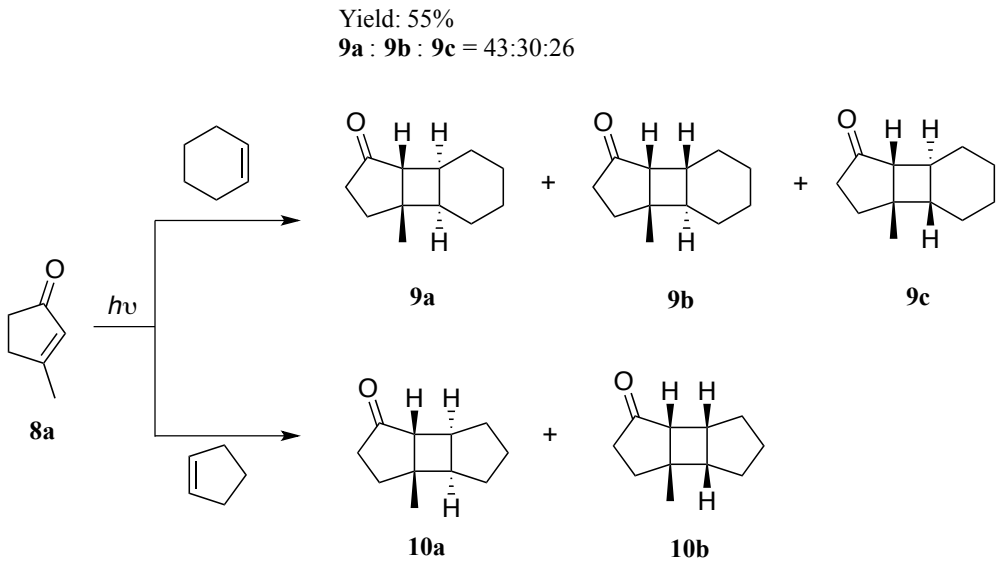

The reaction examples of cyclopentenone with aromatic partners are quite limited. For instance, one report concerning the intramolecular cycloaddition of furan derivative has been published in the study of total sysnthesis of (±)-ginkgolide (Scheme 2).[3]

Scheme 2

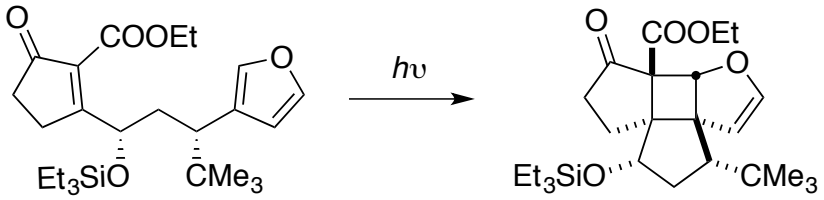

Brooker-Milburn group has accomplished a series of great advances on the intramolecular photochemical [2+2] cycloaddition reactions of simple pyrrole derivatives (Scheme 3).[4] Under the irradiation using low-pressure mercury lamp, the pre-prepared pyrrole derivatives could produce the corresponding cyclobutane species or other product through a path of diradical rearrangement.

Scheme 3. Intramolecular photochemical [2+2] cycloaddition reactions of pyrrole derivatives

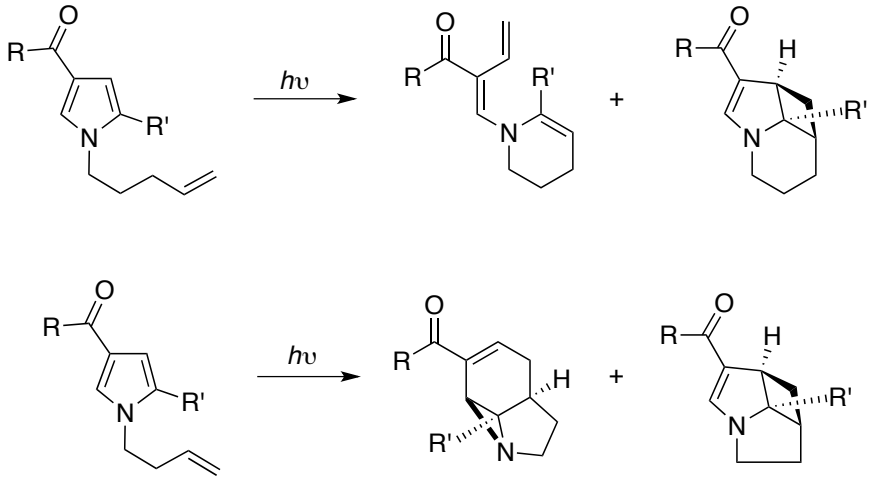

1,4-naphtoquinone is one of the interesting carbonyl compounds with 2 carbonyl groups and lower energy gap between ^{3}n,π* state and ^{3}π, π* state (^{3}π, π* state locates in 25 kJ/mol higher than ^{3}n,π* state).[5] Because of its unique character, much efforts have been made to elucidate the adducts competition between cyclobutane and spirooxetane (Scheme 4).[6] Bryce-Smith *et al.* found that the alkene with higher oxidation potential is more likely to produce cyclobutane adduct rather than spirooxetane adduct.[6e]

Scheme 4. Competition photochemical [2+2] cycloaddition reaction of 1, 4-naphthoquinone with alkene

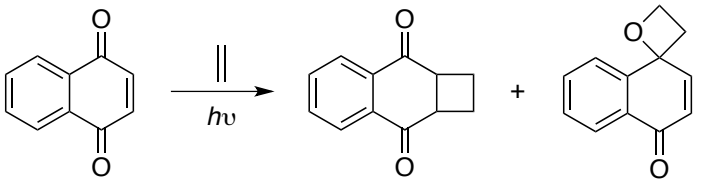

In this chapter, photochemical [2+2] cycloaddition reaction of 2-siloxy-1*H*-pyrrole derivative **1b** and 2-cyclopenten-1-one **8b**, 1,4-naphthoquinone **11** will be investigated. The structure determination of product could be confirmed by several 2D-NMR spectra and the yields have been optimized to be moderate (Scheme 5).

Scheme 5

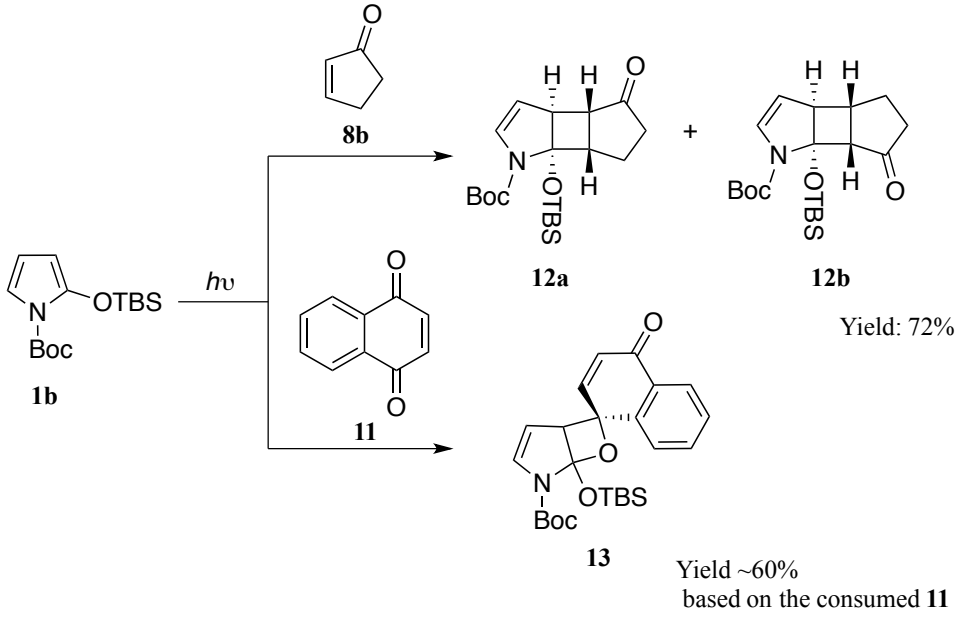

3-2. Results and discussion

The pyrrole, 2-dimethyl(*tert*-butyl)siloxy-N-*tert*-butoxycarbonyl-pyrrole (**1b**), was prepared from the corresponding lactam according to the literature.[7] Firstly, the reaction mixture of **1b** (0.51 M) and **8b** (0.34 M) was irradiated by 365 nm using light-emitting diode (LED) at room temperature in a sealed Pyrex NMR tube in acetone-d_6 after 20 minutes nitrogen bubbling. According to the NMR spectroscopic analysis of the reaction mixture after 24 hours irradiation Figure 1(e), newly appeared signals at δ 6.8, 3.5-2.0 were assigned to the products **12a** and **12b**. After removing the solvent under reduced pressure, the products **12a** and **12b** were isolated in 12% of yield with 64 : 36 isomer ratio by silica gel chromatography (entry 1 in Table 1).

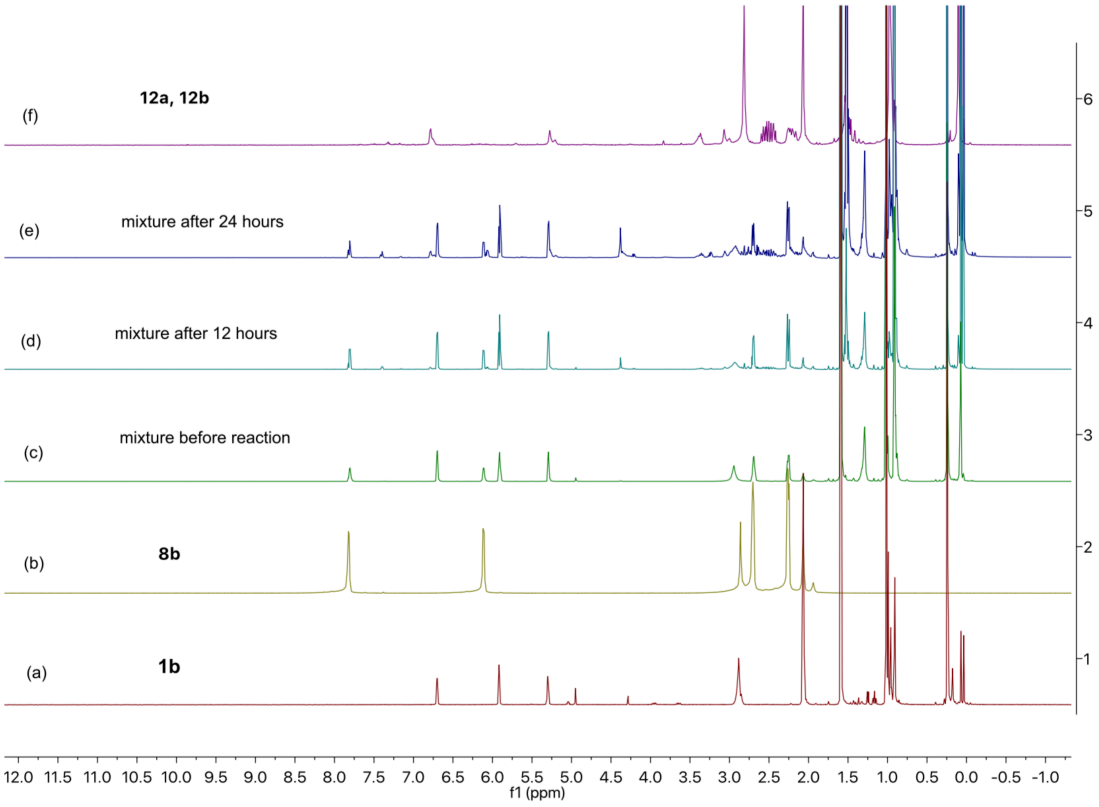

Figure 1. ^{1}H NMR (400 MHz, Acetone-d_6) spectroscopic analysis of the photochemical [2+2] cycloaddition reaction of **1b** and **8b** under irradiation at 365 nm. (a) **1b**, (b) **8b**, (c) before irradiation at r. t., (d) after 12 hours of irradiation, (e) after 24 hours of irradiation, (f) isolated compounds **12a** and **12b**

The structure of **12a** and **12b** was confirmed by 1D-NMR and 2D-NMR spectroscopic analyses, i.e. ^{1}H, ^{13}C, H-H COSY, H-C HSQC, H-C HMBC, H-H NOESY, and high-resolution mass spectroscopic analysis. The formation of other two regioisomers **12c** and **12d** was excluded by the observed two vinyl protons H_a and H_b at 6.75, 6.60 ppm and 5.15, 5.07 ppm, respectively, in the formed cycloadducts (Figures 2 and 3). Because the two protons, H_a (δ 6.75, 6.60) and H_b (δ 5.16, 5.09), were correlated with the sp^2 carbons (δ 132.34, 132.32, 107.4, 107.0), the two protons at ~6.7 and ~5.1 ppm were assigned to the vinylic protons (Figure 3). Furthermore, in the H-C HMBC spectrum (Figure 4), the correlation of H*d* (δ 2.98) and the cyclic carbonyl carbon (δ 219.7) was observed in the major isomer of the products, indicating that the major product was bicyclic cyclobutane **12a, 12b**.

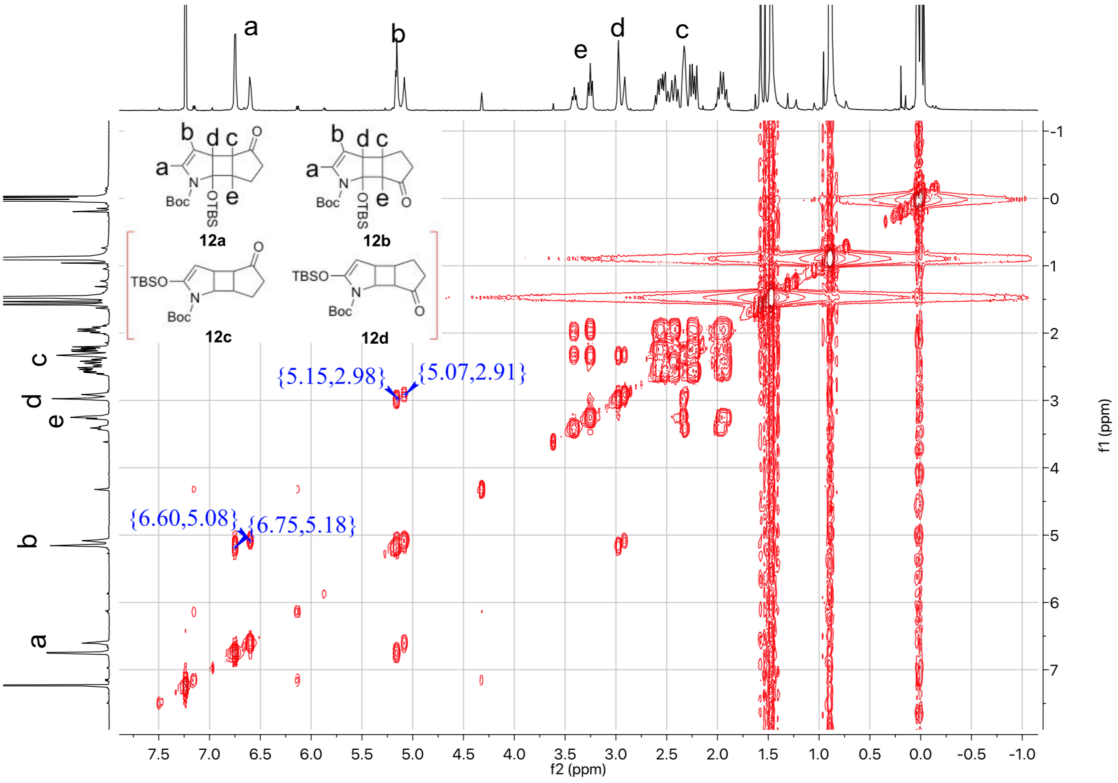

Figure 2. H-H COSY spectrum of a mixture of **12a** and **12b** ($CDCl_3$)

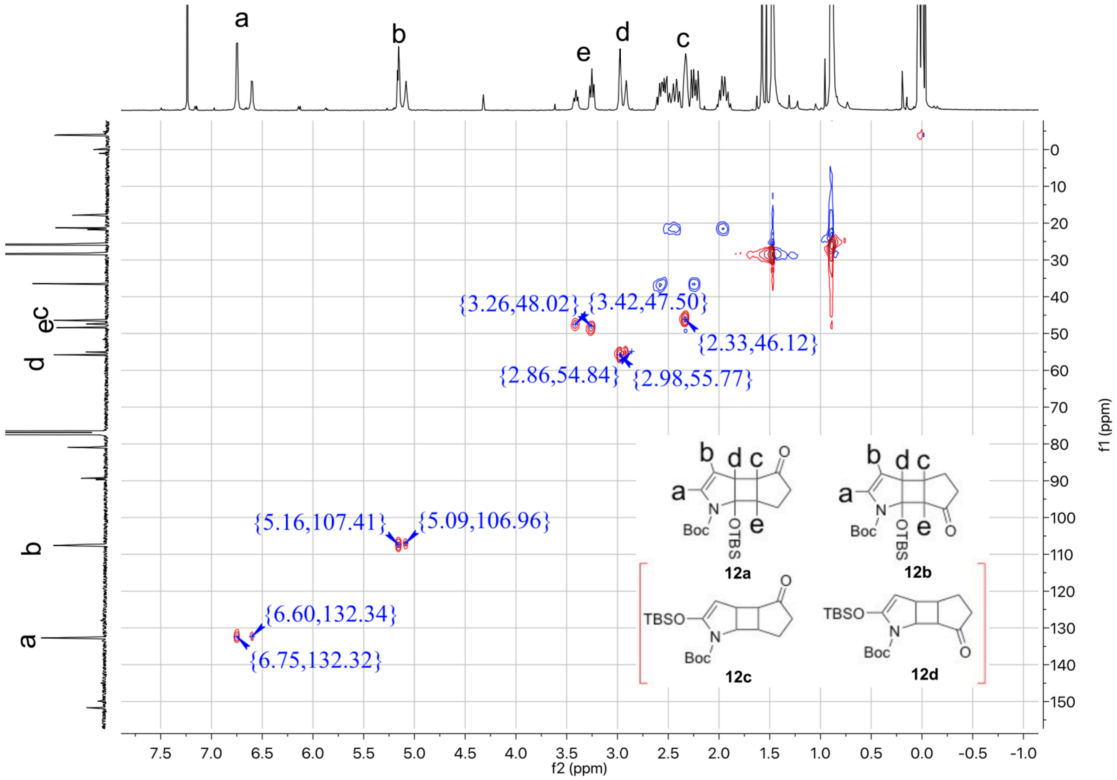

Figure 3. H-C HSQC spectrum of a mixture of **12a** and **12b** ($CDCl_3$)

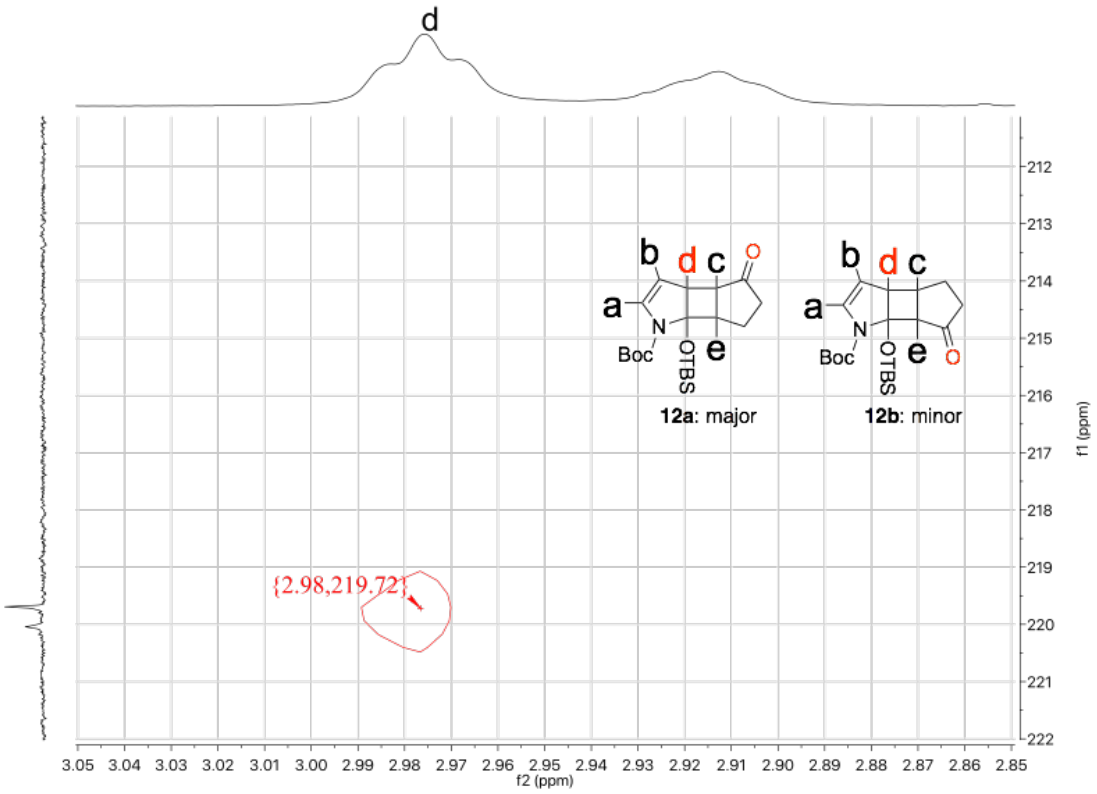

Figure 4. H-C HMBC spectrum of a mixture of **12a** and **12b** ($CDCl_3$)

The stereochemistry of compounds **12a** and **12b**, exo *versus* endo, was determined by their 2D-NOESY spectroscopic analyses. Thus, the correlations between H_b (δ 5.20, 5.13) and H_c (δ 2.38, 2.37) were observed in the H-H NOESY spectrum, indicating that both compounds **12a** and **12b** possess the *exo*-configuration as shown in Figure 5.

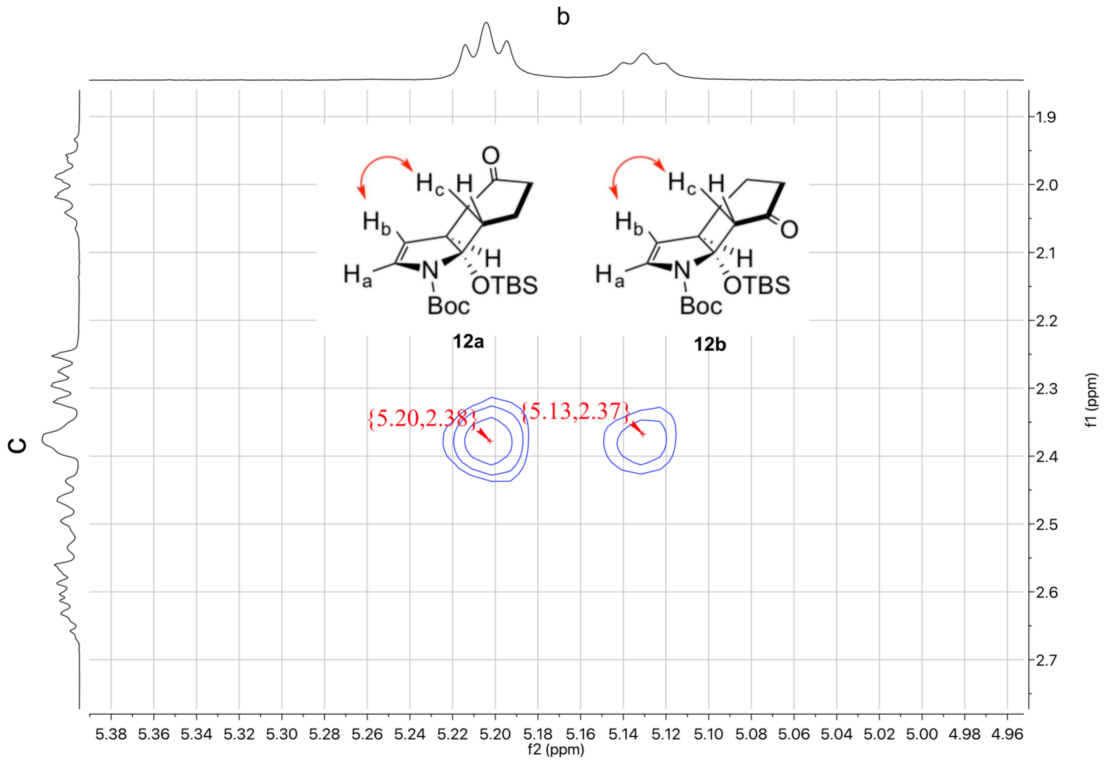

Figure 5. H-H NOESY spectrum of a mixture of **12a** and **12b** ($CDCl_3$)

The reaction conditions were optimized to obtain **12a** and **12b** in high yields, because the large amount of enone **8b** was recovered under the conditions in entry 1 (Table 1). The ratio of compound **12a** and **12b** dramatically influenced the conversion of compound **8b** to give high yields of compounds **12a** and **12b** (entries 1-4, Table 1). When the large excess amount of compound **1b** (15 equiv) was used for the photochemical reaction with **8b**, 72% of compounds **12a** and **12b** were obtained after 24 h using 365 nm-LED in acetone (entry 4, Table 1). The yield of adducts **12a** and **12b** decreased when acetonitrile or benzene was used as a solvent. (entries 5 and 6, Table 1), indicating the reaction occurs in the triplet excited state. The product ratio of **12a** and **12b**, ~65 to 35, was not affected by the concentration or solvent (Table 1).

Table 1. Photochemical Reaction of **1** with cyclopentenone **8b**[a]

Entry	Ratio of **1b** : **8b**	Recovered enone **8b**	Ratio of **12a** : **12b**	Yields of **12a**+**12b**[b]
1	1.5 :1	73%	64:36	12%
2	5 : 1	31%	66:34	57%
3	10 : 1	30%	63:37	64%
4	15 : 1	16%	65:35	72%
5[c]	15: 1	58%	62:38	29%
6[d]	15 : 1	27%	64:36	57%

[a]Acetone was used for the reaction solvent. A light-emitting diode lamp at 365 nm was used for 24 hours irradiation; [b]Isolation yield after silica gel chromatography; [c]Acetonitrile was used for solvent; [d]Benzene was used for solvent.

Next, the photochemical reaction of 1,4-naphthoquinone **11** with **1b** was conducted under the similar reaction conditions (Scheme 5, Table 2). It was worthy to see the product selectivity, cyclobutane *versus* oxetane, since in general the mixture of oxetane and cyclobutane were formed in the photochemical cycloaddition reactions discussed in the *Introduction* part of Chapter 3. After irradiation of **1b** with **11**, the formation of oxetane product **13** was observed. The corresponding cyclobutane products were not observed in the photolysate. The structure of oxetane **13** was confirmed by the measurement of 1D, 2D NMR and HRMS spectra. Except the protons of Boc group and siloxyl group, only one aliphatic proton H_5 at δ 3.80 was observed in the isolated product, which was correlated to the sp^3 carbon at δ 64.19 according to H-C HSQC spectrum (Figure 6). In addition, the findings of correlation of H_1 and H_2 and correlation of H_1 and H_5 in H-H COSY spectrum could also exclude the possibilities of regioisomers (Figure 7). The observation excludes the possibility of the formation of cyclobutanes and the regioisomeric oxetane shown in Figure 6. In addition to the spectroscopic evidence, only one carbonyl carbon at δ 183.9 was found in the photochemical product which is correlated to H_{16} (δ 8.09) and H_{12} (δ 7.30) that also could exclude the possibility of cyclobutane adduct (Figure 8). The

stereochemistry of compound **13** was determined to be *exo*, because the correlation of H_5 (δ 3.80) and H_{13} (δ 8.39) was observed in the H-H NOESY spectrum (Figure 9).

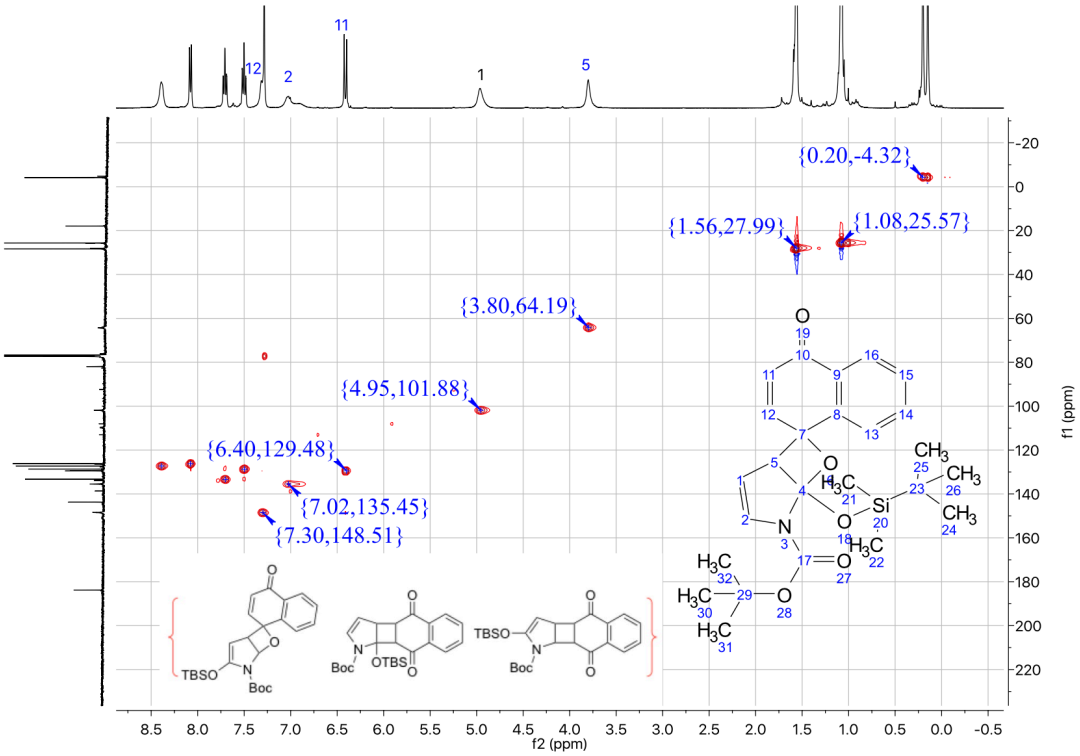

Figure 6. H-C HSQC spectrum of **13** ($CDCl_3$)

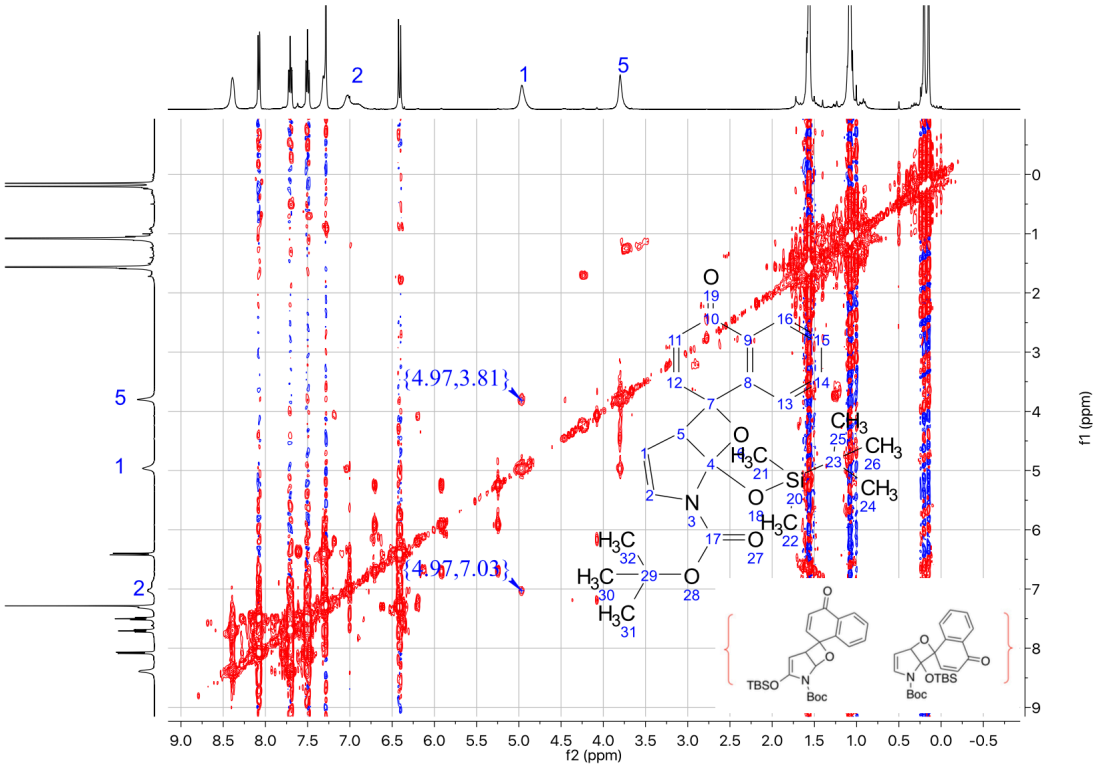

Figure 7. H-H COSY spectrum of **13** ($CDCl_3$)

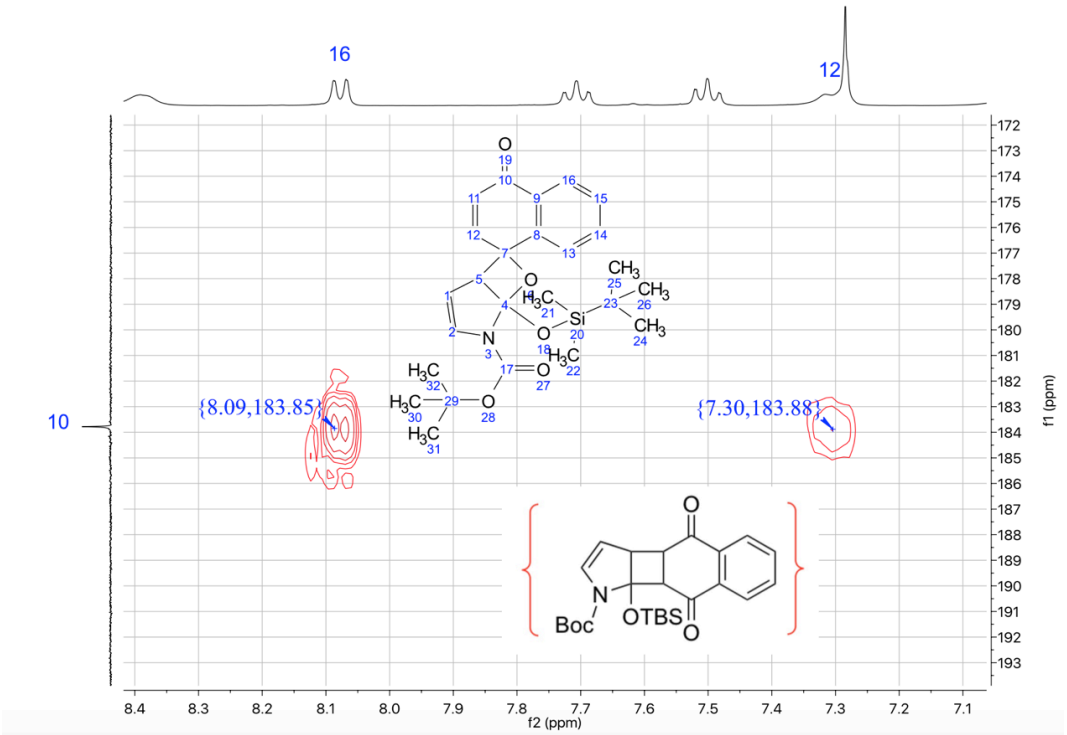

Figure 8. H-C HMBC spectrum of **13** ($CDCl_3$)

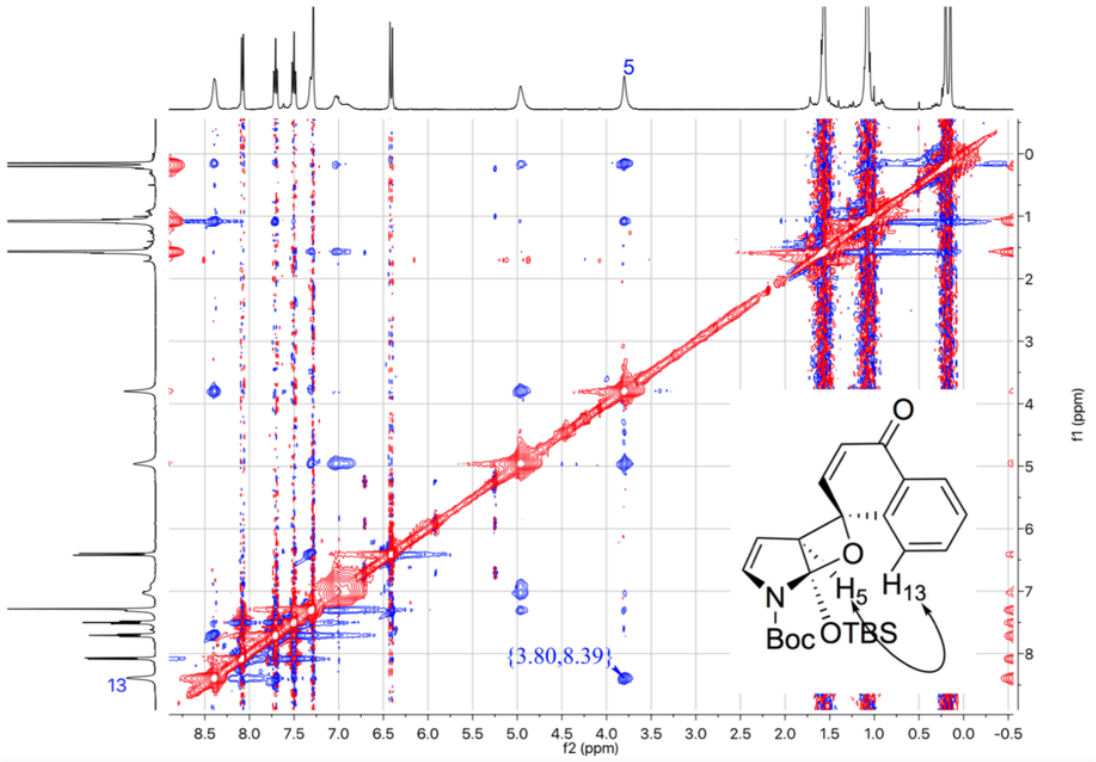

Figure 9. H-H NOESY spectrum of **13** ($CDCl_3$)

The high pressure Hg lamp (300W) through Pyrex filter was found to be better light source than the 365 nm LED lamp for the reaction (entries 1, 2, Table 2). The chemical yield of compound **13** was largely dependent upon the compound ratio of **1b**/**11** and solvent. When the excess amount of compound **1b** was used for the reaction (entries 2-4, Table 2), the conversion yield of **13** was higher than that for the reaction with excess amount of compound **11** (entries 5, 6, Table 2). Acetonitrile was inappropriate for this Paternò–Büchi reaction of **1b** and **11** (entry 7, Table 2).

Table 2. Optimization of the reaction conditions of **1** and **11**[a]

Entry	Ratio of **1b** : **11**	Yield of **13**[b]	Conversion Yield[c]
1[d]	3:1	17%	26%
2	3:1	29%	59%
3	1.5:1	22%	36%
4	1:1	24%	47%
5	1:1.5	26%	40%
6	1:3	13%	16%
7[e]	1.5:1	0	0

[a]Benzene was used for the reaction solvent. High pressure Hg lamp (300 W) was used for 6 hours irradiation; [b]Isolation yield after silica gel chromatography; [c]Conversion yield was calculated based on the consumed naphthaquinone by ^{1}H NMR analysis using Ph_3CH as internal standard; [d]Light-emitting diode lamp at 365 nm was used for light resource; [e]Acetonitrile was used as solvent.

In the chapter, regio- and stereoselectivity of photochemical reaction of the pyrrole derivative **1b** with two types of enone derivatives **8b** and **11** were investigated in detail. In the reaction with 2-cyclopenten-1-one **8b**, *exo*-selective formation of tricyclic cyclobutanes **12a** and **12b** was observed. In contrast to the selective formation of cyclubutane formation, the selective formation of oxetane was found in the reaction with 1,4-naphthoquinone **11**, although the reaction conversion was rather low.

3-3. Experimental section

All the reagents and solvents were obtained at reagent grade and used without further purification except that cyclopentenone **8b** was distilled before use. Thin layer chromatography (TLC) analysis was performed on silica gel plates and imagined under ultraviolet light. ^{1}H NMR and ^{13}C NMR data were recorded with a 400 MHz NMR spectrometer (Bruker Magnet System 400'54 system). $CDCl_3$, C_6D_6 and acetone-d_6 were used as deuterated solvents. Chemical shifts were described in parts per million (ppm) relative to trimethylsilane (δ = 0.00 ppm), and the coupling constants (J) were stated in Hertz (Hz). High-resolution mass spectroscopic (HRMS) analyses were conducted using a Orbitrap XL instrument using the positive ion mode. UV spectra were obtained by SHIMADZU UV-3600 Plus. The photochemical reactions were carried out using the LED lamp *Awill* manufactured by ARK TECH incorporation. The model of high-pressure (300W) mercury lamp is HALoS EH8500 C/S 60.

The synthesis of **1b** was explained in Chapter 2.

General procedure of the photoreaction of **1b** and **8b**, **11**

a. [**8b**] or [**11**] was 340 mM

The solution of starting material in Pyrex NMR tube was bubbled with nitrogen for 20 minutes. After irradiation (high pressure Hg lamp or 365 nm light-emitting diode), the reaction mixture was concentrated under reduced pressure. The desired product was purified by silica gel column chromatography (elution of EtOAc : Hexane = 1:8).

b. [**8b**] or [**11**] was 42.5 mM

The solution of starting material in test tube was degassed by freeze/pump/thaw for 5 times. After irradiation (365 nm light-emitting diode), the reaction mixture was concentrated under reduced pressure. The desired product was purified by silica gel column chromatography (elution of EtOAc : Hexane = 1:8).

***tert*-Butyl 6b-((*tert*-butyldimethylsilyl)oxy)-4-oxo-3b, 4, 5, 6, 6a, 6b hexahydrocyclopenta [3,4]cyclobuta[1,2-b]pyrrole-1(3aH) carboxylate**

and ***tert*-butyl 6b- ((*tert*-butyldimethylsilyl)oxy) 6-oxo-3b, 4, 5, 6, 6a, 6b-hexahydrocyclopenta[3,4]cyclobuta[1,2-b]pyrrole-1(3aH)-carboxylat e** (**12a** and **12b**).

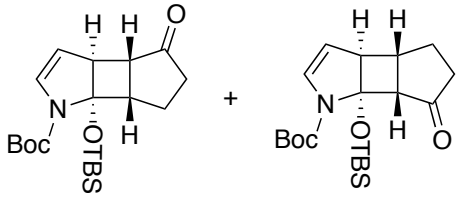

12a **12b**

^{1}H NMR (400 MHz, $CDCl_3$) δ 6.80 (d, J = 4.4 Hz, **12a**-1H), 6.65 (d, J = 4.4 Hz, **12b**-1H), 5.20 (t, J = 3.9 Hz, **12a** -1H), 5.13 (s, **12b** -1H), 3.46 (t, J = 7.7 Hz, **12b** -1H), 3.30 (t, J = 7.9 Hz, **12a** -1H), 3.02 (t, J = 2.9 Hz, **12a** -1H), 2.99 – 2.91 (m, **12b** -1H), 2.72 – 2.41 (m, 2H), 2.40 – 2.37 (m, 1H), 2.29 (dd, J = 17.7, 9.2 Hz, 1H), 2.11 – 1.90 (m, 1H), 1.52 (s, 9H), 0.93 (s, 9H), 0.06 (d, J = 13.4 Hz, 6H). ^{13}C NMR (101 MHz, $CDCl_3$) δ 220.1 (**12b**), 219.7 (**12a**), 151.7 (**12a**), 149.9 (**12b**), 132.74 (**12a**), 132.69 (**12b**), 107.6 (**12a**), 107.3 (**12b**), 89.7 (**12b**), 89.3 (**12a**), 81.0 (**12b**), 80.9 (**12a**), 55.8 (**12a**), 55.0 (**12b**), 48.4 (**12a**), 47.4 (**12b**), 46.4 (**12a**), 46.3 (**12b**), 36.4, 28.4, 25.7, 21.8 (**12b**), 21.3 (**12a**), 17.9 (**12b**), 17.8 (**12a**), –3.9 (**12a**), –3.98 (**12b**), –4.02 (**12a**), –4.3 (**12b**). HRMS (ESI+) m/z: $[M+Na]^+$ anal. calcd for $C_{20}H_{33}O_4NNaSi$ 402.20711, found 402.20728.

***tert*-Butyl-1-((tert-butyldimethylsilyl)oxy)-4'–oxo-4'H-7-oxa-2-azaspiro [bicyclo[3.2.0] heptane-6,1'-naphthalen]-3-ene-2-carboxylate (13).**

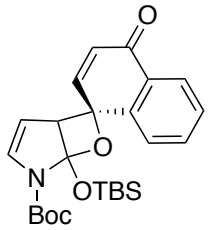

^{1}H NMR (400 MHz, $CDCl_3$) δ 8.39 (d, J = 7.5 Hz, 1H), 8.08 (dd, J = 7.9, 1.5 Hz, 1H), 7.73 – 7.69 (m, 1H), 7.51 (dd, J = 7.6, 1.3 Hz, 1H), 7.32 (s, 1H), 7.02 (d, J = 11.4 Hz, 1H), 6.41 (d, J = 10.4 Hz, 1H), 4.96 (s, 1H), 3.80 (s, 1H), 1.56 (s, 9H), 1.08 (s, 9H), 0.20 (s, 3H), 0.15 (s, 3H). ^{13}C NMR (101 MHz, $CDCl_3$) δ 183.8, 148.4, 143.7, 138.6, 135.5, 133.9, 133.3, 129.5, 129.4, 128.7, 127.2, 126.4, 126.2, 101.9, 81.8, 64.3, 28.3, 25.6, 17.9, –4.15, –4.25.

HRMS (ESI+) m/z: $[M+Na]^+$ anal. calcd for $C_{25}H_{33}O_5NNaSi$ 478.20202, found 478.20209.

3-4. Supporting material

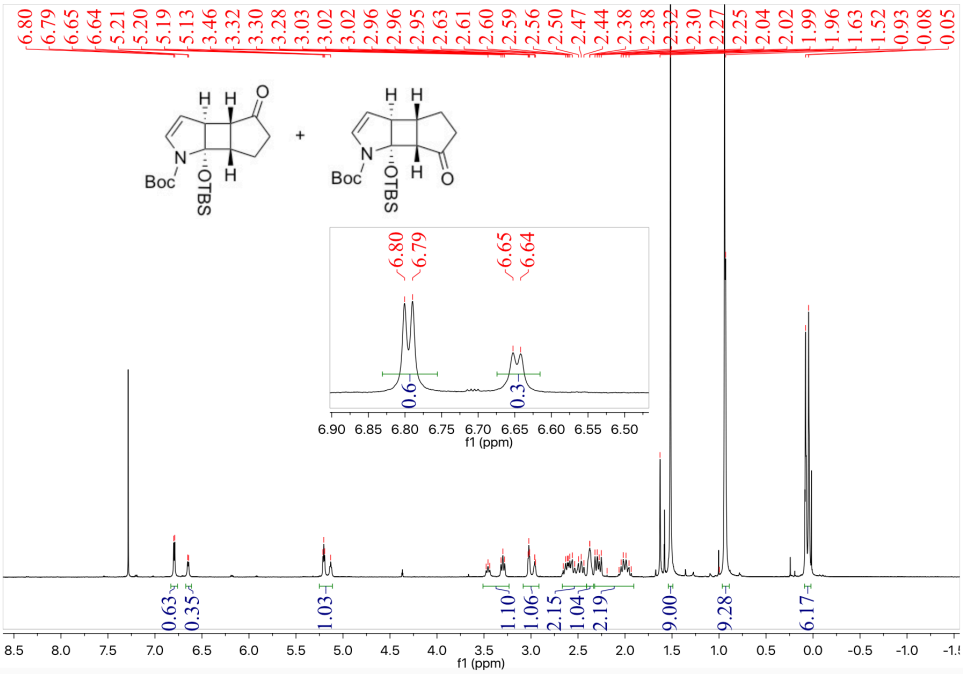

Figure 10. ^{1}H NMR spectrum of a mixture **12a** and **12b** (400 MHz, $CDCl_3$)

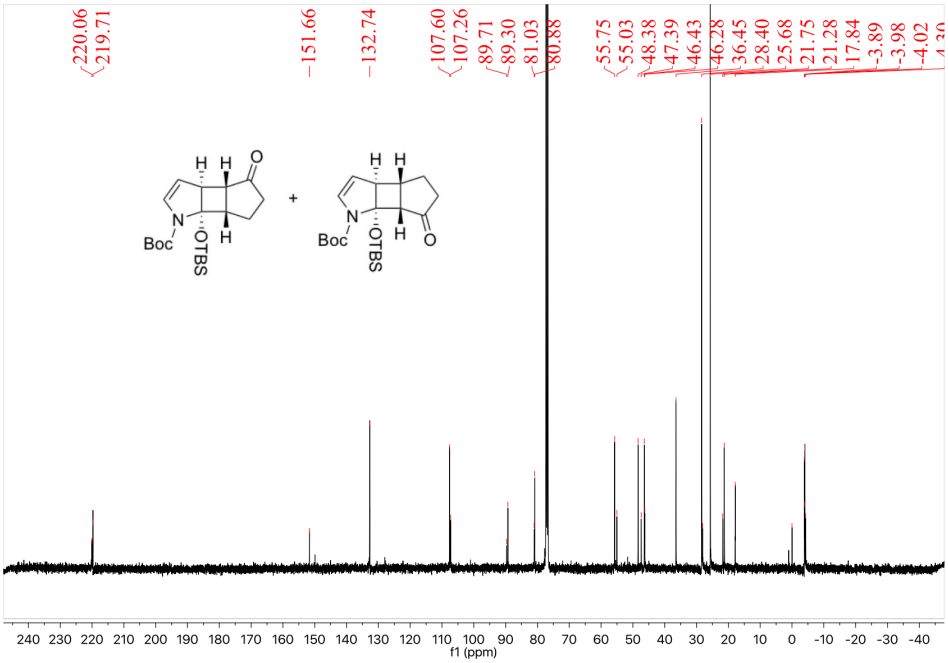

Figure 11. ^{13}C NMR spectrum of a mixture of **12a** and **12b** (101 MHz, $CDCl_3$)

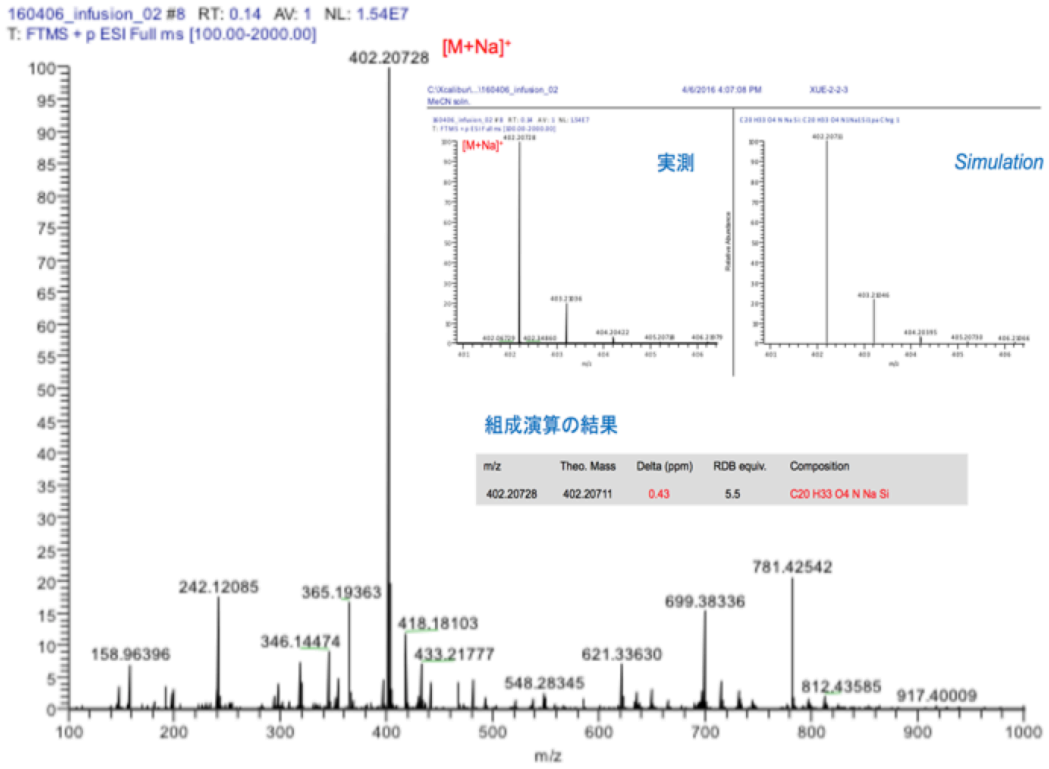

Figure 12. HRMS spectrum of a mixture of **12a** and **12b**

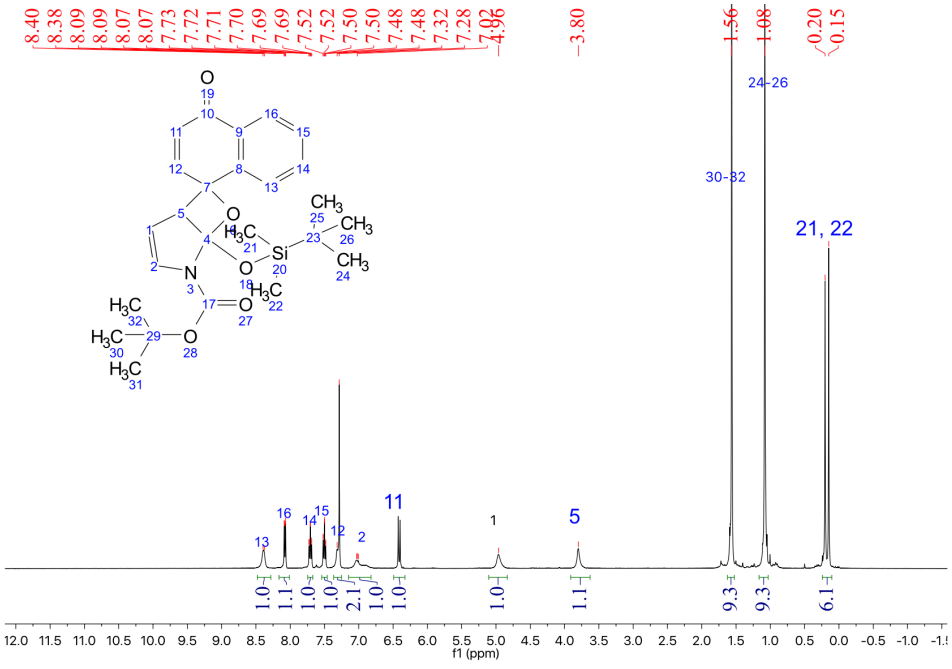

Figure 13. ^{1}H NMR spectrum of **13** (400 MHz, $CDCl_3$)

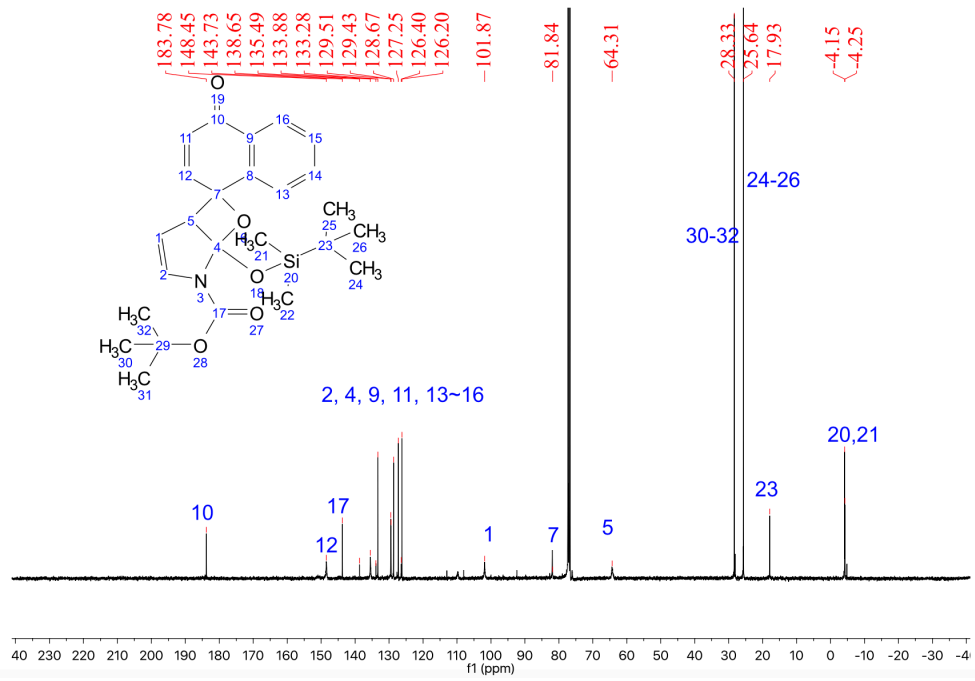

Figure 14. ^{13}C NMR spectrum of **13** (101 MHz, $CDCl_3$)

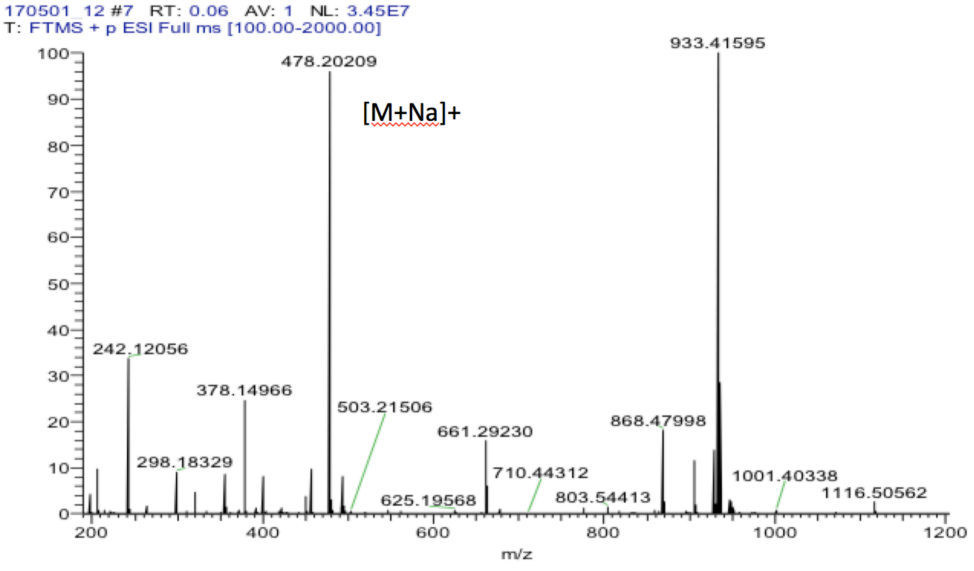

m/z	Theo. Mass	Delta (ppm)	RDB equiv.	Composition
478.20209	478.20202	0.14	10.5	C25 H33 O5 N Na Si

Figure 15. HRMS spectrum of **13**

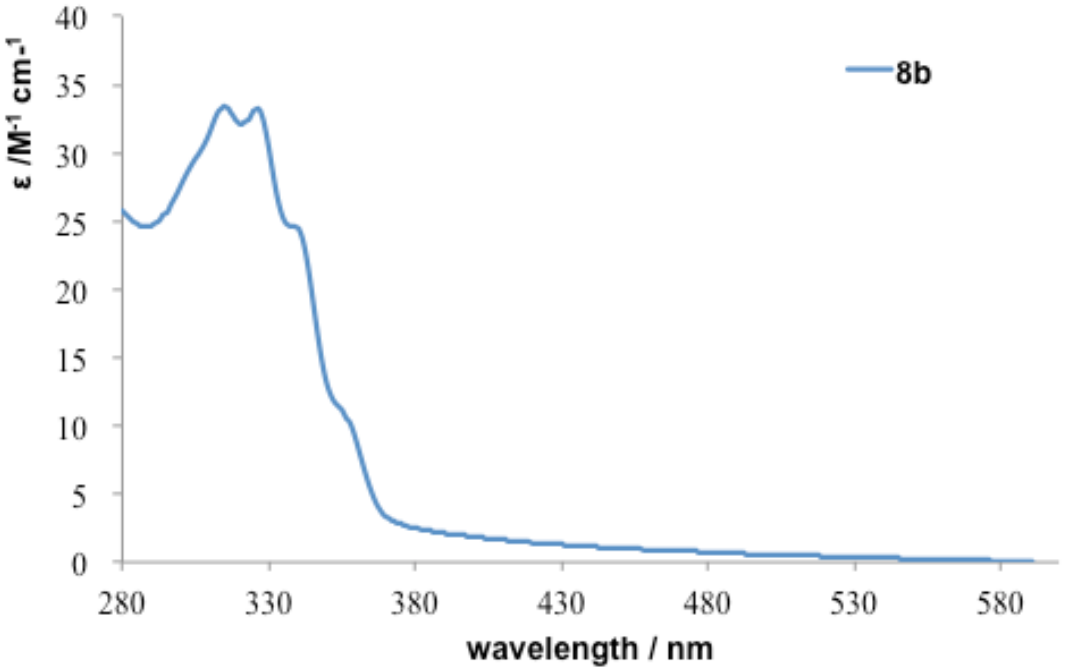

Figure 16. UV-Vis spectrum of **8b** (6.78 mM at benzene)

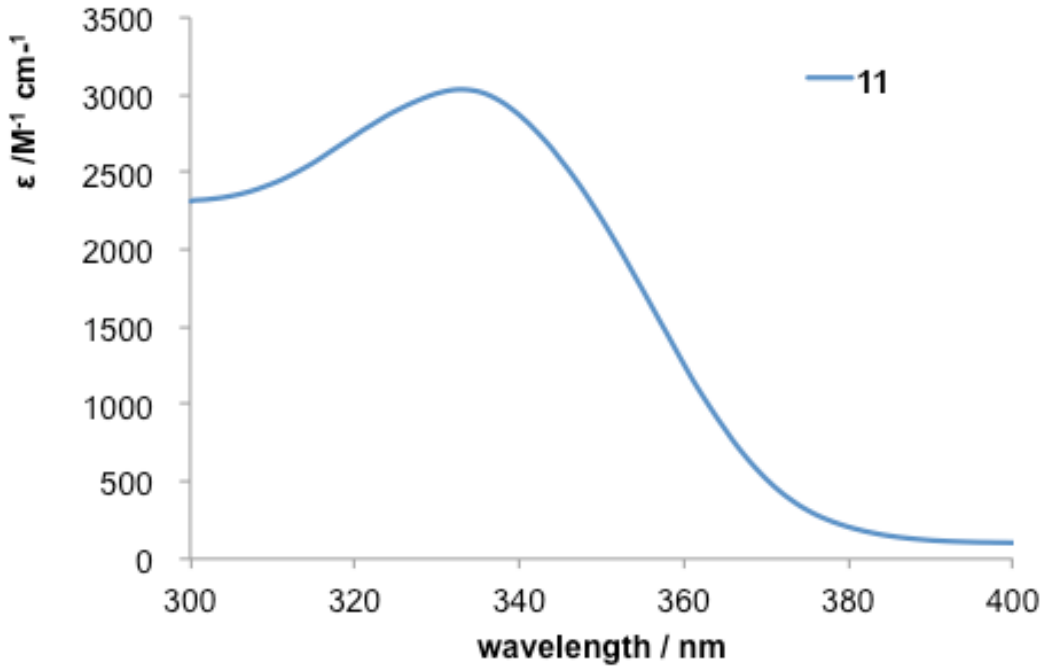

Figure 17. UV-Vis spectrum of **11** (0.285 mM at benzene)

References

1. Poplata, S.; Tröster, A.; Zou, Y. -Q.; Bach, T. *Chem. Rev.* **2016**, *116*, 9748.

2. Grota, J.; Domke, I.; Stoll, I.; Schröder, T.; Mattay, J.; Schmidtmann, M.; Bögge, H.; Müller, A. *Synthesis*, **2005**, 2321.

3. Crimmins, M. T.; Pace, J. M.; Nantermet, P. G.; Kim-Meade, A. S.; Thomas, J. B.; Watterson, S. H.; Wagman, A. S. *J. Am. Chem. Soc.* **2000**, *122*, 8453.

4. (a) Elliott, L. D.; Berry, M.; Orr-Ewing, A. J.; Booker-Milburn, K. I. *J. Am. Chem. Soc.* **2007**, *129*, 3078. (b) Maskill, K. G.; Knowles, J. P.; Elliott, L. D.; Alder, R. W.; Booker-Milburn, K. I. *Angew. Chem. Int. Ed.* **2013,** *52*, 1499. (c) Koovits, P. J.; Knowles, J. P.; Booker-Milburn, K. I. *Org. Lett.* **2016**, *18*, 5608.

5. Bunce, N. J.; Ridler, J. E.; Zerner, M. C. *Theoret. Chim. Acta*, **1977**, *45*, 283.

6. (a) Horspool, W. M. *Enone Cycloadditions and Rearrangements: Photoreactions of Dienones and Quinones* in Specialist Periodical Report on Photochemistry, The Royal Society of Chemistry, Cambridge, **1970-1999**, vol. 1-30 (b) Bruce, M. *Photochemistry of Quinones*, in The Chemistry of Quinonoid Compounds, vol. I, ed. S. Patai, Wiley, New York, **1974**, P465. (c) Ochiai, M. ; Arimoto, M. ; Fujita, E. *J. C.S., Chem. Comm.* **1981**, 460. (d) Maruyama K.; Osuka, A. *Recent Advances in the Photochemistry of Quinones* in The Chemistry of Quinonoid Compounds, vol. II, ed. S. Patai and Z. Rappoport, Wiley, New York, **1988**. (e) Bryce-Smith, D.; Evans, E. H.; Gilbert, A.; McNeill, H. S. *J. Chem. Soc., Perkin Trans 1*, **1992**, 485. (f) Yoshizawa, M.; Takeyama, Y.; Kusukawa, T.; Fujita, M. *Angew. Chem. Int. Ed.* **2002***, 41,* 1347. (g) Yoshizawa, M.; Takeyama, Y.; Okano, T.; Fujita, M. *J. Am. Chem. Soc.* **2003**, *125*, 3243. (h) Wang, W.; Zhang, W. -J.; Wang, L.; Quah, C. K.; Fun, Hoong. -K.; Xu, J. -H.; Zhang, Y. *J. Org. Chem.* **2013**, *78*, 6211.

7. Curti, C.; Ranieri, B.; Battistini, L.; Rassu, G.; Zanardi, F. *Adv. Synth. Catal.* **2010**, *352*, 2011.

Chapter 4

Summary and outlook

Although photochemical [2+2] cycloaddition reaction is such significant in organic synthesis and physical organic chemistry with a history of over 100 years, the pyrrole derivatives are barely addressed because of the instability of product. In this thesis, the reactivity and mechanism exploration of pyrrole derivatives and carbonyl compounds in the photochemical [2+2] cycloaddition reactions were discussed in details.

As shown in Scheme 1, the pyrrole derivative was designed that the siloxyl group (OTBS) is used for the regioselectivity exploration and increase of reactivity of pyrrole; meanwhile, the electron-withdrawing group, *tert*-butyloxycarbonyl (Boc), was introduced to the nitrogen atom of the pyrrole ring to stabilize the bicyclic oxetane product. In the Lewis-acid promoted reaction of the pyrrole and benzophenone, newly formed C-C bond was formed at the most nucleophilic position of pyrrole (C5). However, if the benzophenone is excited to electronically excited state under photo irradiation, the oxygen atom in the carbonyl group will be switched from nucleophilic to electrophilic character that newly formed C-C bond is at C3 of pyrrole ring. The corresponding oxetane product was isolated successfully at the yield of over 90%. In addition, the laser flash photolysis study indicated that almost all of the benzophenone at excited state is quenched by pyrrole though the quantum yield was measured to be 0.02. The computation study showed that another regioisomer was not isolated because 1,4-diradical intermediate is not productive, which also explained why only one regioisomer was obtained.

Furthermore, similar photochemical [2+2] cycloaddition reactions of pyrrole derivatives with 2-cyclopenten-1-one and 1,4-naphthoquinone were also investigated, cyclobutane and oxetane product were obtained respectively in moderate yields (Scheme 1).

Scheme 1

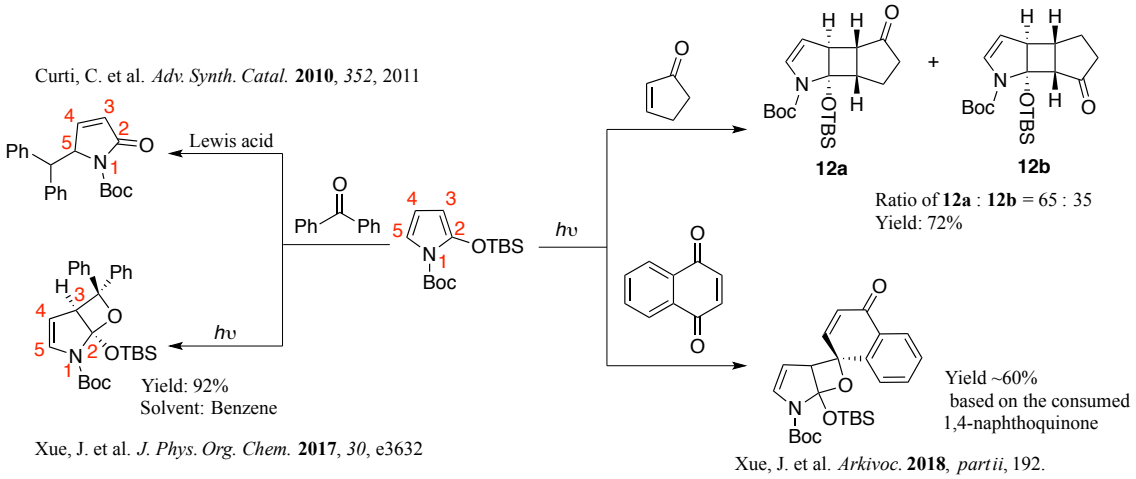

In summary, efforts have been made on the photochemical [2+2] cycloaddition reactions using pyrrole derivatives with carbonyl compounds that oxetane and cyclubutane containing pyrrole moiety were isolated in moderate yields successfully and structures were confirmed by 2D-NMR spectroscopy; meanwhile, the related mechanisms were elucidated by physical chemistry studies.

However, some unknown areas are still remained to explore. The explanation for regio- and stereoselectivity of these reactions needs to be polished in detail; the reactions of pyrrole derivatives with other carbonyl compounds are being waited to investigate in the future.

Acknowledgement

This thesis was accomplished under the guidance of Professor Dr. Manabu Abe belonged to Department of Chemistry, Graduate School of Science, Hiroshima University.

The author would like to thank for the scholarships offered by Japan Student Services Organization (JASSO) and Hiroshima International Center.

The author would like to give heartfelt gratitude to Professor Dr. Manabu Abe for his comprehensive supervision and thought-provoking education. In addition, as an international student, the author is particularly grateful to Dr. Manabu Abe for his generous assistance to the author' s life in Japan.

The author wants to thank all of the group members of Professor Dr. Manabu Abe, Dr. Satish Jakkampudi, Mr. Shohei Yoshidomi, Mr. Kengo Uchihashi, Mrs. Saori Takahashi, Mr. Takaaki Tamura, Mr. Toshiya Ichiki, Mr. Keita Ohnishi, Mr. Naomitsu Komori, Ms. Chie Shimokawa, Mr. Yoshiki Fujita, Ms. Pham Thi Thu Thuy, Mr. Youhei Chitose, Mr. Rikuo Akisaka, Mr. Misaki Matsumoto, Mr. Yuhei Yamasaki, Mr. Yuta Harada, Mr. Kousuke Murata, Mr. Qianghua Lin, Ms. Duong Duyen Thi, Ms. Bui Van Thi, Mr. Norito Kadowaki, Mr. Chihiro Tabuchi, Mr. Ayato Yamada, Mr. Zhe Wang, Mr. Dang Hai Nguyen, Mr. Miyu Sasaki, Ms. Chika Tanabe, Ms. Aina Miyahara, Ms. Ryoko Oyama, Dr. Sujan Kumar Sarkar, Mr. Agung Dian Pangaribowo, Mr. Luan Ngoc Thanh Nguyen, Mr. Kazunori Okamoto, Mr. Satoki Koyama, Ms. Maaya Takano, Mr. Yuki Miyazawa, Ms. Miki Wanibe, Ms. Sayuri Muramatsu, Mr. Hitoshi Dougauchi, especially Dr. Ryukichi Takagi and Dr. Sayaka Hatano for their help in the author' s research and life.

The author appreciates the suggestions and discussion about this research from Dr. Takeharu Haino, Dr. Tsutomu Mizuda and Dr. Yosuke Yamamoto in the organic group seminars of Hiroshima University.

The author also thanks Ms. Tomoko Amimoto from N-BARD, Hiroshima University, who did the contribution to the HRMS measurement.

Mr. Yoshio Tsuru from Global Career Design Center, Hiroshima University did a lot of help to the author for his internship and job searching.

Finally, the author' s parents, Mrs. E Tang and Mr. Huanxin Xue, and girlfriend, Ms. Juan Mao, have been always supporting the author' s life in these three years and encouraging him to be a better person.

List of publications

Articles

(1) Paternò–Büchi photochemical [2+2] cycloaddition of aromatic carbonyl compounds with 2-siloxy-1*H*-pyrrole derivatives

Jianfei Xue, Manabu Abe and Ryukichi Takagi

Journal of Physical Organic Chemistry, 30 (2017) e3632.

(2) Photochemical [2+2] cycloaddition reaction of enone derivatives with 2-siloxy-1*H*-pyrrole derivatives

Jianfei Xue, Ryukichi Takagi and Manabu Abe

ARKIVOC, part ii (2018) 192-204.